Dissertation

submitted to the

Combined Faculties for the Natural Sciences and for Mathematics

of the Ruperto-Carola University of Heidelberg, Germany

for the degree of

Doctor of Natural Sciences

Presented by: Attila Rácz, MD

Born in: Debrecen, Hungary

Oral-examination:

Molecular determinants of hippocampal oscillatory activity

Referees: **Prof. Dr. Peter Seeburg**
             Prof. Dr. Hannah Monyer

In memory of Dr. Ervin Szegedi (1956-2006),
my physics teacher at secondary school

TABLE OF CONTENTS

SUMMARY

In vitro electrophysiological studies in genetically modified mice with a deletion of the GluR-A subunit in parvalbumin-positive GABAergic interneurons (PV-GluR-A KO mice) provided evidence for the involvement of this cell-population in the generation of hippocampal network synchrony. Besides, these mice displayed several alterations in hippocampus-dependent cognitive tasks (Fuchs et al., 2007). To study the characteristics of hippocampal network synchrony thoroughly, we applied *in vivo* electrophysiological measurements in freely moving animals.

We used tetrode and silicon probe hippocampal recordings from mutant and wildtype (WT) animals and compared cellular activity obtained from pyramidal cells and interneurons as well as network activity. The results can be summarized as follows:

1. PV-GluR-A KO mice exhibited increased ripple-power compared to WT mice. The underlying mechanism cannot be accounted for by an augmented cellular activity during ripples but by an increased phase-modulation of both pyramidal cells and interneurons as indicated by the unitary analysis.

2. The decreased gamma-power in the PV-GluR-A KO mice revealed by *in vitro* measurements could not be corroborated by the *in vivo* study. However, a reduction in gamma-frequency could be identified during REM-sleep of the PV-GluR-A KO mice. The phase-preference of pyramidal cells during gamma-oscillations was not different between genotypes. However, there was a delay of the phase-preference of interneurons in PV-GluR-A KO compared with WT mice.

3. The firing rate of pyramidal cells during theta-oscillations was decreased in PV-GluR-A KO mice whereas that of interneurons did not change significantly. We propose that the pyramidal cells' underperformance is due to the altered function of interneurons.

4. Pyramidal cells were more "bursty" in PV-GluR-A mutants. The increased "burstiness" occurred during theta-, gamma- and ripple-oscillations. We think that the suboptimal work of interneurons makes pyramidal cell firing less "predictable" and maybe temporary fluctuations in the excitatory and inhibitory network state can disturb the optimal modes of pyramidal cell-discharge.

In summary, this *in vivo* study provides direct evidence that PV-positive GABAergic interneurons play a crucial role in the generation of synchronous network activity in the hippocampus.

ZUSAMMENFASSUNG

Elektrophysiologische Untersuchungen *in vitro* an genetisch modifizierten Mäusen, in denen die GluR-A Untereinheit in Parvalbumin-positiven GABAergen Interneuronen ausgeschaltet wurde (PV-GluR-A KO Mäuse), ergaben, dass diese Zellpopulation an der Entstehung synchroner Netzwerkaktivität massgeblich beteiligt ist. Des weiteren wiesen Verhaltenstests darauf hin, dass die genetische Modifikation zu Defiziten von Hippocampus-abhängigen Leistungen führte (Fuchs et al., 2007). Um synchrone Netzwerkaktivität im Hippocampus besser charakterisieren zu können, führten wir elektrophysiologische Ableitungen *in vivo* an sich frei bewegenden Mäusen durch.

Wir benutzten Tetroden und Silicon-Proben und verglichen bei modifizierten und Wildtyp-Mäusen (WT) Einzelzellaktivität von Pyramidenzellen und GABAergen Interneuronen sowie oszillatorische Netzwerkaktivität. Die Ergebnisse können wie folgt zusammengefasst werden:

1. PV-GluR-A KO Mäuse zeigten erhöhte "Ripple"-Aktivität im Vergleich zu WT-Mäusen. Wie die zelluläre Analyse zeigt, scheint der zugrunde liegende Mechanismus nicht die erhöhte zelluläre Aktivität in "Ripple"-Oszillationen zu sein, sondern eine erhöhte Phasenmodulation sowohl von Pyramidenzellen als auch von Interneuronen.

2. Die verminderte Gamma-Leistung in PV-GluR-A KO Mäusen, die sich aus *in vitro* Messungen ergab, konnte *in vivo* nicht verifiziert werden. Wir fanden jedoch eine Verminderung der Frequenz von Gamma-Oszillationen während REM-Schlaf in den PV-GluR-A KO Mäusen. Es gab keinen Unterschied in der Phasen-Preferenz von Pyramidenzellen während Gamma-Oszillationen. Interneurone von PV-GluR-A KO Mäusen jedoch waren verzögert im Vergleich mit WT-Mäusen.

3. Die Feuerfrequenz von Pyramidenzellen während Theta-Oszillationen war verringert in PV-GluR-A KO Mäusen, während die von Interneuronen sich nicht signifikant änderte. Die reduzierte Aktivität von Pyramidenzellen ist vermutlich eine Konsequenz der veränderten Interneuronfunktion.

4. Im Vergleich zu WT Mäusen, waren Pyramidenzellen in PV-GluR-A KO Mäusen mehr "bursty" sowohl während Theta- als auch Gamma- und Ripple-Oszillationen. Die suboptimale Funktion der Interneurone ist wahrscheinlich der Grund dafür, warum das Feuern von Pyramidenzellen weniger "vorhersehbar" ist. Eventuell können Fluktuationen von Erregung und Hemmung im Netzwerk das optimale Muster des Feuerns von Pyramidenzellen stören.

Zusammengefasst weisen diese *in vivo* Untersuchungen darauf hin, dass PV-positive GABAerge Interneurone bei der Entstehung synchroner Netzwerkaktivität des Hippocampus eine wichtige Rolle spielen.

LIST OF ABBREVIATIONS

ADAR	Adenosine DeAminase acting on RNAs
AMPA	α-Amino-3-hydroxyl-5-Methyl-4-isoxazole Propionic Acid
BOLD	Blood Oxygen Level Dependent
CA1, 2, 3	Cornu Ammonis 1, 2, 3
CaMKII	Calcium/CalModulin-dependent protein Kinase II
CB	CalBindin
CB1	CannaBinoid (receptor) 1
CCK	CholeCystoKinin
CR	CalRetinin
CSD	Current-Source Density (analysis)
DG	Dentate Gyrus
DSI	Depolarization-induced Suppression of Inhibition
EAAT	Excitatory Amino Acid Transporter
EEG	ElectroEncephaloGraphy
EPSP	Excitatory PostSynaptic Potential
FFT	Fast Fourier Transform
FMRI	Functional Magnetic Resonance Imaging
GABA	Gamma-Amino-Butyric Acid
GAD	GlutAmate Decarboxylase
GDP	Giant Depolarizing Potential
GluR-A, GluR-B, GluR-D	Glutamate Receptor A, B, D
HFS	High-Frequency Stimulation
5HT	5-HydroxyTryptamine, serotonin
IPI	InterPeak-Interval
IPSP	Inhibitory PostSynaptic Potential
I-V	Current-Voltage (curve)
KCC2	Kalium-Chloride Cotransporter 2
KO	KnockOut
LFP	Local Field Potential
LIA	Large-Amplitude Irregular Activity
LTP	Long-Term Potentiation
MEA	Multi-Electrode Array
MEG	MagnetoEncephaloGraphy
NKCC1	Natrium-Kalium-Chloride Cotransporter 1
NMDA	N-Methyl-D-Aspartic acid
NO, NOS	Nitric Oxide, Nitric Oxide Synthase
NPY	NeuroPeptid Y
NR1, NR2	NMDA-Receptor 1, 2
NSF	N-ethylmaleimide-Sensitive Fusion protein
O-LM	Oriens-Lacunosum-Moleculare (cell)
PICK1	Protein Interacting with C Kinase 1
PSD	PostSynaptic Density
PV	ParValbumin
REM	Rapid Eye Movement (sleep)
SAP	Synapse-Associated Protein
SD	Standard Deviation
SOM	SOMatostatin
SPW	SharP Wave

SWS	Slow-Wave Sleep
TARP	Transmembrane AMPA-receptor Regulating Protein
TBS	Theta-Burst Stimulation
TPD	Theta-modulated Place-by-Direction (cells)
WT	WildType

INTRODUCTION

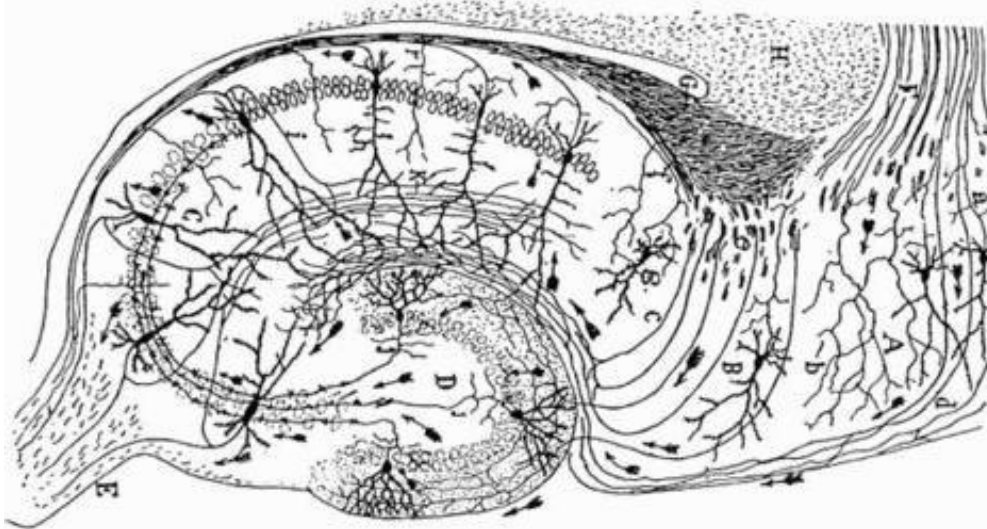**General anatomy of the hippocampus**

The hippocampal formation consists of several subregions, including the dentate gyrus (DG) and hippocampus proper (*Figure 1.*). The hippocampus itself can be divided into subregions named after "Cornu Ammonis" (CA3, CA2 and CA1). Axons from the CA1 form the major output of the hippocampus, the subiculum on one hand and the fornix on the other. The former one feeds information back into the entorhinal cortex (mainly layer 5), which in turn also innervates CA1, CA2 and CA3 via the perforant pathway. The fornix arches towards the mamillary nucleus, from where two main tracts are formed, the fasciculus mamillothalamicus (Vicq d'Azyr) and the fasciculus mamillotegmentalis (named after Gudden). The first one gives input to an anterior portion of thalamic nuclei, which project to the cingulum. The cingulum also volutes back to the parahippocampal structures, thereby closing one of the limbic circles. The hippocampus is a real centre of anatomical connections, not only does it receive inputs from the dentate gyrus and entorhinal cortex, but it is also reciprocally connected to the septal nuclei, which also provide cholinergic and GABAergic (gamma-amino-butyric acid) input to the hippocampus. The dentate gyrus receives noradrenergic input from the locus coeruleus, serotonergic innervation from the raphe nuclei whereas the CA1 receives dopaminergic input from the mesolimbic system, especially the ventral tegmental area. As we shall later see, these modulatory systems may exert a strong influence on learning functions, both in terms of stress-related (Reymann & Frey, 2007) and reward-related learning (Foster & Wilson, 2006). The amygdala comprises a complex of nuclei reciprocally connected with the CA areas and is functionally related to fear-conditioning.

Even though we refer to the hippocampal formation as archicortex, the basic circuitry of the hippocampus shows remarkable differences to other cortical formations. A striking hippocampal feature is its three-layered structure, with cell bodies arranged in the middle, dendritic trees on one side and axons on the other. This is in sharp contrast with the six-layered neocortical microarchitecture. The lamination offers an excellent opportunity for understanding the anatomy of the basic circuitry and for studying its principal physiological functions. The five-layered parahippocampal structures (e.g. the subiculum or entorhinal cortex) are also referred to as periarchicortex because they show a transition between the archi- and neocortical organizing principles (for a more comprehensive treatise see Amaral & Witter, 1995).

Similar to other brain structures, the two major neuronal cell types in the hippocampal formation are the principal cells and interneurons. The archicortex is populated by distinct neuronal

subgroups. The principal cells of the dentate gyrus are called granule cells, those of the hippocampus proper are called pyramidal cells. An interesting glutamatergic cell type in the DG is

Figure 1.: The basic anatomy of the hippocampus, as depicted by Santiago Ramon y Cajal at the beginning of the 20th century. One can clearly identify distinct subregions of the hippocampal formation and basic in- and output routes and internal connections of it: the perforant path coming from the entorhinal cortex, the Schaffer-collaterals and fornix originating from CA3 and CA1.

the mossy cell. It is innervated by granule cells and projects back innervating the dendritic tree of granule cells in the neighbourhood of the cell they receive excitation from. The interneurons of DG are located mainly in the molecular and polymorphic layers, but some, mainly of the basket cell type, can also be found in the granule cell layer. The axons of the granule cells are called mossy fibers, they lack myelin-sheath and form unique synaptic structures onto CA3-cells. CA3-pyramidal neurons receive their input mainly from dentate gyrus mossy fibers, from the perforant path (entorhinal input), from the contralateral CA3 (commissural connections) and via recurrent collaterals from CA3-cells themselves. The latter pathway is called Schaffer-collateral-system, and due to its anatomical organization remarkable auto-associative features are attributed to it that also has behavioural consequences (Nakazawa et al., 2002). CA3-pyramidal cells are quite big (30-35 μm), in comparison to CA1-pyramids (10-15 μm). CA3-cells project both to CA1 pyramidal cells and to CA1 interneurons, thereby ensuring proper feed-forward excitation and feed-forward inhibition. The transition zone between the CA3 and CA1 is called CA2. Here cells are still big, but they do not receive mossy fibers from the DG. The CA1 receives input from the CA3-Schaffer-collateral system mainly via the basal dendrites and apical dendrites located in the stratum radiatum. In addition, the apical dendrites of CA1 pyramidal cells are also innervated by the perforant path, which runs in the stratum lacunosum-moleculare. Apparently the recurrent loop, connecting CA3-pyramids is absent in CA1. CA1-pyramids also drive interneurons that provide feed-back inhibition

onto the pyramidal cells. It is important to note that whereas connections between DG granule cells and CA3-pyramids are rather convergent (a given granule cell innervates 20-30 CA3-pyramids, but a given CA3 cell receives input from roughly 50 granule cells), connections between CA3 and CA1 are more divergent, also due to the Schaffer-collateral system (Amaral & Witter, 1995).

The hippocampus is a special brain-area where the genesis of granule cells continues after birth*. *Other structures possessing this potential are the olfactory bulb (for interneurons) and in distinct species some neocortical areas, such as auditory cortex in some birds, in migrating birds hippocampus as well. After birth the lateral and medial ganglionic eminence and the subventricular zone serve as a place for interneuron precursors generator which then follow certain routes (like the rostral, ventral and dorsal migratory streams) to reach their targets: the basal ganglia or the olfactory bulb. These neuroblasts form the granular and periglomerular cells of the olfactory bulb (for a more complete overview see the reviews of Marin & Rubinstein, 2004 and Wonders & Anderson, 2006).

A number of theories and experiments imply that adult neurogenesis in the dentate gyrus might be associated with hippocampal plasticity, possibly by guaranteeing a continuous rewiring of the system. It is indeed suggested that explorative behaviour promotes neurogenesis in the dentate gyrus (animals living under environmentally enriched conditions show this phenomenon, Segovia et al., 2006). It is also known that cabdrivers have a bigger hippocampus, due to the regular navigation tasks they perform during their everyday routine (Maguire et al., 2000). Interestingly, the right hippocampus is the one which shows this correlation, and the size of the right hippocampus correlates well with the time spent as a taxi-driver as well as with the navigation skills of the given cabdriver (actually this observation also corroborates the old view that the human right hemisphere would be responsible for the integration of spatial information and the left one for the temporal information, Szirmai et al., 2000). On the other hand, early-childhood brain-irradiation (e.g. performed as oncological therapy) can substantially reduce the number of available neurogenic precursors and can lead to learning deficits in later stages of life. In any case, it seems to be important to have ongoing neurogenesis in a brain structure involved in learning and plasticity.

Histology of hippocampal interneurons

There is a wide spectrum of interneurons taking part in the histological architecture of CA3 and CA1. Interneurons can be grouped in distinct classes according to a number of arbitrary features, which in some cases hint to their specific roles in certain neurophysiological processes. Interneurons can be classified based on their morphological properties, their location, the cellular domains that they innervate, their electrophysiological properties, the expression of specific histological markers and proteins, or their participation in distinct oscillatory states (such as theta-off and theta-on cells, Mizumori et al., 1990). Since there are certain correlations between the

above-named criteria, current attempts to classify interneurons aim at taking into consideration as many characteristics as possible (molecular, anatomical, functional).

A large amount of data in this research field was generated in the laboratory of Peter Somogyi and co-workers. These researchers implant sharp electrodes in the hippocampus of anaesthetized rats, adjust the location of the electrode according to the local field potentials and record the activity of individual cells by moving the electrode very close to them. In this way they can follow the behaviour of individual cells during different network-states. The juxtacellular labeling method can be used to fill the recorded cell with a dye (byocitin or neurobiotin) for further anatomical reconstruction. The principle of this method is that during the membrane potential-fluctuations of theta-oscillations the neurons can take up the charged dye-molecules (Pinault, 1996). This way the Somogyi group could establish many correlates between morphology, biochemical markers and electrophysiological properties of certain interneuron subtypes. However, since they examine oscillation-related activity in animals under anaesthesia, it is difficult to extrapolate the results of these findings to a likely scenario as it might occur *in vivo*.

To illustrate interneuron diversity, just a few examples will be discussed. O-LM cells (oriens-lacunosum-moleculare cells) for instance innervate dendrites in the stratum lacunosum-moleculare whereas they sit and expand their dendritic tree in the stratum oriens, to receive input from axons of pyramidal cells. Bistratified cells already innervate stratum radiatum dendrites (Klausberger et al., 2004) whereas basket cells inhibit the perykarion of neurons with basket-like structures. It is estimated that a basket cell can form inhibitory connections on as many as 1800-2000 pyramidal cell somata (Amaral & Witter, 1995; Freund, 2003). Axo-axonic or chandelier cells form synapses on the axon initial segment and since according to the classical view this is the action-potential generation site*, their function can be very important in the output control of pyramidal cells (Klausberger et al., 2003; Szabadics et al., 2005). The neurogliaform cells (Price et al., 2005) are mainly found in the stratum lacunosum-moleculare controlling the perforant path input from the entorhinal cortex. These cells are quite heterogeneous in their electrophysiological properties (Zsiros & Maccaferri, 2005).

*Some studies point out that action potentials may be generated in the dendrites as well (Kamondi et al., 1998), based on the observation that the frequency of dendritic Ca^{2+}-spikes can also exceed that of the somatic action potentials.

A recently identified novel interneuron-type in the hippocampus is the Ivy-cell. These cells are quite numerous, they are located mainly in the pyramidal layer, show very dense axonal fields innervating preferentially the basal dendritic domains and they co-express neuropeptide Y (NPY) and nitric oxide synthase (NOS). It is speculated that they control the input coming via the Schaffer-

collaterals in a rather domain-specific way via the release of NO (Fuentealba et al., 2008). In addition, NO may also regulate blood circulation in the brain, in this manner Ivy-cells might adjust blood and nutrient supply to local needs.

Of interest are also interneurons that innervate (and thus inhibit) other interneurons. The activity of these interneurons can lead to desinhibition of given pyramidal cells (Fonyó, 1995).

Certain immunochemical markers are also used to distinguish between interneuron-subtypes. In many cases they are calcium-binding proteins, such as parvalbumin (PV), calbindin (CB) and calretinin (CR), in other cases neuropeptides, such as cholecystokinin (CCK), somatostatin (SOM) or NPY. According to the current view, the expression of these markers is correlated with the anatomical and physiological subclass to which a given interneuron belongs. Bistratified cells, axo-axonic cells and a great percentage of basket cells are PV-positive, O-LM cells are mainly SOM-positive (Klausberger et al., 2003).

Principles of excitatory neurotransmission

Pyramidal cells constitute the output neurons of the hippocampus. However, pyramidal cells also innervate other pyramidal cells and interneurons in the hippocampus, so excitation is a primary action there. The excitatory drive onto principal cells and interneurons is transmitted mainly via glutamatergic synapses. The receptors, residing on the postsynaptic membranes are ligand-gated ionotropic receptors. According to their pharmacological properties, glutamate receptors can be classified in three major classes: AMPA-, kainate- and NMDA-receptors (AMPA stands for α-amino-3-hydroxyl-5-methyl-4-isoxazole propionic acid, NMDA for N-methyl-D-aspartic acid, reviewed by Mayer, 2005). Each class comprises several subunits. Thus, for instance there are four main subtypes of AMPA-receptor forming subunits (referred to as GluR-1-4 or GluR-A-D) that are differentially expressed with respect to the brain region and cell type. Pyramidal cells preferentially express GluR-A and GluR-B (Geiger et al., 1995). The latter subunits renders heteromeric AMPA-receptors with any of the other three subunits Ca^{2+}-impermeable. The required Ca^{2+} influx via glutamate receptors involved in potentiation of synapses on pyramidal cells has been attributed exclusively to NMDA-receptors. However, the situation is different in interneurons since they express GluR-A and GluR-D but relatively low levels of GluR-B (Geiger et al., 1995) and are thus equipped mainly with Ca^{2+}-permeable AMPA-receptors. Whether AMPA-receptors are involved in synaptic plasticity in interneurons is not clear so far. Overall, synaptic plasticity in pyramidal cells has been much studied over the last two decades and numerous *in vitro* and *in vivo* paradigms have been employed. Synaptic plasticity in interneurons has hardly been studied and in fact was

considered to be absent in interneurons. However, recent studies provide evidence that synaptic strength in interneurons is modifiable (Lamsa et al., 2007).

The functional interplay between AMPA- and NMDA-receptors resides in their different kinetics and functional regulation. Both receptors comprise four transmembrane domains, an extracellular N-terminal and an intracellular C-terminal domain. NMDA-receptors have a higher affinity for glutamate than AMPA-receptors. This means that without any other regulation NMDA-receptors would be activated first upon the presence of environmental glutamate and this would result in a massive Ca^{2+}-influx into the cell even under low external glutamate-concentrations. However, NMDA-receptors at resting membrane potential are "blocked" by Mg^{2+}-ions. The Mg^{2+}-block can only be relieved by strong membrane-depolarization. This mechanism reverses the order so that AMPA-receptors, despite their lower glutamate-affinity gate first and their mediated Na^{+}-current can depolarize the cell to the "threshold" of NMDA-receptor activation (Kandel et al., 2000). Thereby it is ensured that NMDA-receptors can only conduct their massive and relatively long-lasting Ca^{2+}-current, if it is really needed. On one hand this offers specificity for long-term potentiation (LTP) on principal cells, on the other hand it also circumvents possible harmful effects of excessive intracellular Ca^{2+}-concentrations*.

*High intracellular Ca^{2+}-concentrations can lead to the activation of Ca^{2+}-activated proteases, such as calpains, which degrade important molecules, even though calpains are also involved in LTP-induction (see the review of Bliss & Collingridge, 1993). The co-expression of AMPA- and NMDA-receptors on the postsynaptic density further ensures that ectopic or extrasynaptically located receptors alone cannot interfere much with synaptic function. It is speculated that extrasynaptic glutamate-receptors constitute a pool for newly synthesized proteins, which are incorporated later into the synaptic membrane by lateral membrane-diffusion (Ashby et al., 2006).

Glutamate-receptors are formed of tetrameric assemblies. For instance NMDA-receptors of the hippocampus are composed of two NR1 and two NR2 (NMDA-receptor 1 and 2) subunits (Furukawa et al., 2005), the latter being either NR2A or NR2B. NR2 subunits differ with respect to their developmental regulation and kinetic properties. NR2B-containing receptors, which are preferentially expressed at earlier developmental stages, have slower gating kinetics, thereby allowing for longer-lasting Ca^{2+}-currents. The glutamate-binding site is located on the NR2 subunits. For NMDA-receptor activation, binding of the co-modulator glycine is also required and its binding site is on the NR1 subunit.

The C-terminal domain of the NMDA-receptor subunit contains binding sites for Ca^{2+}/calmodulin-dependent protein kinase II (CaMKII) and for proteins possessing PDZ-domains, such as the PSD-93, PSD-95 (postsynaptic density proteins 93 and 95), SAP-97 and SAP-102 (synapse-associated proteins 97 and 102)(reviewed by Kim & Sheng, 2004). In case of the AMPA-receptors the so-called TARPs (transmembrane AMPA-receptor regulating proteins) control the

channel conductivity by bridging the AMPA-receptors and PDZ-domain proteins. The stargazin (TARP γ2) is a classical example of these molecules (Chen et al., 2000). The stargazin receives its name after a mouse mutant with cerebellar deficits (a "stargazer" phenotype), due to the markedly reduced expression of stargazin on cerebellar granule cells of the mutant mouse (Hashimoto et al., 1999).

An immense diversity of glutamate receptor subunits is provided by alternative splicing and RNA-editing (Higuchi et al., 1993). The editing sites in the RNA are located in the region of the 2nd intramembrane helix, corresponding to the so-called pore-loop (translated to protein-structure) of the AMPA-receptors. They have very important functional implications. The Q/R-editing site on the GluR-B is processed by one of the ADARs (adenosine deaminases acting on RNAs). If the editing is compromised with GluR-B-mutations, glutamin will be incorporated into the protein instead of arginin, which renders it Ca^{2+}-permeable. The increased Ca^{2+}-conductance on pyramidal cells leads to epileptic seizures and early animal death in a mouse model (Feldmeyer et al., 1999).

Figure 2.: Schematic view on the domain-structure of AMPA-receptor subunits. The N-terminal domain lies in the extracellular space while the C-terminal domain is intracellular. The second intra-membrane α-helix bends back towards the cytoplasm. The RNA-editing site also lies in that region.
The C-terminal domain comprises binding sites for the PDZ-domain protein PICK1 (Protein Interacting with C Kinase 1, involved in receptor-clustering of the AMPA-receptors, Xia et al., 1999) and NSF (N-ethylmaleimide-sensitive fusion protein, involved in membrane fusion events and also in disassembling the AMPA-receptors from PICK1, Hanley et al., 2002). The structure of NMDA-receptor subunits is basically similar to this principle. The picture is from www.bris.ac.uk, the official website of Bristol University.
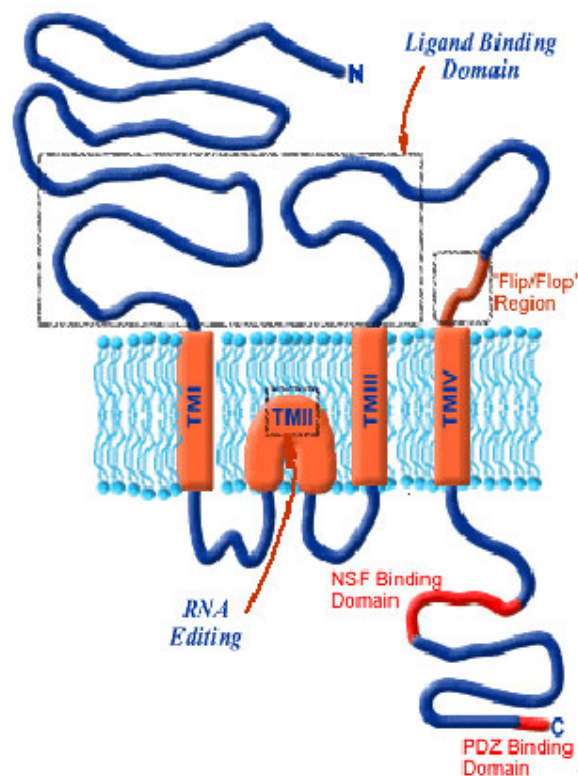
I have not commented on the role of metabotropic glutamate-receptors, they are 7TM-proteins and activate G-proteins upon ligand binding. They are often found on the perisynaptic regions as well, and are consequently activated by higher concentration glutamate-spillover (Somogyi et al., 1998).

Principles of inhibitory neurotransmission

In addition to excitatory synapses there are also inhibitory ones in the nervous system. The former are also referred to as asymmetric, the latter symmetric. These differences rely on electronmicroscopical studies of Gray and the classification of Colonniel, who described a more electrondense material on the postsynaptic side of excitatory synapses whereas on inhibitory synapses this density is more or less symmetrical (Kandel et al., 2000). In addition, granules of excitatory transmitters are mainly big and of round shape while those of inhibitory synapses are smaller and rather ovoid (Uchizono, 1965). Whereas excitatory synapses are formed mainly on dendrites and dendritic spines, inhibitory synapses are usually found on dendritic shafts and on perisomatic regions, such as the soma itself or the axon-hillock. The strategical importance of this arrangement lies in the electrotonic attenuation of postsynaptic potentials and their spatiotemporal summation on distinct parts of the cell (Fonyó, 1997; Kandel et al., 2000).

The two main inhibitory neurotransmitters of the central nervous system are GABA (gamma-amino-butyric acid) and glycine. However, the latter is confined mostly to the brainstem and the spinal chord. Both the ionotropic glycine- and GABA-receptors belong to the acetylcholine-receptor family, a major hallmark of which is the pentameric structure composed of different subunits. The ionotropic GABA-receptors (or $GABA_A$-receptors) are anion-channels, they transport Cl^- and HCO_3^- anions. From the well-known anxiolytics the benzodiazepines and the zolpidem act on $GABA_A$-receptors* (Fürst, 1998). However, different brain regions and different cell types express different receptor-subunits and different cellular domains can also show a different expression-pattern (Mody & Pearce, 2004). This can explain why many of these compounds influence the involved target-mechanisms to a different extent, such as anxiolytic, sedatohypnotic or muscle-relaxant effects and side effects can be of different strength. Nevertheless, these drugs also affect learning.

*Barbiturates also act on $GABA_A$-receptors, but they have a different binding site. Whereas benzodiazepins increase the frequency of channel-opening upon their binding, the barbiturates keep the channels open for a longer time. The most commonly used $GABA_A$-receptor antagonists in electrophysiology are the gabazine, bicuculline and picrotoxin.

GABA as well as glutamate also acts on metabotropic receptors, which are coupled to the function of G-proteins. These receptors are 7TM-receptors. The $GABA_B$–receptors are found mainly presynaptically (Somogyi et al., 1998), very often on the periphery of the synapses. Their effect evolves slower, because of the delay of the intracellular cascades that are activated by the 7TM-receptors. In many cases, the $GABA_B$–receptors can decrease the transmitter-release from the presynaptic active zones (reviewed by Freund & Katona, 2007).

GABA is produced from glutamate via the action of GAD (glutamate decarboxylase) enzymes. Cells take up glutamate with excitatory amino acid transporter (EAAT) molecules, which are also expressed by glial cells. The secreted GABA is bound to the GABA-receptors and after dissociating from the receptor GABA is removed from the synaptic cleft by transporter mechanisms (Kandel et al., 2000). The kinetics of $GABA_A$-receptors is also faster than that of most glutamate receptors. The fast GABA-removal via its re-uptake mechanism and the channel-kinetics in the synaptic cleft are responsible for the phasic component of GABAergic inhibition whereas the tonic inhibition is accounted for extrasynaptic $GABA_A$-receptors, which also have a different subunit-composition (Mody & Pearce, 2004).

Physiology of interneurons

From a general point of view interneurons fulfill a role in the activity-control of local neural circuits. This view is reflected by the name "local circuit neuron". The effect they exert on the innervated cells is mainly inhibitory. This stands in contrast with the principal cells, which are mainly excitatory and are often called projection neurons, for projecting to different or distant brain structures or circuits. However, there are exceptions on both sides. In certain cases GABAergic interneurons can also provide distant projections, such as in case of the interneurons of the septal nuclei (Amaral & Witter, 1995) or Purkinje-cells, the former projecting to the hippocampus, the latter to the cerebellar nuclei. Long-range inhibitory connections constitute an important organizing principle between distinct parts of the basal ganglia as well. Another example is given by the reticular thalamic nuclei, which provide GABAergic innervation for other thalamic nuclei. Excitatory cells can also be local-circuit neurons. The so-called "mossy cells" of dentate gyrus are glutamatergic, but they innervate neighbouring granule cells that they receive input from (Amaral & Witter, 1995).

Inhibition in the cortex is mainly provided by GABA. However, the effect of GABA can also be excitatory. The excitatory action of GABA is very prominent in development when it can also contribute to the plastic formation of microcircuits and can shape early network-patterns (reviewed by Ben-Ari et al., 2007). The effects of GABA are mediated by ligand-gated ion-channels, which are permeable to Cl^-- and HCO_3^--anions. The direction of the current is determined by the membrane potential and the equilibrium potential of the given ions. In certain cases cells have higher internal Cl^--concentrations and according to the Nernst-equation it leads to a smaller (less negative) Cl^--equilibrium potential. When this equilibrium potential exceeds the actual membrane potential, the GABA-current can change its direction and instead of being an inward

negative current, it represents an outward negative current. This can lead to depolarization of the cells (Cohen et al., 2002; Stein & Nicoll, 2003), in certain cases in the form of shunting-inhibition (Vida et al., 2005), in other cases might also induce action-potentials (Szabadics et al., 2005). The cellular Cl^--concentration is regulated by two transporters: the KCC2 (K^+-Cl^-cotransporter 2) and NKCC1 (Na^+-K^+-Cl^- cotransporter 1) channels. The latter imports Na^+, K^+ and 2 Cl^- ions into the cell whereas the former extrudes Cl^- anions coupled to K^+-export (Delpire, 2000). The expression of these molecules is developmentally regulated and this can account for the higher internal Cl^--concentrations during development and early postnatal periods when in many cases GABA is excitatory. Rodent infants are especially prone to seizures, which may reflect the immature inhibitory system in their brain at that age. Another phenomenon, which is generally associated with the switch of Cl^--gradient is the giant depolarizing potential (GDP, reviewed by Ben-Ari et al., 2007). It occurs in cortical areas of newborn or infant mammals but disappears later. However, according to Imre Vida and Marlene Bartos, a large proportion of hippocampal pyramidal cells might also exhibit the same properties as neurons early in development (Vida et al., 2005). In that situation GABA has a shunting-inhibitory effect. In other words it depolarizes the cell to some extent but then it fixes the membrane potential close to the Cl^--equilibrium potential, thereby also inhibiting action potential generation. These effects may have important implications in the generation of oscillations where they might contribute to the precise timing of cell-discharge in large cell-populations.

Interneurons in general fire at a higher rate than principal cells. In case of basket interneurons or axo-axonic cells, the innervation they provide is also more efficient than that of provided by principal neurons that generally innervate distal dendritic domains. The higher discharge-frequency of basket cells is brought about by several mechanisms of which the expression of fast repolarizing potassium-channels such as Kv3.1 or Kv3.4 is of utmost importance (Baranauskas et al., 2003). By their fast action, the depolarization-block of Na^+-channels is relieved very rapidly on the interneurons.

Putative roles of interneurons

As we have seen, interneurons not only can inhibit other cells but in some instances can also excite them. Inhibition is a powerful tool to overcome deleterious effects of spreading excitation (in case of epileptic seizures for example). The principles of "synfire-chains" proposed by Abeles and Aertsen (Gewaltig et al., 2001) describe network-activities lacking a substantial inhibition. In this case, which resembles epileptic seizures, the excitation can propagate and activate an ever-growing cell-population and can only be stopped by the "exhausted" or "pseudo-refractory" state of the

system, determined primarily by neurotransmitter-release and properties of ion-channels (e.g. desensitization kinetics). Interneurons can circumvent these problems purely by their inhibitory action. Interneurons can also have a contrasting effect (collateral inhibition) that makes the output of principal neurons more specific to certain stimuli and thus also minimizes the energy-cost of information-processing. Phasic inhibition imposed on principal-cell-bodies enhances synchrony between distinct cells. In certain ways interneurons can have a role in the generation of gamma- and ripple-oscillations by their rhythmic inhibitory effect that also relieves the depolarization block from the Na^+-channels (Klausberger et al., 2004). As a consequence, a large number of principal cells (and also interneurons) can be available for excitation and fire together. This happens for instance in the hippocampal CA1-region in slow-wave sleep (SWS) when ripples (oscillations in the frequency range between 130 and 250 Hz) occur.

Plasticity at synaptic and network level

Plastic changes belong to the most important ones in our brain-operations and without them we could hardly imagine our daily life. Electrophysiologists often relate certain *in vitro* and *in vivo* paradigms with plasticity. In general, we call synaptic plasticity any change in the efficacy of synaptic transmission. These synaptic changes can affect the release-probability of the presynaptic terminal, the number of released transmitter-molecules, the currents evoked on the postsynaptic side and also the structure of the synapses (Kandel et al., 2000). Plasticity can occur on shorter and longer time-scales at excitatory and inhibitory synapses leading either to an augmentation (potentiation) or a depression of synaptic transmission. The terms "paired-pulse facilitation" or "paired-pulse depression" denote short-term plasticity. Very often the kinetics of vesicular release explain this kind of plasticity. Upon an action potential synaptic vesicles are mobilized and get close to the release sites. When a new action-potential is generated, more or fewer vesicles are available for release, depending on the distance between the release site and the vesicles. Another aspect of short-term plasticity is the polyamine-dependent facilitation that is a postsynaptic mechanism. Certain polyamine molecules, such as spermin, spermidin or putrescin block the internal side of certain AMPA-receptors lacking GluR-B. Upon prolonged depolarization the polyamines exit the channels, thereby allowing a larger pool of channels to conduct ions. This effect is often accompanied by changes of the I-V (current-voltage) curve of the given channels, being inwardly-rectifying in the beginning, and double-rectifying after this form of plasticity takes place (Rozov et al., 1998). Not only interneurons can have this form of plastic change, but also pyramidal

cells, especially when they do not express GluR-B in a sufficient amount (Burnashev, 2003) and this effect can contribute to epileptogenesis.

Long-term potentiation (LTP, originally described by Bliss & Lømo, 1973) requires alterations on either the pre- and/or postsynaptic side of the synapses. Postsynaptic LTP involves the incorporation of different sets of ion-channels on the synaptic membrane for instance or the synthesis of new proteins as well as induction and repression of genes. These different steps are also reflected by the staging of LTP: LTP1 is linked to posttranslational protein-modifications, LTP2 is reflected in changes in protein synthesis without changes at mRNA-levels whereas LTP3 depends on gene-expression alterations (reviewed by Bliss & Collingridge, 1993; Reymann & Frey, 2007). The Ca^{2+}-current of NMDA-receptors is thought to be a key mediator in LTP-induction, however, the activation of Ca^{2+}-permeable AMPA-receptors can also lead to LTP under physiological (Lamsa et al., 2007) as well as pathological conditions (Feldmeyer et al., 1999).

Protocols, most commonly used in slice-preparations to evoke LTP are pairing, tetanic stimulation (Bliss & Lømo, 1973) or high-frequency stimulation (HFS) and theta-burst stimulation (TBS, Larson et al., 1986). As we will see later, the pairing protocol "associates" the activation of presynaptic inputs with the postsynaptic activity of the cell, so it relies on the concept of spike-time-dependent plasticity*.

*When action potentials are generated in neurons, the potential changes propagate back into their dendritic tree. As a consequence, Ca^{2+}-channels open and increase Ca^{2+}-levels in distant dendritic domains. Thus, a well-timed input on a given synapse can gain efficiency and be strengthened (Markram et al., 1997).

HFS also resembles physiological network-processes, such as ripples when cells can fire with a high frequency for a short time-period while TBS consists of a high-frequency input wrapped in 5 Hz clusters (a good example is described by Raymond & Redman, 2006). Since pyramidal cells of the hippocampus tend to discharge during explorative behaviour (ongoing theta-rhythm in the hippocampus in the frequency-range of 4-8 Hz) and place cells often fire in bursts, we can see this protocol as a real counterpart of an *in vivo* situation which potentiates synaptic in- and outputs of place cells or other types of output neurons. Experiments show that the longer a given pyramidal cell is silent, the higher the probability that it will respond with burst firing to a sufficient excitatory input (Harris et al., 2001). The underlying mechanism is probably related to the de-inactivation kinetics of Na^+-channels responsible for action potentials. Interestingly, pyramidal neurons are the most "bursty" not exactly in their place field-centre, but in places where the average spiking-or-bursting-frequency is around 6-7 Hz, a frequency like that of theta-rhythm. In certain cases, this characteristic can make place fields sharper. Overall, it is proposed that single spikes can also gate the efficiency of burst-spikes on dendritic domains, thereby contributing to the dimensions of

plasticity (Harris et al., 2001). Remarkably, LTP can also be induced *in vivo* by certain learning paradigms, like inhibitory avoidance (Whitlock et al., 2006). The resulting increase in field potentials showed resistence to further high-frequency stimulation (LTP-occlusion), suggesting that the electrophysiological basis of learning correlates with changes induced with LTP-paradigms. The hippocampus has an extensive monoaminergic innervation and it is indeed thought that these monoamines play a role in learning. The performance of animals in learning paradigms can be enhanced by a modest stress, such as swim-stress (reviewed by Reymann & Frey, 2007). This observation is also underlined by the fact that ripples show alterations after administration of certain serotonergic (5-HT$_{1A}$ and 5-HT$_3$ receptors) and histaminergic (H$_1$ and H$_2$ receptors) antagonists (Ponomarenko et al., 2003a). Low-frequency stimulation usually leads to depression of synapses.

These processes are extremely important with respect to brain oscillations since rhythmic in- and output during oscillations can underlie synaptic modifications and in turn, these synaptic changes can then alter local or global features of oscillations. Cells firing together within a short time-window determined by an oscillatory cycle can potentiate their connections easier as reflected by the concept of "cell-assemblies". Another eloquent example is constituted by the "spindle bursts", high-amplitude synchronous events of 10-11 Hz, recorded from somatosensory cortices of newborn rat pups. These network patterns are brought about by limb-movements and are supposed to shape the sensory map of their body at that age (Khazipov et al., 2004).

Brain oscillations in general

Network synchrony has been a focus of research in neuroscience for almost hundred years now. Even though basic principles of synchrony and the underlying circuitry have been described, there are still many debates regarding mechanisms and physiological roles of oscillations. The main oscillation-types that can be recorded from the skull surface are usually in the slower frequency-ranges of delta (0.5-4 Hz), theta (4-8 Hz), alpha (8-13 Hz) and beta (13-30 Hz). This is because the slower an oscillation is, the bigger the entrained cell-population and thus one can record these massive effects even from the skull where the signals are heavily attenuated. In other words, the relation between oscillation-frequency and oscillatory power can be described by a power-law (logarithmic relation, Buzsáki & Draguhn, 2004). For the long-range synchrony pacemakers and long-range connections between distant cortical domains are also required in addition to the numerous short-range connections. Theoretical estimations and anatomical measurements suggest, however, that even a small percentage (0.5 %) of connections when long-range can fulfill this function (Buzsáki, 2006). However, they need to be at critical places. For example the thalamic

inputs coming from nonspecific thalamic nuclei (such as the reticular thalamus) provide a major contribution to the generations of delta- and alpha-rhythms, and sleep-spindles as well (both thalamocortical and corticothalamic projections are needed in this process, reviewed by Steriade, 1999). These nuclei are also responsible for generation of cortical UP- and DOWN-states that constitute an ongoing switch between a depolarized and hyperpolarized state of the cellular membrane potential, inflicted by the thalamic pacemakers. One might speculate that for faster rhythms short-range synchrony can be of bigger importance. That is indeed the case but not in an exclusive sense. CA1-ripples for instance, even though being very fast emerge synchronously in the two hemispheres even if they do not show cycle-by cycle coherence (Chrobak et al., 1996). In this case commissural projections between the two hippocampi take part in their synchronization.
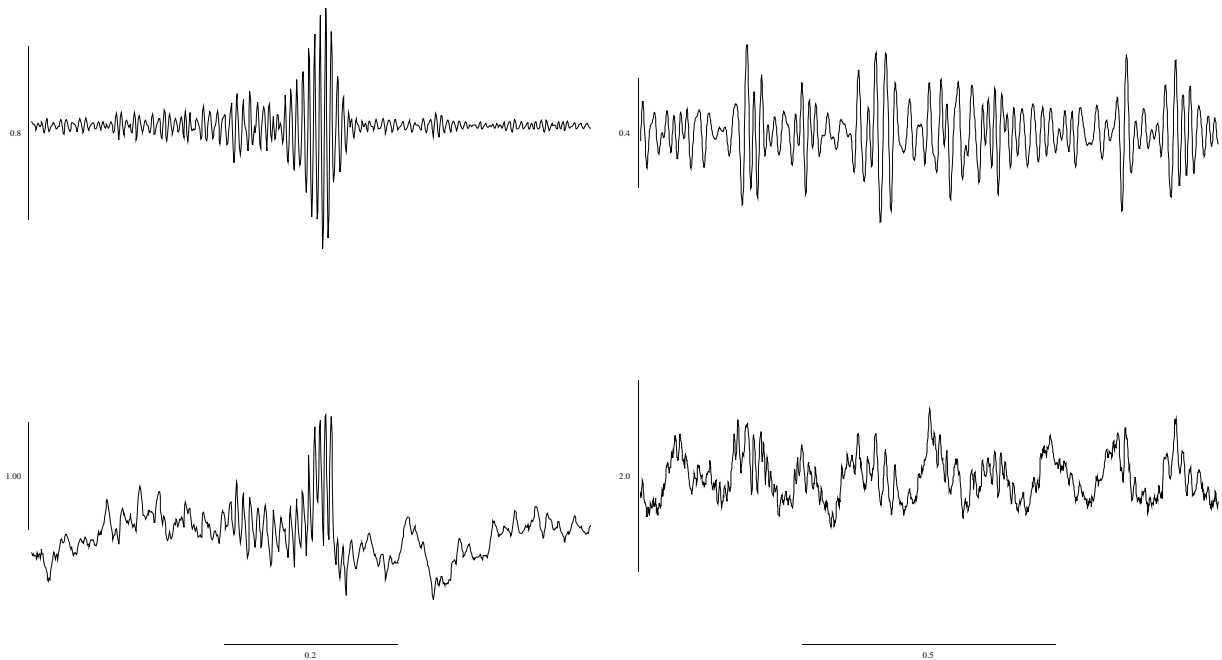
Oscillations of the hippocampus

The hippocampus shows a wide array of oscillatory patterns in the characteristic frequency bands of theta- (4-12 Hz), gamma- (30-85 Hz) and ripple-range (130-250 Hz). These oscillations are spatiotemporal summations of electric currents of orchestrated cell-populations. The laminar organization of the hippocampus is quite suitable for recording purposes because of the high cell-density of the pyramidal-layer resulting in a high density of transmembrane currents. We have to keep in mind that cellular synchrony determines the extracellular rhythms, and what we simply call electroencephalogram (EEG) or local field potential (LFP) is generally a shadow of intracellular events and action potentials.

Ripple-oscillations (*figure 3.*) are characteristic for the CA1-region and even though *in vitro* also CA3 can generate them, CA3-ripples cannot be accounted for as traditional ripples, their frequency *in vivo* also being slightly smaller than those of CA1 (Csicsvári et al., 1999a). Distinct oscillations are characteristic of certain behavioural states, ripples are brought about during slow-wave sleep (SWS), waking immobility, consummatory and grooming behaviour whereas theta-rhythm nested with gamma (*figure 3.*) usually occurs during exploratory behaviour and REM-sleep (rapid eye movement sleep or paradoxical sleep, described by Jouvet; Buzsáki, 2006). The structure of the theta-related EEG also shows species-specific differences. For example theta of the human REM-sleep is rather "fragmented" (Buzsáki, 2006) and also reflects evolutionarily conserved navigation strategies, such as that of bats, in which theta is "packed" synchronously with ultrasound-emission used for echolocation (Ulanovsky & Moss, 2007).

Regarding the theta-rhythm we can claim that its generation is not specific and restricted to the hippocampus and that probably many oscillators interact while bringing it about, involving also the septal nuclei with its cholinergic and GABAergic projections to the hippocampus. Also

GABAergic back-projections from the hippocampus to the septum play a role. Based on pharmacological and behavioural correlates, theta activity is often dissected into type I and type II theta. Both types occur during locomotion, but only type II that is atropin-sensitive can be recorded under urethane-anaesthesia when theta is usually evoked by sensory-stimulations, such as a tail-pinch (Yoder & Pang, 2005). As determined form partial coherence analysis, even the hippocampal formation contains two theta-generators, one of them mediated by the entorhinal inputs via the perforant path terminating in the stratum lacunosum-moleculare, the other by the CA3-Schaffer-collaterals, innervating dendritic domains of the stratum oriens and radiatum (Kocsis et al., 1999).

Figure 3.: Examples of hippocampal oscillations. On the left side a ripple is shown (lower trace is raw signal, upper trace after filtering between 130 and 250 Hz). On the right side a very short segment recorded during REM-sleep is shown, with characteristic theta- and gamma-oscillations (lower trace is the raw signal, the upper one is the filtered signal between 30 and 85 Hz). The time bar for ripples is 0.2 s, for gamma 0.5 second. Note that the amplitude of these events in the mouse hippocampus is in the mV-range.

The gamma-rhythm is not specific for the hippocampus but can also occur in distinct neocortical domains. The most well known examples are the visual and the auditory cortices where the incoming input promotes network oscillations (Gray & Singer, 1989). In their classical experiment these scientists recorded from the visual cortex of anaesthetised cats with extracellular electrodes while they projected moving bars onto the retina of the animals. They found that at certain recording locations the power of gamma showed a tuning-curve depending on the direction of the bar or arrow they moved. Interestingly, but not surprisingly they also found that the cells

showed very similar tuning curves on that location and those cells which had the same directional preference showed a quite remarkable phase-locking to the ongoing gamma-rhythm. Gamma-synchrony in the visual cortex is not only promoted by sensori stimuli but is also influenced by stimulus-selection* (Fries et al., 2002), implying that perceptual differences can adjust the level of "synchrony" and can also gate sensori inputs.

*Stimulus-selection means a "decision" on which one of the stimuli projected onto the eyes separately would be the dominant one if there are contrast- or illumination-differences between them or if they are projected onto the retina of the dominant or subdominant eye.

The hippocampal gamma-rhythm in classical situations, such as locomotor behaviour and REM-sleep, is nested within theta-rhythm. In addition, given parameters, such as amplitude and frequency of the gamma are modulated by characteristics of theta, such as the phase of theta but also amplitude of the underlying slower rhythm (Bragin et al., 1995).

It is not entirely correct to speak about a given gamma-rhythm in the hippocampus. It seems that this structure has two gamma-generators, one of them being the DG (driven by the entorhinal cortex), the other the CA3-CA1 circuitry, and these two systems interact with each other (Csicsvári et al., 2003b). It is generally accepted that the UP and DOWN states of the neo- and paleocortical areas influence these generators. UP-states can drive a specific set of dentate granule cells, which can oscillate at gamma-frequency and can activate a selective set of pyramidal cells in the CA3 whereas most of the pyramidal cells are inhibited by interneurons. In this scenario the CA3-CA1 gamma- and ripple-generator would be suppressed whereas the generator in DG would be active. During a DOWN-state, however, the DG would not exert suppression on the CA3-CA1 axis, allowing the generation of CA3-CA1 gamma and ripples (Isomura et al., 2006). The suppressive effect of entorhinal inputs is corroborated by the fact that by dissecting entorhinal inputs, the gamma-power in the CA3-CA1 system shows a strong increase (Bragin et al., 1995). The function of CA3-pyramidal cells is of utmost importance in the gamma-synchrony of CA1 since by removing CA3-inputs to CA1, one can extinguish oscillations in the latter (Fisahn et al., 1998). It seems that both the recurrent excitatory loops within CA3, as well as the monosynaptic drive of CA3-pyramidal cells onto CA1-pyramids and CA1-interneurons contribute to synchronous network activities of CA1 (Csicsvári et al., 2003b). Since pyramidal cells show the tightest coupling to the gamma-rhythm recorded on the same electrode, it has been speculated that the local gamma-power is the reflection of EPSPs (excitatory postsynaptic potentials) and IPSPs (inhibitory postsynaptic potentials) in the neighbourhood of the recording site. That way, an analogy with the visual cortex can be drawn since the local gamma-power would be determined by the actual spatial input and the receptive field of the given cells of a particular location (Gray & Singer, 1989).

Ultrafast (above 100 Hz) synchrony resembling ripples can occur in the neocortex also normally but more often under pathological conditions. Epileptic activity is an extreme grade of ultrafast synchrony. However, ripples represent a physiological mechanism, thought to be important for memory-consolidation processes. It is estimated that roughly 10-15 % of all hippocampal neurons can be active during a given ripple, hence during a short time-window spanning no longer than 100 ms. This extreme temporal synchrony is supposed to bring together cells in the form of "cell-assemblies" that might be the primary storage-place for memory-traces. Ripples are not specific for the hippocampus but also occur in the amygdala (Ponomarenko et al., 2003b) and in certain output routes of the hippocampal formation, such as the subiculum and entorhinal cortex (Chrobak & Buzsáki, 1996) and unitary analysis confirms that ripples are indeed generated there. Ripples are thought to be dependent on the CA3 subregion and the Schaffer-collateral inputs and in slice-preparations spontaneously occurring ripples travel from CA3 towards CA1 (Maier et al., 2003). Interestingly, one can also induce ripples with LTP-protocols in slices, in which previously no ripples occurred spontaneously (Behrens et al., 2005). This observation would imply that ripple-generation relies on cell-assembly formation in the CA3-network. The CA3 region cannot be considered homogeneous regarding either its histology or its involvement in the generation of ripple oscillatory epochs. The CA3a and CA3b domains are characterized by extensive recurrent collaterals that can recruit subsequently more and more cells in the beginning of sharp waves whereas CA3c would rather be an "output-connector" towards CA1. Interestingly, at least 10 % of CA3 pyramids need to be recruited in a 100 ms window to have a considerable effect on CA1-synchrony in forms of ripples (Csicsvári et al., 2000). Remarkably, lower grade synchrony is associated with a smaller increase in firing rates of CA3-pyramids than of CA1-pyramids, but this relation is completely the opposite for higher-grade synchrony (synchrony meaning the number or percentage of cells firing in a short time-window), which probably also reflects the activity of recurrent loops. On the other hand, József Csicsvári and his colleagues made very interesting observations and distinctions based on the actual ripple-amplitude generated in CA1. They classified ripples into big (>7SD above threshold) and medium size (7SD>size>4SD above threshold) categories and they saw that high-amplitude ripples are more coherent across different recording sites of CA1 whereas smaller ripples are not so much. Besides, they found that the activity of given CA3 neurons could be predictive of the character of the upcoming CA1-ripple. This leads to the idea that ripples might reflect the coherent and synchronized activity of CA1- (and also CA3-) microdomains, CA1-neurons being strongly correlated with certain CA3-pyramids on one hand, on the other hand it suggests that ripples of different amplitude or morphology represent different activated cell-assemblies. Similarly to gamma, pyramidal cells show the strongest

coherence with "their local" ripples and show much weaker with distant ones whereas interneurons show a high coherence with distant locations as well, suggesting a more general role for them in the generation of gamma- and ripple-oscillations.

To nail it down to an anatomical scheme, the story begins in the CA3 where the recurrent loops gather more and more CA3-cells firing and bringing about a sharp-wave, which is equivalent to the excitatory input via the Schaffer-collaterals. In CA1 this input excites pyramidal cells and interneurons in parallel (feed-forward excitation and feed-forward inhibition). The inhibitory effect of the interneurons on the pyramidal cells then will be delayed by one synaptic delay with respect to the maximal excitation of pyramids. The CA1-pyramids also activate CA1-interneurons, which exert inhibition on them (feed-back inhibition). The interneurons hyperpolarize the cells, which ensures the relief from the Na^+-channel block and therefore pyramidal cells can fire synchronously again, activating again the interneurons that will inhibit them. The "energetic drive" is the CA3 and the ripple lasts until the underlying sharp wave lasts.

We know very little about the subcellular and molecular details of the generation of ripples and in many respects of gamma-rhythm. Besides chemical neurotransmission recent studies also suggest the involvement of gap junctions in this process (Draguhn et al., 1998; Traub & Bibbig, 2000; Whittington & Traub, 2003), even though the importance of "electrical synapses" in higher-order brain functions of phylogenetically more developed species has been underestimated for a long time. Gap junctions are molecular complexes that allow for an intercellular transport of molecules smaller than 2 kDa. The gap junctions are usually formed from two hemichannels, expressed on the neighbouring cells, these are called connexons, and each connexon is built up from six connexin molecules (Kandel et al., 2000). Since there are many types of connexins expressed in the brain, the subunit-composition of each connexon can vary to a great extent, this also leads to a great versatility of the conducted currents. There are connexins, for instance connexin36, which are expressed exclusively on neurons whereas others, for instance connexin43, are expressed both on neurons and glial cells. Pannexins are also supposed to form gap junctions (Bruzzone et al., 2003). As far as we know the mostly known pannexins: pannexin1 and pannexin2 are specific neither for pyramidal cells nor for interneurons, but can be expressed in both neuronal populations (Vogt et al., 2005). Connexin36, however, seems to be more specific for interneurons (Hormuzdi et al., 2001). Certain connexins, such as connexin36 are located mainly on dendrites whereas pannexins are supposed to be mostly located on axons. It seems that both axonal (Schmitz et al., 1996) and dendritic gap junctions can facilitate the rhythmogenesis in the gamma- and ripple-frequency range since action potentials or postsynaptic potentials can propagate between cells practically without any synaptic delay. Slices from the hippocampus of connexin36 knockout mice displayed reduced

gamma-oscillations *in vitro* (Hormuzdi et al., 2001) and certain alterations in ripples as well (Maier et al., 2002). The connexin36-deficient mutant mouse also showed diminished gamma-power during exploratory behaviour (Buhl et al., 2003).

Based on the findings of Dietmar Schmitz it was speculated that the average number of gap junctions that an axon forms with other axons is actually very low, 1 or 2. However, as also modeling studies (Traub & Bibbig, 2000) show, even that number can make ripple-oscillations very robust since the excitatory output of the network would not depend so much on the individual excitation of pyramidal cells. Roger Traub and his colleagues developed an interesting multicompartmental model composed of both principal cells and interneurons in which in addition to chemical synapses axo-axonal gap junctions are also present between principal cell axons. Based on their computation, axons can "fire" with a very high frequency, even if the cell somata cannot follow this high frequency. The major requirements for this are a critical density of axo-axonal coupling (the before mentioned 1-2, on average 1.6 per axon), a sufficient conductance of the gap junction channels (so that the action potential can jump quickly from one axon to the other or at least can induce spikelets) and some ongoing firing of certain pyramidal cells, which becomes more robust upon dendritic depolarization occurring in the form of sharp waves. Their prediction is that the frequency of the evolving "rippling" is higher when either the conductance of a single gap junction is increased or the density of the gap junctions on an axon is increased. However, by increasing the strength of inhibition, the oscillation-frequency approaches the gamma-range, so it slows down. The weaker inhibition also favours the antidromic propagation of action potentials whereas stronger inhibition and lower frequency is favourable for orthodromic spike-propagation. Even though the principle of axo-axonal coupling is thoroughly discussed nowadays (however, with a lot of debate), it raises certain problems regarding the specificity of output processing since principal cells are considered the output neurons of our brain.

Another remarkable feature of the gap junctions is that they connect almost exclusively neurons of the same type, either principal cells or different subclasses of interneurons (Blatow et al., 2003). This might indicate a developmental role for gap junctions as well, expressed already at earlier stages of the ontogenesis in precursors of specific neuronal subclasses.

Even though gap junctions might have a role in the generation of gamma- and ripple-rhythms, inhibitory neurotransmission is indeed involved in oscillogenesis. One can record very small amplitude intracellular membrane potential-fluctuations in synchrony with ripples and the polarity of these oscillations reverses around the Cl$^-$-equilibrium potential, indicating that GABAergic transmission is most probably involved in their generation (Ylinen et al., 1995). Besides, ripples show changes after the application of different GABAergic agonists and

antagonists, such as benzodiazepines, zolpidem and flumazenil (Ponomarenko et al., 2004). These and other experiments (Penttonen et al., 1998) also suggest that IPSPs and also EPSPs on both pyramidal neurons and interneurons contribute to the extracellular LFP-oscillations, be they ripples or gamma-oscillations.

Network synchrony in vitro

Many of the mentioned rhythms also exist in brain slices, suggesting that the mechanisms bringing them about rely on smaller circuitries. Spontaneously occurring ripples can easily be recorded from CA3 and CA1 in slice-preparations (Draguhn et al., 1998), but they can also be induced by electrical stimulation. The application of the GABAergic blocker gabazin actually facilitates the ultrafast oscillations, even if not in the form of sharp wave-ripples (SPW-ripples, Maier et al., 2003) which often leads to the hypothesis that GABAergic transmission is not necessary for the generation of high-frequency oscillations. Besides, since these oscillations are sensitive to the gap-junction-blockers octanol and carbenoxolon, it has been hypothesized that axo-axonal gap junctions may contribute to their generation (Draguhn et al., 1998; Maier et al., 2003). On the other hand, the slicing procedure can destroy longer axons which might also be coupled via gap junctions. One might thus underestimate their importance in network synchrony or depending on the orientation of slices one might get different results.

Gamma-oscillations can also be induced by tetanic stimulation or pharmacologically in hippocampal (Fisahn et al., 1998; Bartos et al., 2007), entorhinal (Cunningham et al., 2003) and auditory cortical slices (Cunningham et al., 2004; Traub et al., 2005). The most commonly used drugs in these protocols are kainate, domoate and the cholinergic agonist carbachol. However, one must be aware that the mechanisms underlying the rhythms in these *in vitro* models do not necessarily match each other or either the real *in vivo* situation. Carbachol for instance activates metabotropic cholinergic-receptors on pyramidal cells first and interneurons are activated secondarily via the principal cells. This type of oscillation is both sensitive to the AMPA-receptor blocker NBQX and the GABA$_A$-blocker bicuculline (Fisahn et al., 1998). However, when the network is activated via kainate-receptors, pyramidal cells and interneurons are activated simultaneously and since kainate can provide sufficient excitation, it is not sensitive to NBQX (Bartos et al., 2007). Furthermore, mechanisms can be different in hippocampal subregions. Last, but not least, gamma-oscillations in slice-preparations occur in absence of theta-rhythm, which is normally not the case *in vivo*.

Interestingly, interneurons can also synchronize when glutamatergic neurotransmission is blocked in the network, indicating that via GABAergic inhibition they can pace each other (Traub et al., 1998). However, since GABA might also have a shunting inhibitory effect and gap junctions may also contribute to synchrony, we cannot clearly attribute a major role to phasic inhibition in this process.

Slower oscillations can also be induced pharmacologically, in neocortical preparations for instance where the application of carbachol evokes synchronized intracellular membrane potential-oscillations in mutually coupled interneurons (multipolar bursting cells) in the theta-frequency-range (Blatow et al., 2003).

However, not only electrophysiological paradigms can be helpful in understanding the principles of network synchrony. A newly developed method, the two-photon microscopy offers an excellent opportunity to investigate synchrony in smaller local circuits using optic principles. The application of Ca^{2+}-sensitive dyes allows for pursuing the activity-state of a given neuron while the use of a shorter wavelength irradiating laser source enhances the penetration depth of the light beam, thus expanding the histological volume one can examine (Denk & Svoboda, 1997). One can then correlate the state of neighbouring neurons with a relatively good time-resolution, in the range of tens of milliseconds.

Multi-electrode arrays (MEAs) can also be used to record from several sites of an *in vitro* preparation (Mann et al., 2005). The application of voltage-sensitive dyes can also inform us about the coherent activity of bigger cell-populations, their depolarized and hyperpolarized states. However, their use is limited due to the toxicity of the dyes.

Brain synchrony in vivo

Neuronal synchrony *in vivo* can be measured with a wide array of methods. The EEG can be recorded either on the skull or from the brain *in situ* using implantable electrodes or grid-electrodes which are usually applied to the cortical surface. In certain pathological conditions, such as pharmacologically untreatable epilepsy, intracerebral recordings can help localize the seizure-center and can lead to a full recovery of the patient after the operation. We have to be aware that with skull-EEG one obtains only attenuated signals that are furthermore restricted to a lower frequency-range due to the bone capacitance. Besides, signals are usually summations of a larger brain surface, which can lead to imprecision. The magnetoencephalography (MEG) uses the principle that alternating currents (such as our neural postsynaptic and action potentials) generate magnetic fields which can be recorded with loop-like devices. Since for the recording an optimal orientation of the

magnetic field is required, the MEG is usually more straightforward in following the activity of brain sulci and fissures than that of planar cortical regions (Buzsáki, 2006).

Implantable electrodes are of wide use in neurophysiology of animals, especially in rodents but also in monkeys. In general, one uses extracellular electrodes, such as single-wires or stereotrodes, the latter being better in unitary recordings since they enhance the efficiency of unit-separation. The most commonly used is the tetrode. Tetrodes consist of four very thin metal wires that are twisted around each other. The thickness of one such wire is precisely in the range of cellular size. Thus, the distinct channels will give an excellent spatial resolution since action potentials recorded on different channels will be of different amplitude due to the very steep decay of the recorded action potential with distance (McNaughton et al., 1983; Buzsáki, 2004). Indeed, tetrodes were first applied to reconstruct spatial arrangement of closely spaced cells. The "extracellular" action potential is not simply a mirror image of the intracellular one but can be approximated with the first derivative of it in time. With the help of tetrodes one can relate LFP-oscillations with single cell data. Silicon probes also show the stereotrode principle, however, their major aim is different. Their big advantage is that one can record from many histological layers simultaneously (Csicsvári et al., 2003) and thereby reconstruct current-source density (CSD) profiles to reveal what kind of currents underlie the rhythms and to determine in which layers they are generated (Mitzdorf, 1985). This computation can be complicated since the relation between intracellular currents and their extracellular "reflections" are quite complex. In case of an action potential the cell gets temporarily positive relative to its resting potential, due to the cation-influx. Since these charges stem from the extracellular space, their close environment gets temporarily negative, that is why we normally see action potentials as negative deflections on extracellular recordings. However, LFP-oscillations are not only a summation of action potentials of the neighbouring neurons, but postsynaptic potentials of large neuronal populations most probably have an even larger contribution. When a cellular domain gets depolarized, the extracellular space around shows negativity. However, on other parts of the cell positive charge will be released to compensate for the depolarization, that is why the extracellular space surrounding those cellular domains will become slightly positive. If we record from different histological layers simultaneously, we normally find these sink-source pairs. In this case there will be an active sink and a passive source representing a so-called return current. This can also be the opposite, in case of inhibitory neurotransmission. To find out, which is the active and passive current of the sink-source pair, one usually needs unitary analysis as well.

The optical methods used in *in vivo* functional imaging have a much lower spatial and temporal resolution than electrophysiological methods. Nevertheless, they can provide useful

information on the function of distant brain regions in different cognitive tasks. Functional magnetic resonance imaging (fMRI) and the resultant blood oxygen level dependent (BOLD) signal relies on the principle that the blood supply of active brain regions increases (Kandel et al., 2000; Buzsáki, 2006). Due to the delay of intracellular cascades involved in blood-vessel regulation, the temporal resolution of this method is in the range of seconds.

Interneurons in oscillations and plasticity

Certain interneurons are active at distinct behavioural states and distinct phases of oscillations (*Table 1.*). One of the most synchronous oscillatory events of the brain is the previously described "SPW-ripple" complex. Axo-axonic cells are active usually in the very beginning of the ripples and they seem to be silent afterwards (Klausberger et al., 2003). Both PV-positive basket cells and bistratified cells increase their firing during ripples (Klausberger et al., 2004), but CCK-positive interneurons (CCK-cells) do not change their activity (Klausberger et al., 2005) whereas O-LM cells are silent during these events. Interneurons are also active at distinct phases of the theta-cycle (*Table 1.*), thereby leading to the assumption that CCK-cells might be important in the phase-precession of pyramidal cells for instance and that O-LM cells might be important in theta-generation. The methodology used in the Somogyi-lab allows for a good *post hoc* identification of the recorded cell-type but urethane-anaesthesia used in their experiments is a certain limitation. Tetrode-recordings from freely behaving animals allows for the distinction between pyramidal cells and interneurons, but the identification of interneuron-subtypes can be more problematic. Studies from the Buzsáki-lab confirm that interneurons also tend to fire on the ascending phase of ripple-waves (whereas pyramidal cells in the troughs) and generally on the descending slopes of theta-waves (Buzsáki et al., 2003 for mice; Csicsvári et al., 1999b for rats), as we see for PV-positive basket cells in anaesthetized rats.

Cell type	*Theta-phase*	*Ripples*
Basket cell	Descending (PV), or ascending (CCK)	Increases, ascending phase (PV), does not change (CCK)
Chandelier (axo-axonic) cell	Peak	In the beginning
Bistratified cell	Trough	Increases, ascending phase
O-LM cell	Trough	Silent

Table 1.: Interneurons functioning in distinct ways during different oscillations. Table is based mainly on data obtained in the Somogyi-lab.

Very important distinctions between interneurons can be made according to biochemical markers that they express. The PV-positive basket cells also express certain K$^+$-channels (Kv3.1

and Kv3.4) that ensure their fast repolarization after action potential generation (Baranauskas et al., 2003). These K⁺-channels also ensure that they can fire with a high frequency, in slice-preparations up to 100 Hz. CCK-cells on the other hand can follow a frequency only up to about 40 Hz (reviewed by Freund, 2003). Glutamate receptor expression on interneurons is also different: PV-positive basket cells express kainate- and AMPA-receptors at a great density, but only very small amount of NMDA-receptors whereas CCK-cells have a much higher density of NMDA-receptors on their surface. Therefore, PV-cells might be more static actors whilst CCK-cells more plastic. CCK-cells also express CB1 (cannabinoid) receptors, to whom an important role in DSI (depolarization-induced suppression of inhibition) has been attributed. When a pyramidal cell is active and emits "bursts" (let us imagine a place cell at a given location during active exploratory behaviour), cannabinoids are synthesized in the pyramidal cell and diffuse to the inhibiting basket cells. Since CCK-cells express cannabinoid receptors, they can sense the endocannabinoid. This leads to a decreased GABA-release from their synaptic terminal (Klausberger et al., 2004). Therefore the given pyramid is not inhibited so much and it can emit spikes even with a smaller degree of excitation. So it can slide downwards on the slope of the theta-wave, and thus accounts for phase-precession. Not surprisingly, the consumption of marihuana leads to learning- and memory-deficits. Application of cannabinoid agonists *in vivo* resulted in decreased LFP-power especially in the ripple-frequency range, which was not associated with any change in the discharge-rates of neurons. However, the coordination in cell-assemblies and the spiking-regularity was influenced by the drugs explaining the oscillatory-findings and also the learning-deficits (Robbe et al., 2006). GABA$_A$-receptor subtypes are also differentially expressed
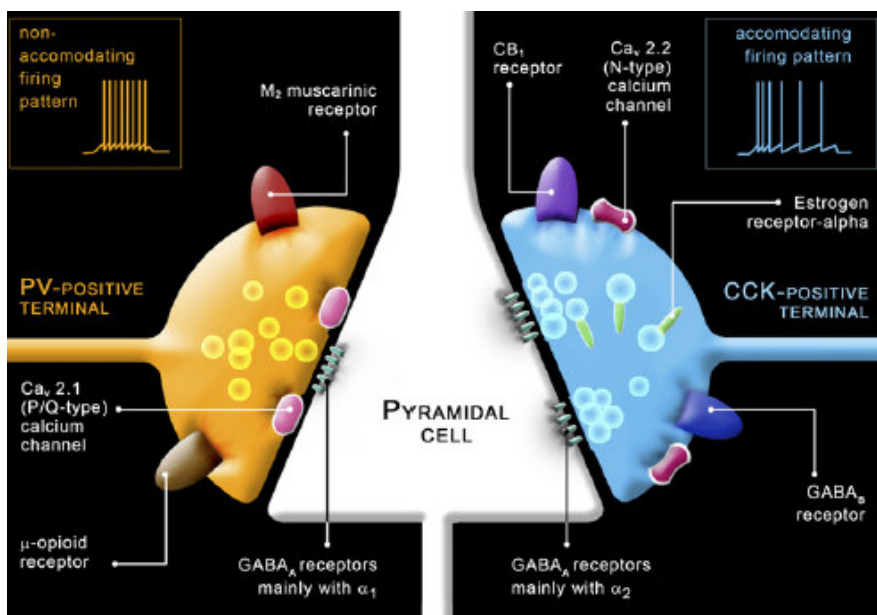

Figure 4.: Distinct basket cell populations may perform distinct functions. CCK-cells and PV-cells express different receptors on their synaptic terminals and their electro-physiological properties are different as well. Picture comes from Freund & Katona, 2007, Neuron, artwork was done by Gábor Nyíri.

on the synapses formed by the diverse basket cell-population: PV-cells having mainly α1, CCK-cells α2 on their postsynaptic targets. It is important to note that α2 subtypes of GABA$_A$-receptors are responsible for the anxiolytic effect of benzodiazepins (reviewed by Freund, 2003).

I mentioned the absence of plasticity in interneurons that do not or only weakly express NMDA-receptors. Certain LTP paradigms almost exclusively point to the importance of NMDA-receptors in the induction of Hebbian LTP (which means that pairing stimulation of a given pathway with the depolarization of the postsynaptic cell leads to strengthening of the "targeted" synapses). This can be more or less true for CCK-cells since they express NMDA-receptors in a good quantity which conduct Ca^{2+}-ions at a relatively positive membrane potential. However, in case of oriens or alveus-associated interneurons that only have Ca^{2+}-permeable AMPA-receptors activated at a more negative voltage, LTP is anti-Hebbian, meaning that pairing of hyperpolarization with the stimulation of a given pathway leads to synaptic strengthening (Lamsa et al., 2007). This holds true for PV-cells as well, due to their low-level NMDA-receptor expression.

There are also other differences between PV- and CCK-cells that suggest a more plastic role of the latter type in network phenomena. Ca^{2+}-channels on the presynaptic terminals of PV-cells are of the P/Q-family, with a strong coupling between these channels and the Ca^{2+}-sensor required for vesicular GABA-release. This kind of mechanism usually excludes short-term facilitating effects on these synapses. In contrast, CCK-cells express N-type Ca^{2+}-channels on their presynaptic boutons. These channels are located further away from the sensor, thereby allowing facilitation to occur on those GABAergic synapses that are formed by CCK-cells (reviewed by Freund & Katona, 2007). CCK-cells are also modulated by a number of modulatory afferents, such as serotonin (5HT). Besides, GABA$_B$-receptors expressed on their axon-terminals extrasynaptically can inhibit GABA-release in an autocrine manner. These observations attribute a more rigid role to PV-cells in network synchrony whereas the CCK-cells would have a more delicate, tuning role, which requires certain plastic capabilities of course.

Proposed functions of the hippocampus

We have seen the anatomical architecture and histological constitution of the hippocampus and have hints, how these can serve electrophysiological phenomena, such as oscillations or plasticity. Now we have to see, what cognitive tasks this structure performs and if there is any correlation between network synchrony and cognitive behaviour. The hippocampus has been implicated in many cognitive functions and depending on the animal species the hippocampus might perform different sets of "intellectual" tasks. The importance of the hippocampus in learning

was first supposed in the mid of the 20th century when clinical and neurosurgical cases proved that without an intact temporal lobe, learning of new information is impossible. A patient often referred to (H.M.) suffered a complete loss of the capability of acquiring new information after a surgical bilateral lesion of his temporal lobes, even though his memories from his life before the operation were more or less preserved (Scoville & Milner, 1957)*. Another important cause for hippocampal destruction can be a herpes-encephalitis, which destroys the temporal structures with a great propensity, or the Wernicke-Korsakow-syndrome, a dietary B1-vitamin deficiency. The latter, however, is not specific for the hippocampus but rather to its fornical and mammillary projections. The recurrent wiring of the hippocampus (especially that of CA3) via its activity-related energy consumption also makes it quite vulnerable to hypoxia. Probably it is also related to the hippocampal wiring that the seizure threshold for this brain area is low and epilepsy eventually leads to neurodegeneration. The pathological changes of Alzheimer Disease in its classical form are first seen in the temporal lobe and also hippocampus (for a complete view on the pathology of hippocampus see Szirmai, 2005). All the named diseases perturb learning-mechanisms and memory. An interesting aspect of H.M.'s postoperative deficits reflects a contextual retrieval problem. The patient remembered persons he had just met before, as long as these persons were in the same context, for instance the same room. When they moved to a new room he could not recognize the same persons any more.

*However, other symptoms caused by the loss of the temporal lobes might not be directly related to the hippocampus proper. The Klüver-Bucy-syndrome for instance, which is characterized in monkeys, is due to the loss of the corpus amygdaloideum. Since the amygdala is involved in fear conditioning, the animals usually exhibit a loss of fear even towards noxious or dangerous factors, such as snakes. In addition, they become hypersexual and develop oral tendencies.

The classical idea is that the hippocampus would be a temporary storage place of newly acquired information and thereby the residing place of memory traces shortly after their acquisition. According to this view, the information would be "written out" from the hippocampus to neocortical areas during SWS (Buzsáki, 1989; Buzsáki, et al., 1994). This memory-consolidation process would require the strengthening of synapses between hippocampal output neurons and their targets. Ripples represent a highly synchronized hippocampal activity and it is supposed that they have an important role in the consolidation process. Besides, pyramidal cells often fire with a high frequency during ripples, which is quite suitable for modifying neocortical synapses (just as an *in vivo* LTP-protocol). It was shown that performance in certain cognitive tasks increases after sleep, and the performance correlates well with the time spent in SWS (Buzsáki, 2006). However, ripples can also occur in awake immobile periods and sometimes also during exploratory behaviour (O'Neill et al., 2006). The role of these ripples (with theta-rhythm interspersed SPW-ripple

complexes) would be to provide a better update of the recently learned environment and to cope with the huge place-related information coming in during exploration. During REM-sleep, the period when normally dreams occur, most of the potentiated cells also show a reactivation (it can be considered a replay-mechanism). Since inhibition is somewhat looser during sleep than during wakefulness, some previously not perfectly potentiated output neurons can also be activated. This effect might be responsible for the somewhat confounding and very often quite creative character of our dreams*.

*As we shall later see, memories are often thought to be stored in the coherent activity of cell-assemblies, via their well-correlated activity. As Freud points out in many of his clinical cases ("Dora: An analysis of a case of hysteria" or "Little Hans"), subjects or locations in dreams are mainly transferred to other subjects or places (which could coalesce with a slightly perturbed assembly-coordination). On the other hand he implies that in many cases the logical relations between subjects are preserved, sometimes are turned to opposite and mimic that of the original persons and objects. Thus, it might be that more stable connections between cell-assemblies would be representing logical operations.

According to evolutionary psychiatrists, dreams could also have an adaptive role during phylogenesis by providing subjects with "novel ideas" during their everyday struggle for potential resources (Stevens & Price, 1996). An alternative proposal relies on the analysis of the most frequent dream contents. The fulfillment of basic instincts in many dreams (sexual contents), the quite frequent archetypal contents (such as proposed by Jung) and behavioural patterns often performed when arousal happens in the middle of a dream ("flight and fight" for instance) imply that genetic determinants can be involved in the programming of dream contents. These programs could have a role in "pretraining" subjects in infancy or childhood for dangers lurking around them in prehistoric times (actually a similar thing happens in the well-known movie "Matrix"). However, evolutionary studies also suggest that REM-sleep has something to do with the economy of brain in terms of memory storage. Certain egg-laying mammals, representing a very early stage in the mammalian development do not have REM-sleep at all, on the other hand they have a huge neocortex compared to their overall body-size. It may well be that sleeping also has a role in removing unnecessary memory-traces, and keeping only the really necessary ones, thereby minimizing the spatial requirements for memory storage (for more details see Stevens & Price, 1996).

However, certain theories imply that the hippocampus is also involved in memory retrieval. According to these ideas the two hippocampi would not be equal but one of them rather specialized for memory acquisition and the other to memory retrieval. In this case the latter would function as a "librarian", who, according to the "memory-indexing hypothesis" would provide access to the information stored in the neocortex (Lytton & Lipton, 1999).

An interesting theory proposes that the information can be stored in the form of cell-assemblies, like small engrams and with time these engrams would be transported along the temporoseptal axis of the hippocampus. According to this model the oldest information would be stored around the temporal pole of hippocampus whereas newer engrams would be located closer to the septal pole (temporoseptal engram shift model, Lytton & Lipton, 1999). However, a theory like this might be difficult to reconcile with the stability of place fields observed in rodents and with the memory-indexing hypotheses since it would require a day-to-day update and continuous change in the indexing synapses' strength. However, certain imaging studies seem to support this idea in human subjects. Since the rodent and human hippocampus is of different size and the proposed size of engram-modules is roughly the same, the information would need more time to travel along the human hippocampus than it would need in rodents.

In rodents, however, the hippocampus performs navigational tasks as well. As an animal explores and learns a new environment, it uses certain navigation strategies. The intellectually most demanding is called taxon navigation that uses allocentric (meaning external) cues, usually distal landmarks for its spatial navigation (for example trees, hills, the sun, rivers, etc.). A major hallmark of this strategy is a multimodal perceptual integration of all incoming environmental information. Indeed, the hippocampal formation receives extensive innervation from brain regions involved in visual and olfactory processing. As an animal is getting acquainted to an environment, it develops alternative strategies to navigate in it. First, it might memorize turning or intersection points of the maze, just as we learn to find our goals using streets of a town. This form of orientation is called praxic navigation and is usually related to the striatum. In the next step of abstraction the animal plans its trajectory based on earlier experience just by knowing its initial location, the goal location, its speed and the direction of its own movement. This type of navigation, also referred to as path integration, does not require external cues, but egocentric (or idiothetic) ones. Different brain regions might be involved in this form of orientation, supposedly mainly the entorhinal cortex. In the next part we shall discuss the different cell types involved in the navigation (for a more complete view an spatial navigation see Redish, 1999; on path integration see McNaughton et al., 2006). A navigation strategy for a given environment does not exclude others, the animal might switch back to the hippocampal one when its striatum is compromised in its function, as was shown by experiments in which lidocain-injections were administered (reviewed by Redish, 1999).

Distinct subregions of the hippocampus might perform different tasks in orientation and spatial navigation. Nakazawa et al. (2002) showed that a CA3 region-specific NMDA-receptor knockout mouse is impaired in a pattern completion task (after an already learned environment is represented with certain external cues, some of them are removed and then an experimental subject

has to recognize the same environment based on the remaining cues). According to their hypothesis, this would be accomplished by the autoassociator CA3-loops, which can "fill in" the missing gaps with the help of their recurrent connections (reviewed by Nakazawa et al., 2004). The CA3 also seems to be important for the acquisition of one-time experience (Nakazawa et al., 2003). Another phenomenon, the pattern separation (discrimination between superficially similar but basically different environmental arrangements) would be performed by the dentate gyrus (McHugh et al., 2007).

Cells specialized for navigation

In the seventies an interesting observation was made by O'Keefe and Dostrovsky. They found that the activity of a great percentage of hippocampal pyramidal cells is bound to the location of a rat in a given recording environment (O'Keefe & Dostrovsky, 1971). They christened them place cells since they were only active when the rat was at a given location and remained silent in other places (*figure 5.*). In parallel, other cells were described in certain thalamic nuclei, in the mammillary nucleus and in the retrosplenial cortices that fired only when the animal's head faced a certain direction. These cells were named head-direction cells (Ranck, 1984). Both the animal's position and the head-direction that usually indicates the direction of motion contain indispensable information for path integration.
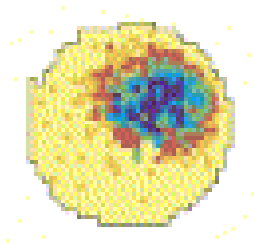
Figure 5.: Place cells are usually represented by firing rate maps. A typical CA1 place cell (picture is from Kentros et al., 2004, Neuron) has a single receptive field where its firing is maximal (peak frequency, indicated with dark blue) while its activity sharply decreases with increasing distance from the centre. Different species have different place field sizes.

Place cells can be found in the CA3 and CA1 areas as well. However, their characteristics are somewhat different. One should note that place fields are context-dependent. They display a given field in a specific environment but they can fire in a different place in a contextually different one. Besides, the animal's near past and future can also influence their activity. This is called retrospective and prospective coding (Wood et al., 2000). Place fields might be bidirectional or unidirectional (normally it is only visible on tracks where the animal can explore a given location only from two directions and cannot make "junction crossings" such as in open fields or more realistic environments). What makes place cells interesting with respect to oscillations is their phase-precession. This means that while the animal approaches and traverses the receptive field of a given cell, the cell emits spikes on earlier and earlier phases of subsequent theta-cycles. This

phenomenon is often explained by the interaction of two oscillators, a somatic and a dendritic one, the former representing perisomatic inhibition and the latter dendritic excitation upon environmental exploration. The dendritic excitation depends on the animal's spatial position. Since the extracellular local field would be generally composed of the interference of the "two theta-oscillations" but the action potential emission is rather determined by the excitation strength which invades the soma upon dendritic depolarization, the spikes come earlier and earlier, as the drive is getting stronger (Harris et al., 2002). As the animal traverses many place fields while moving in the environment, several place cells are activated in a sequence. As the animal reaches the center of one place field, cells which predict the animal's future location are already activated but the neurons representing the present and near past locations are still active, although on different phases of the theta-rhythm. Given the principle of phase-precession, there would be many cells firing in one theta-cycle, in different phases of the ongoing theta-rhythm. Thus, both the animal's past, present and future is represented this way in a compressed time-scale and to pack this spatial information in cell ensembles the theta-clockwork seems to be a prerequisite (Buzsáki, 2006).

There are several models describing the coordination of neurons in this cell-assembly. The pacemaker-model suggests that the cellular activity would solely be determined by an external pacemaker representing environmental input. However, the cell-assembly model proposes that there is also an internal coordination between members of the cell-assembly in the hippocampus itself (Dragoi et al., 2006). According to the cell-assembly model the precision of information processing would be enhanced, since the firing-order of pyramidal cells would also be determined by the synaptic interactions between assembly members. Taken together, it appears that space-representation involves distinct computational strategies within the same system: spatial location is represented by the phase of the theta-cycle when a given place cell discharges (temporal- or phase-code), by the spike frequency generated by a cell (frequency-code) as the animal gets closer to the center of the place field and by the combination of active cells at a given time thus denoting a cell-assembly (population code).

Place fields are not rock-solid entities, they can change in a dynamic way. The stability of place fields is strongly influenced by the attention level of the animal when it learns its environment. For example, the performance of an intellectually demanding task in a maze leads to more stable place fields (Kentros et al., 2004). In an interesting experiment Dragoi and his colleagues used LTP-protocols on the Schaffer-collateral inputs to modulate place cell activity of an already learned environment. This way they found certain changes and rearrangements of place fields, which in many cases turned out to be reversible (Dragoi et al., 2003). As also these

electrophysiological insights suggest, NMDA-receptors play a role in place encoding. Indeed, mice with a CA1-specific NR1-deletion display smeared hippocampal place fields (McHugh et al., 1996). As mentioned earlier, animals may recognize the same environment even after slight changes. This is generally reflected by the behaviour of place cells that fire in similar locations although small alterations are carried out in the environment. However, the firing frequency of pyramidal cells might change, this is called partial or rate remapping. When the environment is changed to a different one, cells do not preserve their original place field but fire on distinct locations and with distinct characteristics. In this case also the spatial interrelation between distinct place fields is lost compared to the original environment. This is called global remapping, which implies a contextual shift regarding the animal's place-representation. These phenomena can be investigated with so-called "morphed environments", which involve gradual alterations on the maze the animal learns (Leutgeb et al., 2005).

Place cells are not only active during exploration but in sleep they show "reactivation". As we have seen for the cell-assemblies during theta-rhythm, it has been proposed that the sequential order of reactivated cells firing inside ripples during SWS reflects the order of activation during the exploration (Buzsáki, 1994). However, when reactivation occurs in ripples of waking immobile periods, the reactivation order is just the opposite of the "place-acquisition-order" (Foster and Wilson, 2006). It is thought that this "reverse replay" would enhance the efficiency of reward-related learning. Since normally an animal has to reach its target-location first to get a reward, the reverse-order would ensure the activation of cells related to reward (maybe somehow connected to dopamine-release) already in the beginning of an oscillatory epoch and thus it would "mark" (so to say enhance the potentiation on) the whole sequence of the activated place cells.

Sometimes one can find cells with more complex properties in the parahippocampal structures, such as the pre- and parasubicular cortices. These include the TPD-cells (theta-modulated place-by-direction cells, Cacucci et al., 2004). The activity of these neurons is not just simply a function of the animal's location but also shows a dependence on their head-direction. Interestingly, in remapping experiments the two modalities were independent of each other since place-related activity showed global remapping while the directional preference of these cells remained constantly the same.

A recent discovery suggests that place-related activity is not unique for pyramidal cells but can be found for interneurons as well (Ego-Stengel & Wilson, 2006; Maurer et al., 2007). It has been proposed that those interneurons can inherit activity-patterns from the innervating pyramidal cells but the function of this phenomenon is still unknown. In many cases interneurons show phase-advancement, meaning that they are activated at later and later phases of subsequent theta-cycles.

This phenomenon is explained by the differential kinetics of excitatory and inhibitory drive that interneurons receive, which can be different from that of pyramidal cells.

In 2005 an interesting cell type was found in the entorhinal cortex, a structure that provides a substantial input to the hippocampus. These cells discharge when the animal is located in the vertices of a hexagonal spatial matrix and are called grid cells (Hafting et al., 2005). The geometry of this system can be described with three major parameters; the grid spacing (the distance of vertices from each other), the phase of the grid (describing the orientation of the matrix or the axes of the lattice) and the gridness score (describing how well a given cell can be fitted with grid-like properties). Interestingly, grid cells recorded from the same location show very similar features (*figure 6.*) and there is a correlation between anatomical position in the dorsomedial entorhinal cortex and the grid spacing for instance. In one report the grid spacing was also correlated with intrinsic cellular properties, such as resonance-frequency in the theta-range (Giocomo et al., 2007), implying a relation with oscillations. The formation of grid-structure is dependent on distal cues and landmarks but it persists without them (for example in darkness). By rotating cue-cards in the environment the grids move together with them, suggesting a remapping-phenomenon.

Figure 6.: Grid cells from the entorhinal cortex, picture from Hafting et al., 2005, Nature.
On the upper part one can see firing rate-maps and grid centers of three grid cells. In the lower row spatial cross-correlograms for pairs of three distinct grid cells recorded on the same tetrode are seen. The orientation and spacing of the grids are quite similar to each other, as shown by the cross-correlograms and grid centres can be superimposed on each other by a simple translocation.
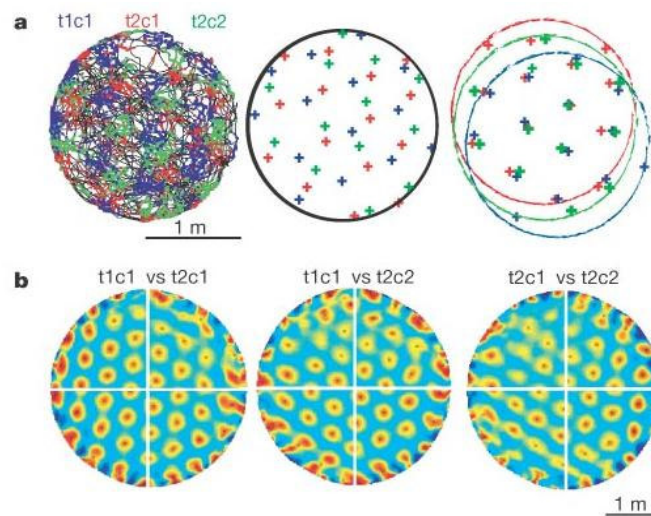
The entorhinal cortex also possesses head-direction cells and cells that comprise both grid-like- and head-direction-properties. These cells are the so-called conjunctive cells. Interestingly, when researchers rotate the cue-configuration in the animal's environment, grid cells and head-direction cells rotate their tuning-curves to the same degree, suggesting that they are involved in the same sort of place-representation (this behaviour is different from that of the TPD-cells where after remapping directional tuning remains the same even with a different place-preference). The activity of the conjunctive cells is modulated by the speed of the animal. Altogether these facts suggest that

the entorhinal cortex could be sufficient for the generation of path integration (Sargolini et al., 2006). Thus, the entorhinal cortex would provide a spatial metric system for navigation while the role of the hippocampus would be to integrate multimodal information from the environment. Which mechanism is the primary one, needs to be verified.

The importance of PV-positive interneurons and their involvement in learning

In the previous parts I summarized current knowledge on hippocampal oscillations and explained with a few examples how these oscillations can be related to plasticity and to the roles the hippocampus performs in behaviour. But is there anything known regarding the link between hippocampal interneurons specifically and behaviour?

PV-positive interneurons (PV-cells) comprise roughly 25 % of the hippocampal interneuron population, this number and their diversity (both axo-axonic, bistratified and a great percentage of basket cells belong to them, and many O-LM cells also express PV weakly, Klausberger et al., 2003) also suggest an important role for hippocampal physiology. Indeed, malfunction of PV-cells may be involved in the pathogenesis of human psychiatric disorders, such as schizophrenia (Zhang & Reynolds, 2002). Basket cells are responsible for perisomatic inhibition and together with the axo-axonic cells their basic presumed function would be the output-control of principal cells. However, axo-axonic cells might not exclusively be inhibitory, but in many instances they are excitatory. PV-cells have an exquisitely high density of excitatory terminals on their dendritic tree compared to other interneuron types (Gulyás et al., 1999, see also *figure 7.*), which suggests a very reliable coupling to synchronous excitatory events.

We have seen that PV-cells are coupled to ongoing oscillatory rhythms, both to theta and to ripples, but different PV-positive subpopulations might be involved in different ways in these processes. Axo-axonic cells are active just in the beginning of ripples and stay silent afterwards whilst PV-positive basket cells increase their activity throughout ripple activity, just as bistratified cells do. PV-cells express NMDA-receptors at low levels, therefore they are considered less plastic than CCK-cells (Freund, 2003).

In our laboratory Elke Fuchs generated transgenic mice that express Cre-recombinase in PV-cells. By crossing these mice with floxed GluR-A mice (Zamanillo et al., 1999) she obtained offsprings in which PV-cells lose their GluR-A-expression (PV-GluR-A KO mice). She also generated and analyzed GluR-D knockout (GluR-D KO) mice, with the advantage that normally GluR-D-expression is almost restricted to PV-cells. *In vitro* electrophysiological insight into these
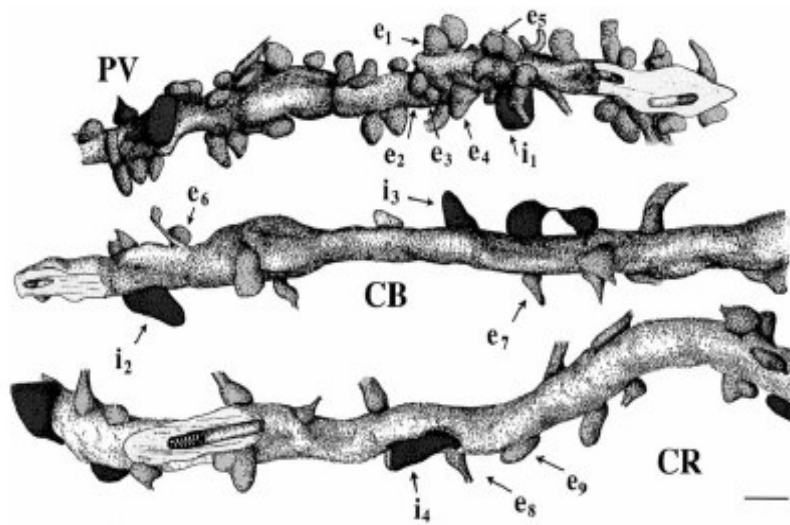
Figure 7.: PV-positive cells receive a robust excitatory innervation on their dendrites compared to CB- and CR-positive cells (electronmicroscopic studies by Gulyás et al., 1999).

mice revealed that they have smaller AMPA-currents on their PV-cells than normal mice have and pharmacologically induced gamma-oscillations were decreased in their power in both mouse mutants (Fuchs et al., 2007). She also analyzed the animals in learning-paradigms, in spatial working memory (T-maze), reference-memory (Y-maze and hidden platform Morris water-maze) tests and novel object recognition*. Interestingly, the animals underperformed in spatial working memory (*figure 8.B*) and novel object exploration but were practically normal in reference memory (*figure 8.A*), indicating a defect in the early phases of memory-acquistion.

*In the T-maze an animal initially finds a food pellet in a given arm of the maze. In the next run the food pellet is placed in the other arm and the animal has to remember for a short time that it already consumed the food in the first arm. Therefore in an optimal case he will turn to the actual, food-storing arm. In the Y-maze the animal always finds the food pellet in a given location but its initial location is kept flexible. So this test is designed for spatial navigation and long-term memory functions. In the novel object exploration test the animal explores distinct objects placed in a cage for a certain time, and the time it spends with each object is measured in a session. Subsequently one object is displaced by a new one and the time spent with the two objects is measured again. In a normal situation the animals prefer exploring the new object.

These data underline the possible involvement of PV-cells in learning processes and their involvement to alterations in network synchrony.

Figure 8.: Both the general GluR-D KO and the PV-cell specific GluR-A KO mice display normal spatial reference memory (A), but have deficits in spatial working memory (B). In the reference memory-test one can see the gradual increase in performance from 50 % (chance-level) towards higher values. Thus, with time even these mutant animals can learn to navigate in that environment. The test for working memory shows that the mutants perform significantly worse than WT mice (B). The figure is from Fuchs et al., 2007, Neuron.
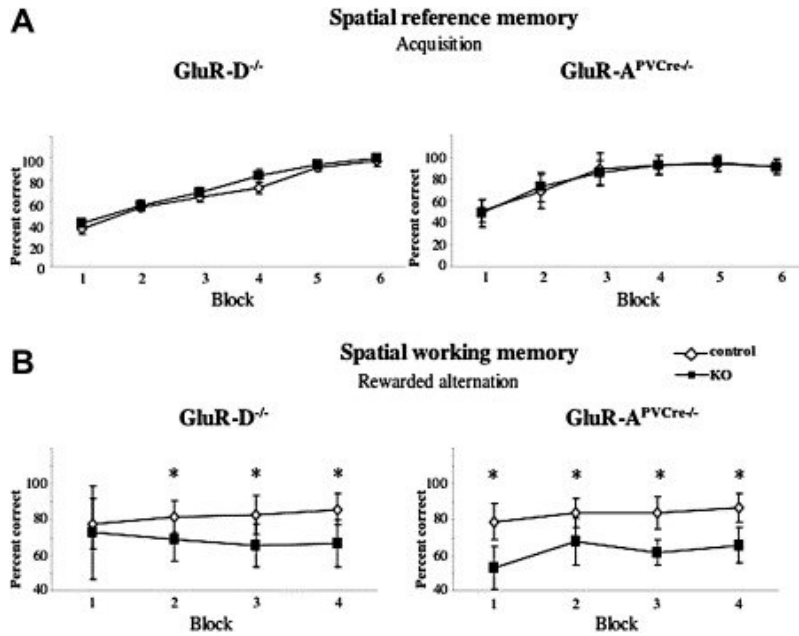
THE MAIN SCIENTIFIC QUESTIONS OF THIS STUDY

Brain oscillations are supposed to provide a temporal frame for information processing and many cognitive functions, as suggested by a wide literature (Gray & Singer, 1989; Buzsáki et al., 1994; Buzsáki, 2006). However, so far this assumption turned out to be difficult to prove experimentally due to the lack of appropriate model systems.

In vitro electrophysiological and behavioural studies (Fuchs et al., 2007) carried out in our lab showed that the mice in which GluR-A has been knocked out specifically in PV-positive interneurons (later on referred to as PV-GluR-A KO mice) exhibit a complex phenotype, involving perturbed network synchrony and deficits in hippocampus-specific behavioural and learning paradigms (*see the respective part of the Introduction*). Based on these findings and the literature, we wanted to investigate, whether certain aspects of synchronous network activities and various forms of cognitive behaviour can be correlated with each other.

In my experiments the main goals and questions were the following:

I. What kind of changes if any do different hippocampal oscillations show in the PV-GluR-A KO mice *in vivo*? Given the proposed roles of PV-positive cells in gamma- and ripple-rhythms, we hypothesized that gamma- and ripple-oscillations show alterations *in vivo*. In other words, what is the function of PV-positive interneurons (mainly PV-positive basket cells) in the generation of hippocampal gamma- and ripple-oscillations?

II. What features can we extract from unitary analysis in the mutant animals? How do these alterations on a cellular level (pyramidal cells and interneurons) translate into modifications on a multicellular network level? To answer this, we analyzed unitary activity in wildtype (WT) and PV-GluR-A KO mice and tried to correlate unitary results with oscillations.

III. Can we draw any correlation between network synchrony (in the form of oscillations and unitary activity) and the behavioural deficits in these animals?

To address these questions we applied *in vivo* electrophysiological measurements in freely moving and behaving mice using three types of electrodes: single tungsten wire-arrays, tetrodes and silicon probes.

MATERIALS AND METHODS

Animals

In this study we used fourteen mice, seven WT (mostly floxed GluR-A mice), and seven KO (floxed GluR-A animals with Cre-expression under the PV-promoter). The PV-GluR-A KO mice were generated by Elke Fuchs based on the floxed GluR-A mice (Zamanillo et al., 1999), which were crossed with the PV-Cre mice (Fuchs et al., 2007). The floxed GluR-A, PV-Cre or complete WT littermates served as negative controls in our experiments (*Table 2*).

Wildtype mice	PV-GluR-A KO mice
M60 (floxed GluR-A)	M187
M210 (3 tetrodes)(WT)	M209
M221 (floxed GluR-A)	M220
M1096 (PV-Cre)	*M486 (7 tetrodes)*
M1097 (floxed GluR-A)	M1086
M671 (floxed GluR-A)	**M672**
M701 (WT)	**M700**

Table 2.: The animals used in this study, numbers mean identification numbers in the Central Animal Facility of the Heidelberg University. In case of the pairs 209-210, 220-221, 1086-1097 (together with 1096), 671-672 and 700-701 WT controls were littermates of the KO mice, in case of the remaining animals this was not so. Animals implanted with silicon probes are marked with bold signals and gray shading.

Eight mice were implanted with single tungsten wire-array electrodes (tungsten wires of 45 µm, obtained from California Fine Wires Company), two with tetrodes (a WT with 3 and a KO with 7 tetrodes) and four with silicon probes (*Table 2*). The age of the animals on the day of the surgery was between three and four months on average (101±33 days for WT and 94±27 days for KO, means and standard deviations). The average weight of the mice was in the range of 25-30 gramms, they were provided with food and water *ad libitum*.

Electrodes

The electrode drives were prepared manually from prefabricated elements. They consisted of movable pieces (their number ranging from 3 to 7 for tetrodes or just 1 in case of wire-arrays or

silicon probes), which could be advanced or retracted with a screwdriver. The connection board and the PIN-connector were fixed with a small and thin metal framework on the drives. The electrodes were guided by silica-tubes with 75 μm internal and 150 μm of external diameter (from Polymicro LLC, www.polymicro.com), they were fixed in the tubes with glue and protruded from them 3-4 millimeters. Tetrodes were prepared from polyimide-coated platinum-iridium wires 12 μm in diameter, obtained from the Kantal Palm Coast company. Since the impedance of the tetrodes was above 1 MΩ, we had to decrease the capacitance of their tip by using a gold-chloride ($AuCl_3$) solution (SIGMA, 200 mg/dl). After plating their impedance was around 250-400 kΩ. The connection between the tetrode-channels and the connection-board was established with a silverprint (Auromal 38, AMI DODUCO GmbH). The respective channels of the board and the PIN-connector were soldered together with an aluminium-based soldering pen.
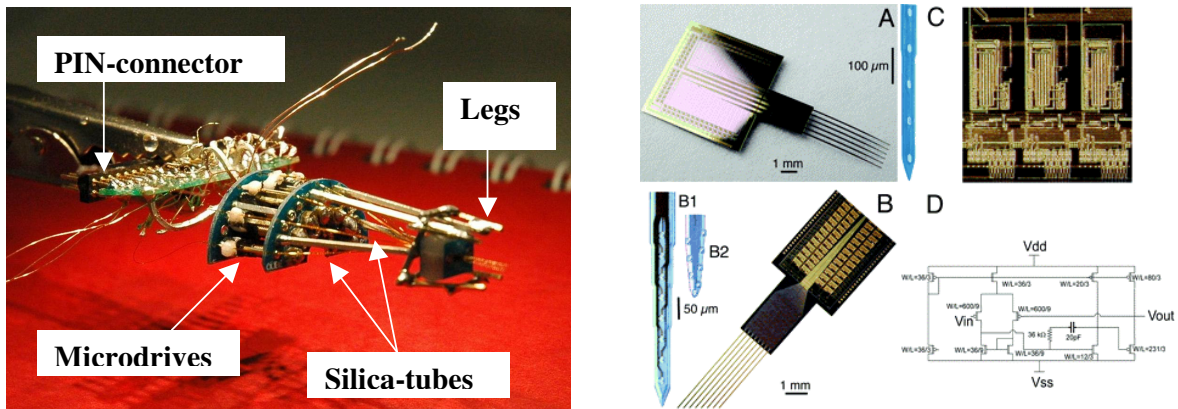
Figure 9.: Two special electrode-types used in this study. On the left side a tetrode-drive is shown. One can see the seven microdrives that can be moved independently from each other and the very thin tetrodes protruding from the silica-tubes. The small "legs" at the very right of the picture are used for the fixation on the animal's skull. On the right side a characteristic design of silicon probes is shown (picture from Csicsvári et al., 2003a, Journal of Neurophysiology). A: global view of a probe, B: the connector side, B1-B2: shanks magnified with the arrangement of recording sites, C-D: connection schemes of preamplifier modules used with silicon probes.

Silicon probes have been purchased from a company (ACREO). In these experiments 8-shank, 64-site probes were used, comprising 8 recording sites on each shank, their vertical spacing being 50 μm. The distance of the shanks from each other was 60 μm, thereby creating an 8 times 8 rectangular matrix spanning more than 400 μm of the hippocampus in lateral direction, and allowing for recording from both the stratum oriens, stratum pyramidale and stratum radiatum simultaneously. To protect the drives and to provide a good electromagnetic "shielding" we applied an aluminium foil-based coverage to the drives, which we hardened with epoxy-glue (R&G GmbH,

www.r-g.de). The shielding was also grounded. The recording sites of the probes were connected with two flexible circuits comprising 32 channels to a small board, which ensured a proper contact between the probe itself and the preamplifiers. We used 32-channel preamplifiers with an input-resistance of 10 MΩ to minimize the signal amplitude-decrease resulting from the use of high-impedance electrodes, such as silicon probes. These preamplifiers were ordered from the Brain Technology Team (www.braintelemeter.atw.hu, Pécs, Hungary).

Surgery

Animal handling, anaesthesia and surgery were carried out in accordance with the German Laws for Animal Care and Animal Wellfare. For operation narcosis we used volatile isoflurane anaesthetic. The mice were preanaesthetised in a chamber in a way that they were dizzy enough to endure the fixation on the stereotaxic frame meanwhile they also inhalated the gas (1 liter of atmospheric pressure air/minute supplied with required amount of isoflurane, around 4-5 % for anaesthesia-induction and later on around 1 % for the maintenance of the narcosis), which provided a smooth continuum for the deeper anaesthesia stages. The very fast equilibrium between brain tissue, blood and inhalation mixture allowed for an excellent control over the depth of narcosis. The depth of anaesthesia during the operation was controlled frequently by the hindpaw-reflex and cornea-reflex. No incision took place until these reflexes disappeared. During the operation the eyes were covered with a polycarbohydrate-based gel (Vidisin Optic from Dr. Mann Pharma) and the thermal stability of the mice was ensured by a heating pad. The very top of the mouse head was shaven, the skin above the skull after desinfection was incised and the skull surface was disclosed. For the later fixation of the electrode head-set and for grounding and referenceing purposes stainless steel screws were also implanted, two above the prefrontal cortical region and two above the two cerebellar hemispheres respectively. We also implanted wire-electrodes into their neck-musculature for electromyography (EMG) recording purposes. Subsequently a small hole (1-1.5 mm in diameter) was drilled into the skull above the parietal cortical areas. The centre of the hole was located 2 mm posterior and 1 mm lateral to the bregma (the implantation coordinates were based on George Paxinos & Keith B. Franklin: The mouse brain in stereotaxic coordinates). The dura mater was removed using a small pincette and electrodes were implanted in the neocortical layers or the corpus callosum of that region. Silicon probes were implanted in a "coronal" plain to provide a "coronal electrophysiological section" of the respected hippocampi. After the implantation the electrode-parts lying free and the brain surface in between the borders of the hole were covered with

wax, and the "legs" of the drive were fixed on the skull and onto the screws with dental acrylic (Paladur).

EEG-recordings

After the recovery of the animals, the electrodes were slowly advanced to the hippocampal pyramidal cell layer where recordings were obtained using an MCP Plus system (and AlphaMap software, from Alpha Omega) in the frequency range from 1 to 10000 Hz. For recordings, animals were placed in a circular arena of 48 cm in diameter with plastic walls of 50 cm height. The floor and walls of the arena were cleaned with ethanol after every recording session. The animal's headset was connected with the preamplifier and the preamplifier was connected with a cabel to the amplifier channels of the recording setup. Signals were digitized with an analog-digital conversion board allowing for a sampling rate of 20 kHz. In addition to recordings in CA1 stratum pyramidale, we also acquired recordings from the stratum oriens and stratum radiatum and in some cases from CA3 and DG. After completion of the experiments the mice were deeply anaesthetized with ketamin (Ketavet, Pharmacia GmbH) and an electrolytic lesion was induced via a selected electrode located in the stratum pyramidale. For the lesion a square-wave pulse of 150 µA and 2 sec duration was applied with a Digitimer Ltd. stimulator. Subsequently mice were perfused transcardially with 20 ml physiological saline solution followed by the same amount of 4 % PFA (para-formaldehyde). Their brain was removed, sliced on a vibratome and stained with cresylviolet. In all cases the successful positioning of the electrodes in CA1 was verified histologically.

Analysis of the data

Analysis of oscillations

Recordings were analyzed off-line with the Spike2 software and MatLab-scripts (see Matlab-website at www.mathworks.com), and occasionally also with GraphPad Prism (www.graphpad.com). For LFP- and oscillation-analysis preselected recordings were split based on a 700 Hz low-pass and high-pass filter into EEG-signal and spike-related potentials (Spk-files) (mprocess-algorithm, designed by József Csicsvári). The EEG-files had a sampling rate of 1250 Hz. We selected recordings from stratum pyramidale where ripple amplitudes were maximal from a given animal and where sharp waves preferentially showed a biphasic profile (according to the pyramidal layer). The recordings (roughly 1.5-2 hours in length) were scored according to the behavioural state of the animals with a 10 sec bin-size. The behavioural staging was performed

using the prefrontal cortical EEG-signal, the EMG-signal and in certain cases the hippocampal EEG itself. Awake exploration was characterized by so-called "desynchronized" signal on the prefrontal and theta-oscillations on the hippocampal channels combined with phasic muscle-activity. To fulfill criteria for slow-wave sleep (SWS) the prefrontal and hippocampal EEG had to show large amplitude slow-waves (so-called "synchronized" patterns) corresponding to delta waves and sleep-spindles and the EMG-channels had to display a lack of considerable muscle-related activity. REM-sleep criteria were desynchronized cortical activity and hippocampal theta-rhythm with muscle atonia. Intermediate stages were allocated to segments, which did not fit to either of these groups but they were not included in the analysis later.

Ripples (selected from SWS) and gamma-oscillatory events (selected from REM-sleep and awake exploration) were first analyzed as events with a threshold-based peak-detection algorithm (Ponomarenko et al., 2004). For ripple-analysis, recordings were filtered in the 130-250 Hz range with a 15 Hz transition band, for gamma a 30-85 Hz range was used with a 5 Hz transition. The filtered signals were also rectified and smoothed with 0.005 s windows for ripples and 0.015 s for gamma-analysis. Detection thresholds were computed based on the smallest variance 3 s long recording segment from the rectified and smoothed signal. The mean (M) and standard deviation (SD) of this baseline segment served later for computing thresholds for ripple-detection (M+7SD) and gamma-envelopes (M+2SD). As additional criteria, these signal-segments had to be at least 15 ms long in case of ripples and 25 ms long in case of gamma-envelopes. The final length of these events was determined based on the points where they fall below M+0.5SD and M+1SD (ripples and gamma respectively) on the rectified signal. The amplitude of the detected events was calculated from the filtered (but not rectified) signals and was normalized later to the SD and threshold values of the baseline: (amplitude-threshold)/SD. For frequency-analysis a wavelet-function (Morlet) was applied in the region of the ripple- and gamma-peaks on the filtered signal. This analysis was followed by a power spectral analysis (multi-taper method, modified by Partha Mitra). This algorithm used the peak-amplitude points of the ripples and computed the frequency-composition in the time-segment located 64 ms around the amplitude-peak using a 2048-point Fast Fourier Transform (FFT) function. The power spectrum was computed as a second power of the Fourier Transform. We also analyzed ripples of different amplitude-ranges, most prominently ripples bigger than the median of amplitude distributions but smaller than those belonging to the upper 5 percentile. This way our estimates were more robust against threshold-differences and outliers. Ripples whose prominent frequency was higher than 140 Hz in their power spectrum were also compared between the animals and animal groups.

To gain insight into the theta- and gamma-bands, a similar multi-taper method was used, with the exception that we selected REM-sleep and awake exploratory episodes from representative recordings based on hypnograms and these segments were used in total for spectral decomposition. The spectrum of SWS was analyzed in a similar way. We also analyzed amplitude- and frequency-modulation of gamma-rhythm by theta. First we computed the Hilbert-transform of the selected signals in the theta-band to get the most precise approximation of the theta-phase at each sampled point. This way the precise and corrected theta-phase could be allocated to the gamma-peaks. A complete and Hilbert-transformed theta-wave was split into 24 equal phase-bins (15 degrees or actually $\pi/12$ radians) and the mean gamma-wave amplitude (from filtered gamma) in each particular bin was computed by averaging the gamma-waves peaking in that particular phase-bin. In a similar way the frequency-modulation was computed using the interpeak-intervals of gamma-cycles covering the theta-wave and the values were arranged according to the timing of the gamma-waves they stem from. In these cases gamma was treated as a continuous oscillation. These measures, however, were also analyzed separately for gamma-cycles of detected gamma-events. For ripple-waveform analysis, ripples extracted from the EEG were aligned to each other with their positive peaks. For coherence-studies cross-spectral coherence and interpeak-intervals were calculated. To achieve that, time-lags between peaks of successive oscillatory cycles were computed on different positions (actually different channels) and their difference served as a base for frequency comparison with IPI (the difference between the interpeak-intervals on the compared channels). The cross-spectral coherence of different channel-combinations was computed from the multi-taper Time Frequency Cross-Spectrum of the respective channels (originally developed by Partha Mitra). The cross-spectrum is practically the FFT-based spectrum of the reference channel multiplied with the spectrum of the respective channel. To make this measure insensitive to the signal-amplitudes, the second power of the cross-spectrum was divided by the multiplied product of the cross-spectra of the individual channels (the cross-spectrum of an individual channel is practically the second power of its individual spectrum). Thus, in other words NormCrossSpectralCoh$_{12}$ = (CrossSpect$_{12}$)^2/(CrossSpect$_{11}$*CrossSpect$_{22}$). To describe phase-coherence, phase-shifts between the peaks of oscillatory cycles on the compared channels (any given channel relative to a reference channel) were computed separately for gamma- and ripple-envelopes.

We also applied current-source density (CSD) analysis to uncover the underlying currents of ripple-oscillations. To do so, different channels (on the same shank) of silicon probe recordings were used. Average waveforms were computed on the different channels triggered by the ripple-peaks on a given pyramidal-layer channel. From the average waveforms spanning 240 ms centered

at the ripple peak, the second spatial derivative was derived for each sampled point. For the derivation we used a spatial difference of 2 channels (practically 100 microns). Finally, to make the results more comprehensive, a linear interpolation was used and the results were plotted with a colour-code in the two-dimensional time-depth matrix.

Unitary analysis

For spike-sorting the above-mentioned Spk-files were used for feature-extraction which was based on Principal Component Analysis. These features (altogether 17) were used later for a 17-dimensional hierarchical clustering (KlustaKwik, written by Ken Harris, available at http://sourceforge.net/projects/klustakwik). The resultant clusters were verified and merged manually by using the Klusters software (designed by Lynn Hasan).

For the identification of units we used distinct criteria for pyramidal cells (less than 3 Hz average firing rate, a characteristic autocorrelation function with "bursty" sidepeaks and more than 0.35 ms spike-width) and interneurons (more than 7 Hz average firing rate, distinct autocorrelation, lack of "burstiness", spike-width shorter than 0.35 ms, *figure 10.*). The autocorrelation of a given cell describes the relation of its spikes to each other in time, and thus is very similar in its meaning to the interspike-interval histogram. The spike-width was computed between the points of 25 % of the maximal spike-amplitude (Csicsvári et al., 1999b). The units characterized by firing between 3 and 7 Hz were classified as "intermediate type cells", they might include very fast pyramids or special, slower interneuron-types.

Units were considered "clean", if they did not contain any spikes in their autocorrelogram in the first 2 ms bins. For the analysis of interneurons, also some units containing a lower number of spikes in the respective bins of their autocorrelogram were used as multiunits. In this case their "contamination" was estimated by relating the firing rate in the refractory period (refractory rate) to the "asymptotic firing rate" reflecting the average firing rate. A refractory rate of 100 would mean that in the given multiunit every second action potential stems from a contaminating unit. However, we included only much "cleaner" multiunits in the analysis. The isolation-quality was described with the isolation distance or Mahalanobis-distance, reflecting the overlap between the cluster-clouds (Harris et al., 2000). An isolation distance above 30 indicated a good isolation quality and above 40 an excellent separation (Harris et al., 2000). To minimize the inclusion of cells which were recorded more than once (and therefore could have biased the distributions), we applied an electrode-advancement protocol and also a redundancy-screen that compared features of the units

from subsequent recordings. In this way one cell was usually represented by one recording session in our database.

Recordings were also analyzed in distinct EEG-states based on an automatic theta- and ripple-detection routine. The automatic ripple- and gamma-detection was performed as described previously. For automatic theta-detection a 2048-point FFT-analysis was performed on the selected
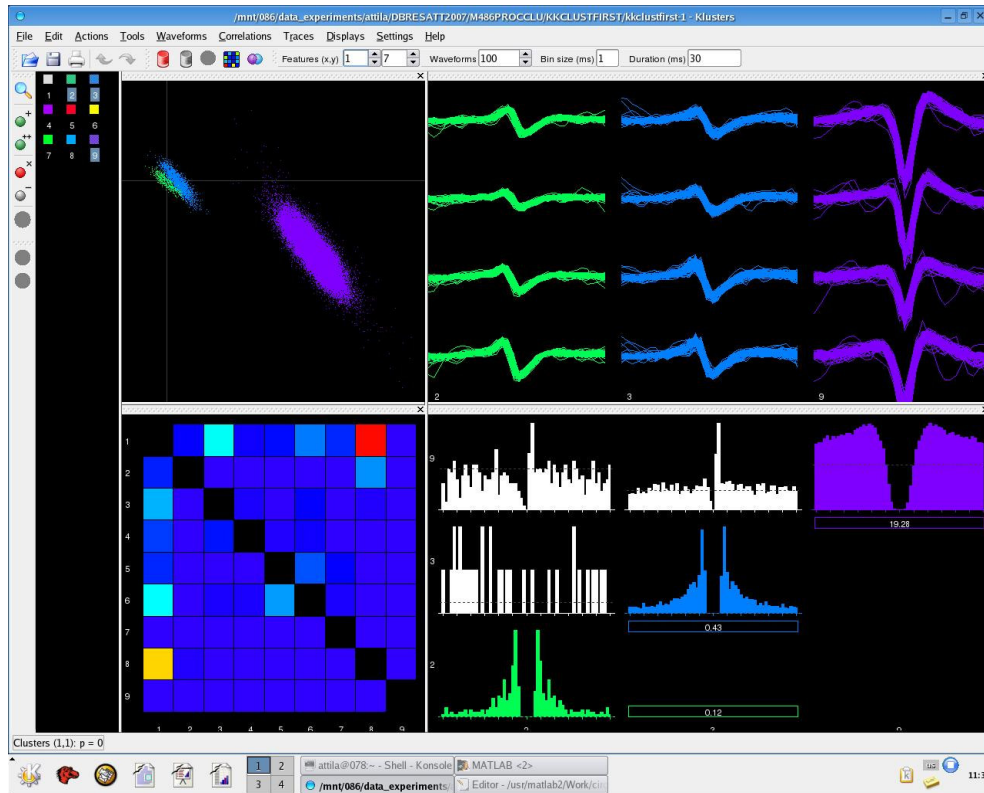

Figure 10.: The Klusters software (Hazan et al., 2006) was used to analyze multiunit recordings. The platform shows four windows illustrating cluster-clouds of three selected units, the waveforms of these three cells on the four tetrode-channels, the cluster-similarity matrix and the interspike-interval histograms (or so-called autocorrelations). The purple cell is a putative basket cell, the other two are pyramidal cells. Cross-correlations (relation between the firing of distinct neurons) are indicated in white.

EEG-file with a 2.5 s bin-window size and 1.25 s overlap between them. Segments were selected as theta, if the ratio of the spectral power between 6-12 Hz (theta) and 2-5 Hz (delta) exceeded 6 in a given bin. For oscillatory phase-computations the peaks and troughs of oscillatory waves (theta, gamma and ripples) were determined and these time points were set as π (or 180 degrees which is equal to - π or -180 degrees due to the circular nature of oscillations) and 0 respectively, and the phase values between these points were interpolated. Since theta-waves show a physiological asymmetry (their descending slope lasting longer than the ascending) and cannot be described

perfectly with harmonic oscillator models (Siapas et al., 2005), a correction of non-uniformity distribution was also applied for their analysis. This way, unitary activity could be investigated during distinct oscillatory types (theta, gamma and ripples). In addition to average firing rates, faster spike-trains (more than 50 Hz, corresponding to spikes omitted in a time-window shorter than 20 ms) were described with the instantaneous or "bursting" frequency. The phase-locking of isolated units was analyzed in distinct ways. The number of spikes of a given cell was computed in 20 bins covering a complete wave (from $-\pi$ to π), and the spike-phase histograms were averaged after normalization to the overall number of spikes emitted by a given unit. In a complementary way the phase-preference of units was estimated with the Rayleigh test. We also estimated the modulation-strength with the so-called "modulation depth", the relative difference in the spike count between the phase-bins with the maximal and minimal counts.

Statistical analysis

The examined parameters from WT and KO animal groups were compared using the Wilcoxon rank sum test, and in case of normal distributions with the t-test. Regression slopes were compared with covariance analysis. We used the statistical toolboxes of the Matlab and GraphPad Prism packages. We applied the Watson-Wheeler test to compare circular distributions. If not otherwise indicated, distributions are represented by their mean values and standard errors.

RESULTS

Hippocampal oscillations in PV-GluR-A KO mice

Earlier *in vitro* experiments on the PV-GluR-A KO mice were performed by Aleksandar Zivkovic, Andrey Rozov and Marc Cunningham. Their most important finding was that AMPA-currents on PV-cells were decreased. In addition, pharmacologically induced gamma-oscillations were reduced in the KO mice. These effects were even more pronounced in a similar mutant, the complete GluR-D KO (GluR-D is expressed almost specifically in PV-cells). In the GluR-D KO mice, the precision of spike timing of CA3-interneurons was reduced in terms of gamma-phase-locking as well (Fuchs et al., 2007). Since PV-positive basket cells are supposed to play an important role in the generation of fast oscillations and in the PV-GluR-A KO mice PV-positive cells receive much less excitatory drive, our prediction was that both gamma-synchrony and ripples would be perturbed in these mutants *in vivo*. To our surprise gamma-oscillations and ripples were preserved in the hippocampus of the PV-GluR-A KO mice, although there were certain alterations.

To analyze these events we have to extract them from a composite "material", namely the hippocampal EEG. By looking at EEG-recordings from this brain-structure, one has the feeling of traveling on a fantastic highland (like Tibet), involving big mountains (delta-waves and sharp waves), sometimes these mountains have refined riffs on their top (ripples on the sharp waves), sometimes there are deep canyons (radiatum sharp waves), and often there are flat plains situated between the mountains. This pattern, occurring usually during SWS, is called large-amplitude irregular activity (LIA), sometimes comprising slow oscillations as well (Wolansky et al., 2006). Another time one can find a regular pattern of mountains with faster riffs located on them (theta waves nested with gamma), this is what we see during active exploration and REM-sleep. To navigate this landscape we have to subdivide it into smaller pieces based on the bigger and slower components, which also reflect behavioural stages (hypnogram-scoring), and then look at its components in different frequency-ranges.

After sorting according to behavioural stages we analyzed the power of gamma- and ripple-oscillations (frequency-bands are 30-85 Hz for gamma and 130-250 Hz for ripples) using two approaches. We applied a threshold-based event-detection algorithm which one can run on the recording-signals already filtered in the appropriate frequency bands. This gives us information on the amplitude, duration and leading-frequency of a given event. However, since the recorded signal-amplitude also depends on the electrode-impedances, we could not use the voltage values directly, but only after normalizing them to the detection threshold and standard deviation of the baseline

(*see Materials and Methods*). After computing the event- (ripple- and gamma-) arrays of individual animals, we also pooled the data for WT and PV-GluR-A KO mice. It turned out that neither gamma-oscillations, nor ripples show statistically significant alterations in the mutant mice in either of the examined parameters (*figure 11.*).
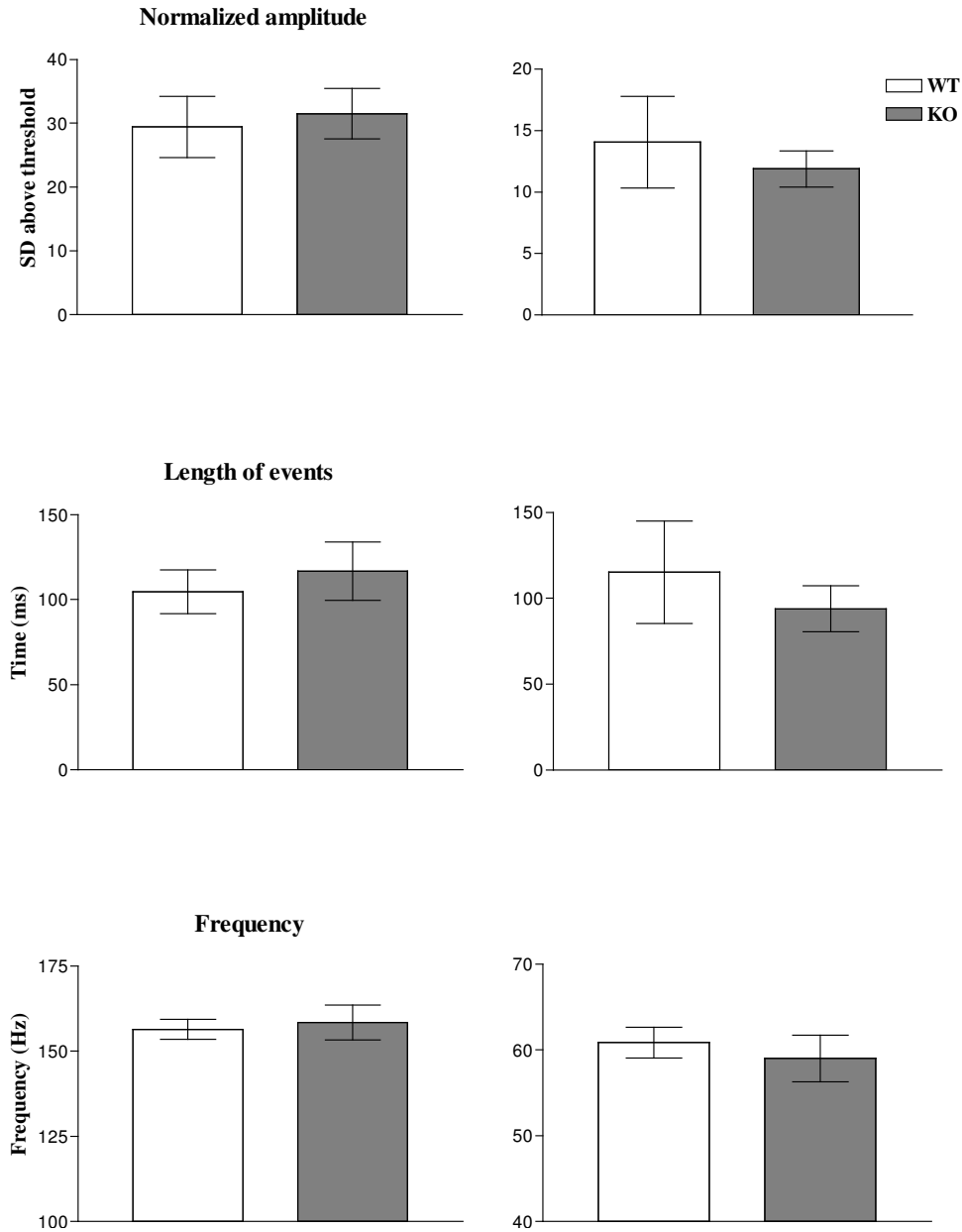

Figure 11.: Ripples and REM-gamma as events based on a peak-detection algorithm. Columns on the left refer to ripples (from SWS), those on the right to gamma-epochs from REM-sleep. The mean of medians of the individual animals from the WT and KO group are plotted indicating standard deviations as well.

Interestingly, when we grouped the animals according to the implanted electrode-types (wire-electrodes, including tetrodes versus silicon probes), we found different results regarding the

amplitude of ripple-oscillations: ripples were of higher amplitude in wire-implanted KO mice and smaller in probe-implanted mutants than in WT mice. Wire-electrodes have a low impedance while tetrodes have intermediate resistance but uncomparably smaller than silicon probes. The high impedance of the latter devices can account for a bigger signal-amplitude loss in our amplification system (*see later, figure 17.*). In addition to this, silicon probes implanted in KO mice had a higher impedance than those implanted in WT animals and this unfortunate circumstance can explain, why we did not find bigger ripples in the KO mice implanted with silicon probes. We also compared the ripple-oscillations in yet another way to obtain the power spectrum of the ripples. For this analysis we detected the ripple-peaks in the recordings and computed the power spectrum in the EEG-segment 64 ms around the ripple-peak (*figure 12.*). We also selected those ripples whose peak-frequency was above 140 Hz and plotted their power spectrum separately.
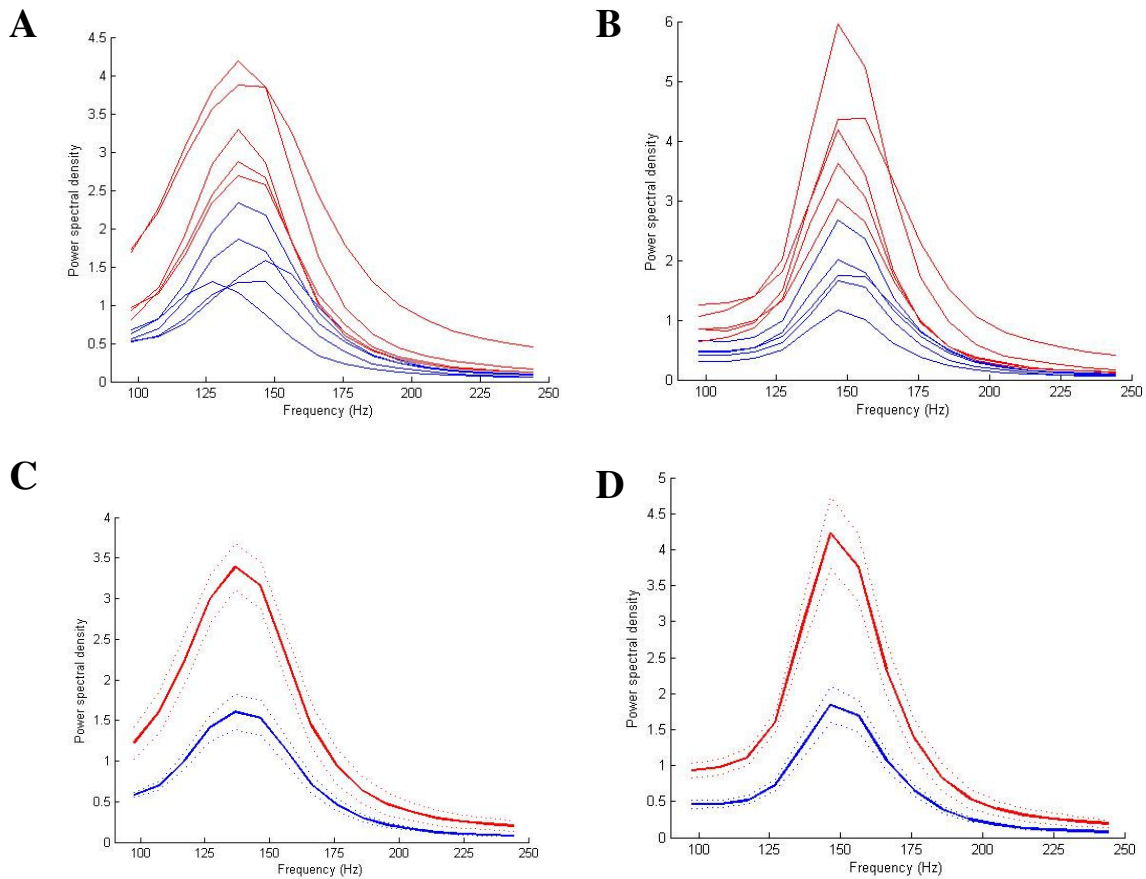
Figure 12.: Power spectrum of ripples (A) and "real ripples" (B, peak-frequency above 140 Hz) from 5 WT and 5 KO mice implanted with wires (blue indicates WT, red KO mice). The power spectra are based on EEG-segments comprising 64 ms around the ripple-peaks. In panels C and D the mean power spectra plus standard errors are shown for the wire-implanted mice.

The power spectral analysis takes into account that the power a given oscillation conveys is proportional to the second power of the voltage (just as sound intensity is proportional to the second power of the sound pressure). With this method we see an increased ripple-power in the individual as well as in the pooled power spectra of PV-GluR-A KO mice compared to that of WT mice. However, as before, the increased ripple-power holds for the wire-implanted mice whereas it is just the opposite in case of silicon probe-implantations. An explanation for that can be that the ripple-detection thresholds were very similar among wire-implanted mice but unfortunately were different for probe-implanted WT and PV-GluR-A KO mice. Thus, the considerably lower detection-threshold (which also reflects the mentioned impedance-differences between silicon probes) in KO animals can account for the lower ripple-power among probe-implanted KO mice. As can also be seen later on *figure 17*, the power-decrease is practically homogeneously affecting the complete frequency-spectrum of the SWS- and REM-sleep of the mutants, which is also an indication that the impedance of silicon probes implanted in the KO animals was unfortunately higher compared to those used for WT mice.

Interestingly, ripples from the PV-GluR-A KO mice very often looked "strange", meaning that many of them showed huge variability in their cycle-to-cycle wave-amplitude and morphology. To approach this problem more precisely, we computed average ripple-waveforms by aligning ripples to each other by their peaks but surprisingly the average waveforms looked normal in the KO mice (*figure 13.*). The mean ripple-frequency (as determined by Gaussian fittings of the ripple-power spectra) did not show a significant difference between the groups (138.23±2.25 Hz in WT and 136.70±2.17 Hz in KO, means and standard errors, p=0.63, t-test).
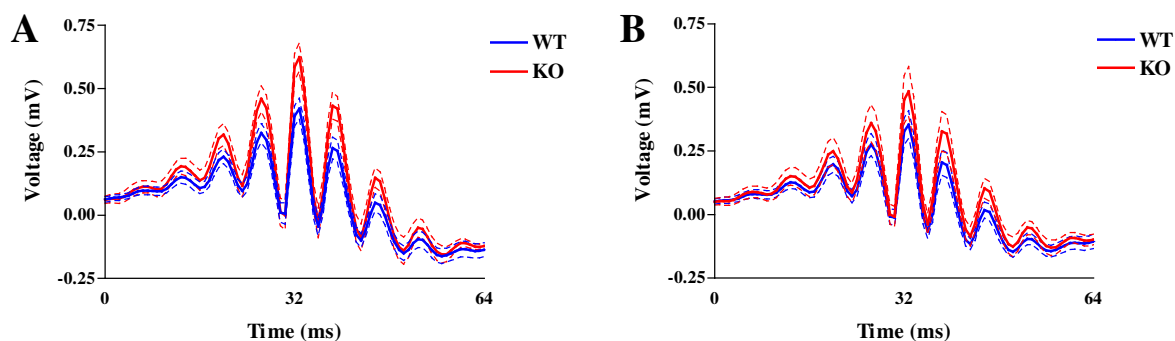
Figure 13.: Average ripple-waveforms from 5 WT and 5 KO mice implanted with wire-electrodes (A). Ripples from the raw signal were aligned with their positive peaks. A 64 ms time-window is shown with mean waveforms and standard errors. B: average ripple-waveforms with the inclusion of probe-implanted animals (altogether 7 WT and 7 KO mice). KO mice display bigger amplitudes.

Thus, this method could not reveal these slight disturbances, however, one might try to subgroup ripples according to distinct features and to cluster them in distinct groups. Another characteristic feature of ripples is the "intraripple frequency accommodation", meaning that the

frequency of the ripple is maximal in its beginning and slightly decays towards the end of the event due to the spike-frequency-accommodation of the participating cells. Since ripples change this "deceleration-profile" upon application of various GABAergic agonists (Ponomarenko et al., 2004), it is thought to be a sensitive measure of inhibitiory network state during ripples. We used a wavelet-based method to determine the ripple-frequency every 5 ms after its beginning and analyzed it between 15 and 50 ms, since in the very beginning of these ultrafast events there is a frequency-peak that we cannot fit with linear models. Interestingly, we did not find any significant alteration in the intraripple frequency accommodation in the PV-GluR-A mutant mice (*figure 14*.).
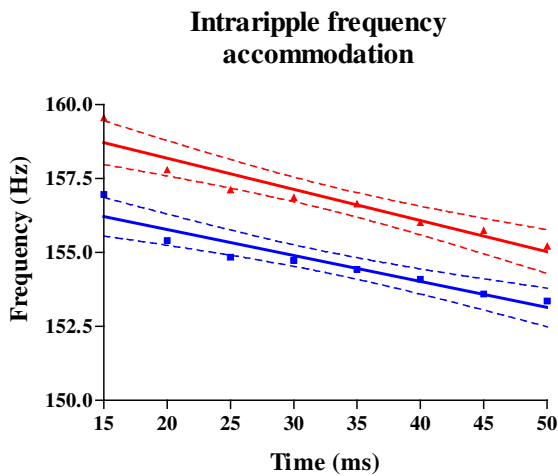
Figure 14.: Intraripple frequency accommodation is a sensitive measure of network mechanisms underlying ripples. We did not find any significant change in the deceleration profile in KO mice compared to WT animals. Linear regression analysis indicates that the deceleration rate for WT: 0.087 Hz/ms and for KO: 0.105 Hz/ms (p=0.37, analysis of covariance). The mean of the ripple-frequency medians of the individual animals in the two groups is plotted as a function of time. 95 % confidence intervals are also indicated.

To analyze the overall spectral composition of the hippocampal EEG in distinct behavioural states, we performed a Fourier Transform based power spectral analysis on SWS and REM-sleep EEG-segments in WT and KO mice. As *figure 15*. shows, the power-increase in the ripple-band in KO animals is also quite conspicuous in this analysis. There is also a slight increase in the gamma-band but to a lesser degree.

Figure 15.: Power spectrum of SWS-periods from WT (blue) and KO (red) animals. In this analysis all 7 WT and 7 KO mice (implanted with wires and silicon probes) were included. The respective EEG-segments were selected based on hypnograms. Even though we find a slight increase in theta- and gamma-power as well, the ripple-power increase is much more pronounced. Plotted were the logarithms of the mean power values with standard errors on a decibel scale.
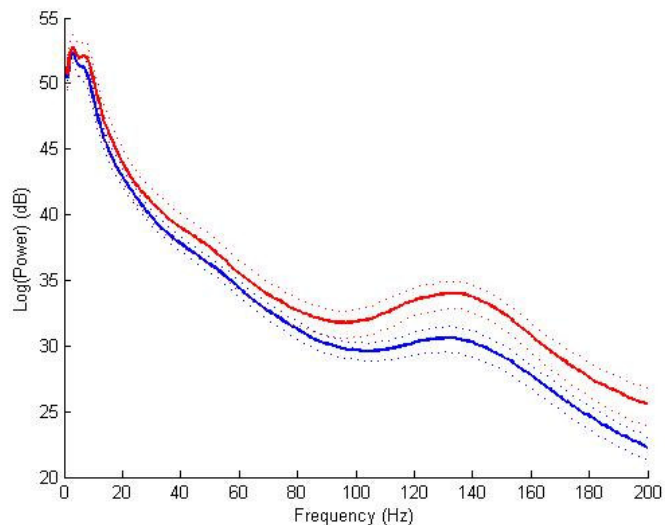
The power-increase in the ripple-band in the PV-GluR-A KO mice, however, may not only be an indication of increased ripple-size but can also result from an increase in the occurrence-frequency or duration of ripples (this tendency, even if not significant is present; ripple-length in WT: 104.690±3.455 ms, in KO: 116.800±4.615 ms, means and standard errors of the median values from 7 WT and 7 KO animals, p=0.16, t-test). We also looked at the ripple-occurrence frequency and found that in KO mice they are generated a bit more frequently, however, this effect was not significant (1.43±0.128 Hz in WT and 1.77±0.159 Hz in KO, p=0.12, t-test). Thus, it seems that we have a complex phenotype in which ripple-generation is affected at multiple levels.
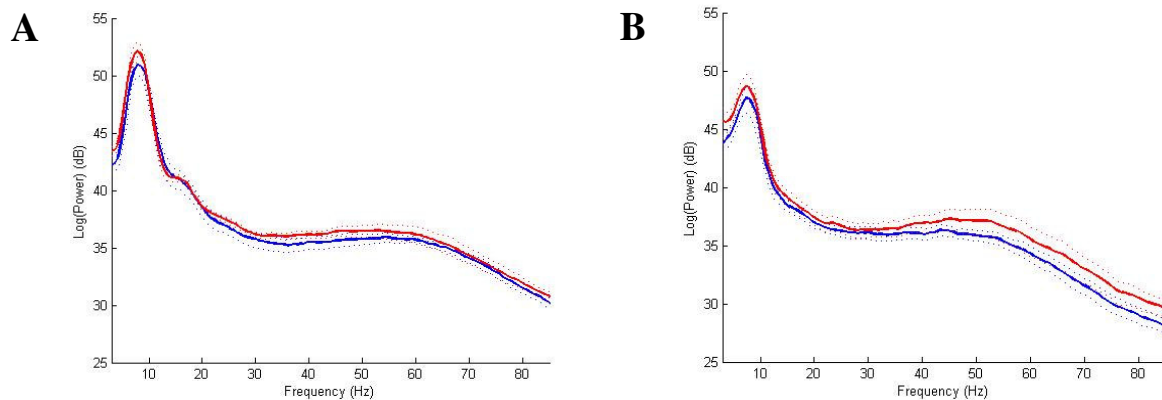
Figure 16.: Theta- and gamma-power in REM-sleep episodes (A) and during awake exploration (B), WT is indicated in blue, KO in red. There is a modest power-increase in the KO mice in both the theta- and gamma-band, which is, however, much smaller than that in the ripple-band. Power spectra of 5 WT and 5 KO animals were averaged for REM-sleep and for awake exploration (animals with silicon probes were omitted due to impedance-differences and the high noise-levels that silicon probes show during awake exploration). Logarithms of the mean powers with standard errors are plotted using a decibel scale.

The gamma-power was slightly increased in REM-sleep and during exploration, which was paralleled by a modest increase in the theta-power in these states. However, these alterations were much lighter than those of the ripples and were practically due to one outlier animal in the KO group. One can also see on the power spectra that the maximal amplitude-peak of REM-gamma is shifted to lower values in the KO mice (*figure 16.*), a result which is corroborated by the analysis of theta-gamma comodulation (*figure 18.*). Silicon probe-implanted mice were treated separately (*figure 17.B*) due to the electrode-impedance problems.

We also looked at the relation between theta- and gamma-oscillations. It is known that theta-oscillations modulate certain features of gamma-oscillations (Bragin et al., 1995). Theta-oscillations are in phase in the stratum oriens and pyramidale but in the stratum radiatum their phase changes and gradually turns to a phase-reversal. To minimize the variability resulting from different locations, the modulations were always computed from pyramidal layer recordings. There are

distinct features of oscillations that can modulate other oscillations. The phase of theta modulates both the amplitude and frequency of gamma-oscillations. The maximal gamma-frequency we normally find around the peak of theta-waves whereas on the slopes of the theta-waves the gamma-rhythm is somewhat slower. The maximal gamma-amplitude we find on the peak or on the descending slope, slightly after the peak of the theta-waves. Sometimes these gamma-waves can be as huge in amplitude as the underlying theta, thus we can call them "gamma-spikes" (Buzsáki et al., 2003). There is also a positive correlation between the theta-amplitude and gamma-power and frequency. Interestingly, there is a weak negative correlation between the amplitude and frequency of theta, meaning the bigger a theta-wave the slower it is (data not shown). In case of ripples, this relation is usually positive (Csicsvári et al., 1999a). As most of the features of the two oscillations are somehow modulated by each other, it is very difficult to say in the end, which feature modulates exactly what, so the term "co-modulation" may be more correct to describe this phenomenon. We also looked at how the gamma is modulated by theta in the PV-GluR-A KO mice. To our big surprise we find that gamma is nicely modulated by the phase of theta both in amplitude and frequency in the PV-GluR-A KO animals (*figure 18.*). This effect can be seen both during REM-sleep and awake exploration. We find a slower gamma-rhythm in the REM-sleep of the mutant mice, this difference is 2.13 Hz if we account for the complete theta-wave and 2.87 Hz when we look at the region around its peak. These differences are significant ($p < 0.0001$, paired t-test comparing respective phase-bins of the theta-cycle). Theta-power seems to be very slightly increased in the PV-GluR-A KO mice both in REM-sleep and explorative behaviour (again due to an outlier animal, *figure 16.*), but frequency-composition in the theta-range seems to be unaltered.
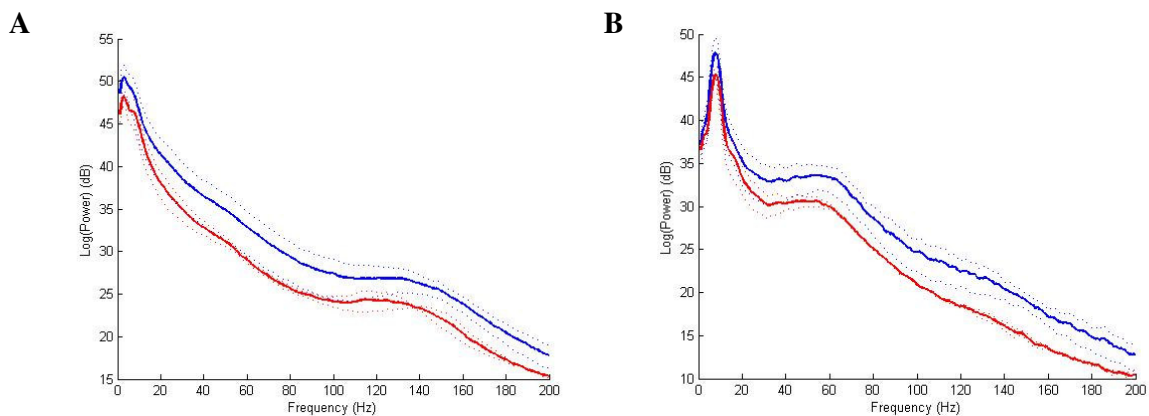
*Figure 17.: Power spectra of SWS (**A**) and REM-sleep (**B**) from silicon probe recordings. The blue colour indicates WT and the red KO mice. One can see an overall decrease in the powers of KO mice, which is, unfortunately, due to the impedance-difference of these high-resistance electrode types, which affected more seriously the KO group. Logarithms of the mean powers with standard errors are plotted on a decibel scale.*
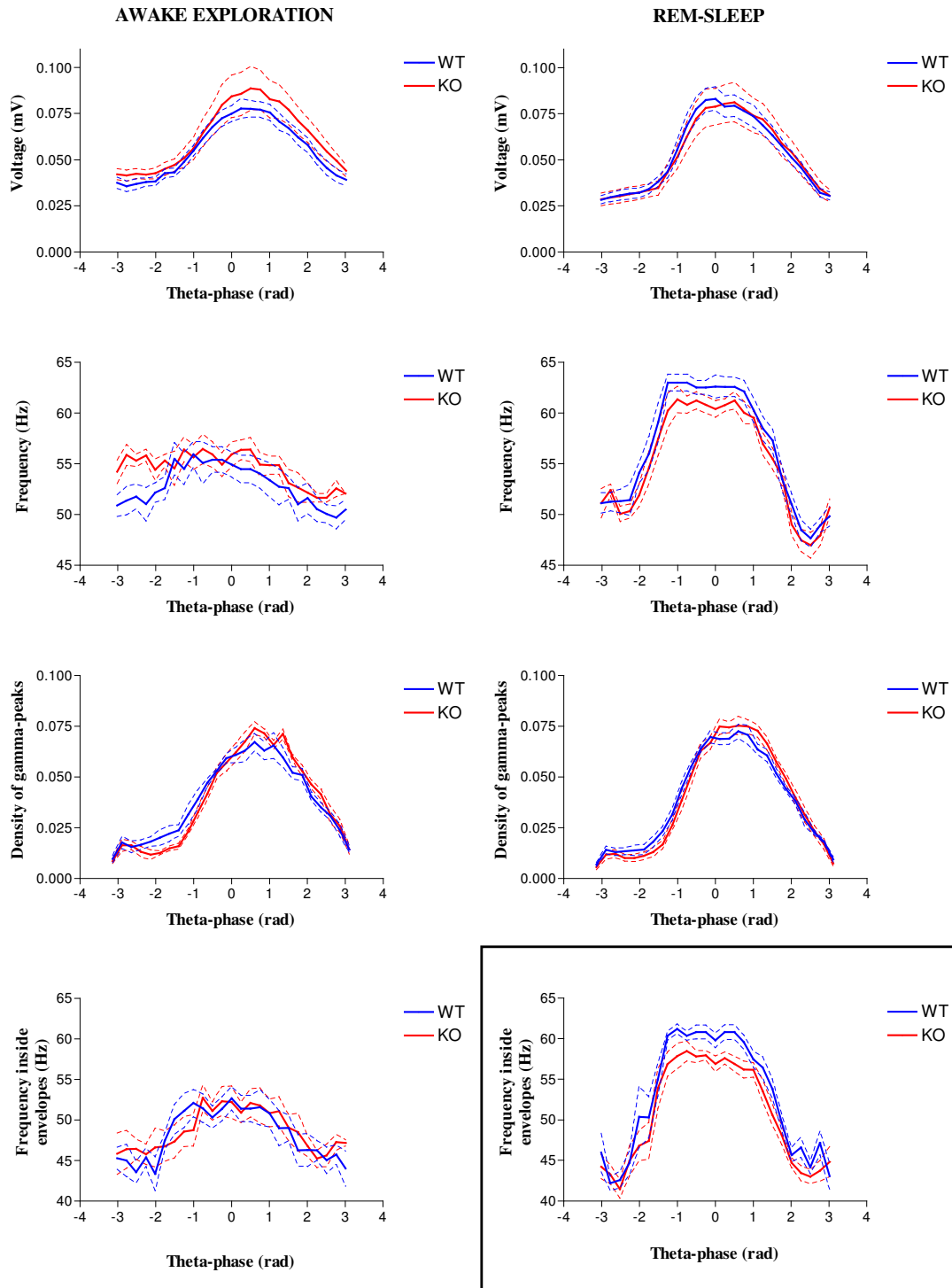
Figure 18.: Co-modulation of theta- and gamma-rhythms is preserved in the PV-GluR-A KO mice both during REM-sleep and awake exploration. This holds true also for the amplitude of gamma-peaks (first row) and the frequency of the gamma-rhythm (second row) all over the selected theta-ranges and also for the number of gamma-cycles and gamma-frequency in detected gamma-envelopes (third and fourth rows). One can see that there is a slight decrease in REM-gamma-frequency in mutants, which is, however, not seen during explorative behaviour. Nevertheless, this can also be the consequence of the overall slightly slower gamma-rhythm in exploration where the capacity for gamma-frequency increase is not exploited maximally.

Hippocampal oscillations measured in defined layers

EEG-oscillations are brought about by the spatiotemporal summation of extracellular currents propagating in three dimensions. In the hippocampus these spatial dimensions are represented by different histological layers and the precise topological arrangement of the histological constituents underlies the remarkably different and very characteristic EEG-profiles. Basic oscillatory features as described in the previous section were analyzed in the pyramidal cell layer of CA1. However, most of the investigated patterns are also visible in other layers. Thus, gamma-oscillations can also be recorded in the stratum oriens and stratum radiatum. This applies to ripples as well, with the difference that ripples vane in the stratum radiatum whereas gamma-oscillations become stronger there. However, this is due to the fact that ripple-generation is unique for the stratum pyramidale whereas gamma-oscillations are also generated in the DG. Thus, the gamma-oscillations we record in the deep stratum radiatum and in the stratum lacunosum-moleculare are actually mixtures of gamma-oscillations passively volume-conducted from the hilus and from the pyramidal cell layer. Gamma-oscillations show phase-reversal in the stratum radiatum, suggesting that dendritic excitation from the Schaffer-collaterals is involved in their generation. This idea was also proven *in vitro* with the use of voltage-sensitive dyes and current-source density analysis (Mann et al., 2005). Theta-oscillations reverse their phase below the stratum pyramidale, therefore also the phase-relation between theta and gamma changes there, the maximal-amplitude gamma-waves sliding to the theta-troughs. This feature and the constantly increasing gamma-amplitude towards the DG is responsible for the fact that in the stratum lacunosum-moleculare gamma looks even more prominent than the theta-rhythm. Coming to SWS, ripples look the most robust in the pyramidal cell layer, however, their underlying driving force, the sharp wave is not always visible there but is more intense at the border of the stratum oriens and stratum pyramidale (in the form of a positive deflection) or is dominant in stratum radiatum in the form of a big negative deflection (positive and negative refer to the appearance but following convention the radiatum sharp wave is called "positive"). The bigger sharp waves usually represent a bigger drive of the Schaffer-collaterals, therefore the ripples associated with them also tend to be of higher amplitude. Silicon probes are extremely suitable for examining oscillations in many histological laminations simultaneously (Csicsvári et al., 2003a). In *figure 19.* two short segments from a probe-recording are visible, the first one exemplifying SWS with ripples and the second a fragment of REM-sleep. These recordings make it possible that by a computational procedure one can determine which layers take part in the generation of different rhythms, whether they participate actively or passively and whether they constitute a current-source or current-sink.

To gain insight into the histological profile of gamma- and ripple-oscillations we analyzed silicon probe recordings. The depth-profiles look very similar in the WT and PV-GluR-A KO mice for gamma- and ripple-rhythms and also sharp waves.

We also performed current-source density (CSD) analysis to determine the generation site of ripple-oscillations (*figure 20.*).

Figure 19.: Silicon probe recordings from a WT mouse. The 8 channels shown are spaced 50 μm apart from each other. The upper trace is from the stratum oriens, the following four represent stratum pyramidale and the lower traces were recorded in stratum radiatum.

A: A segment from SWS with ripples and sharp waves which are very prominent in the stratum radiatum.
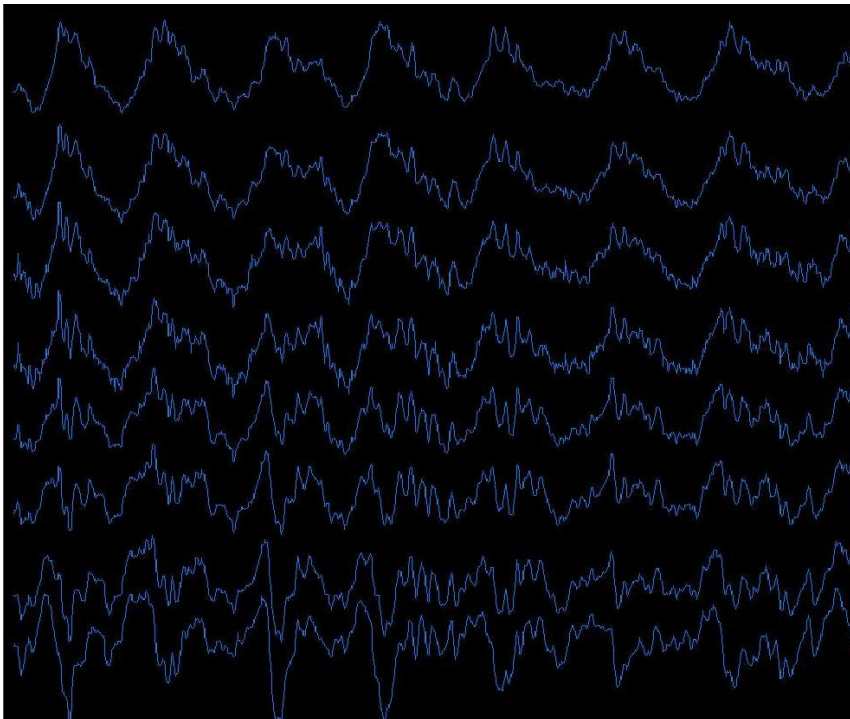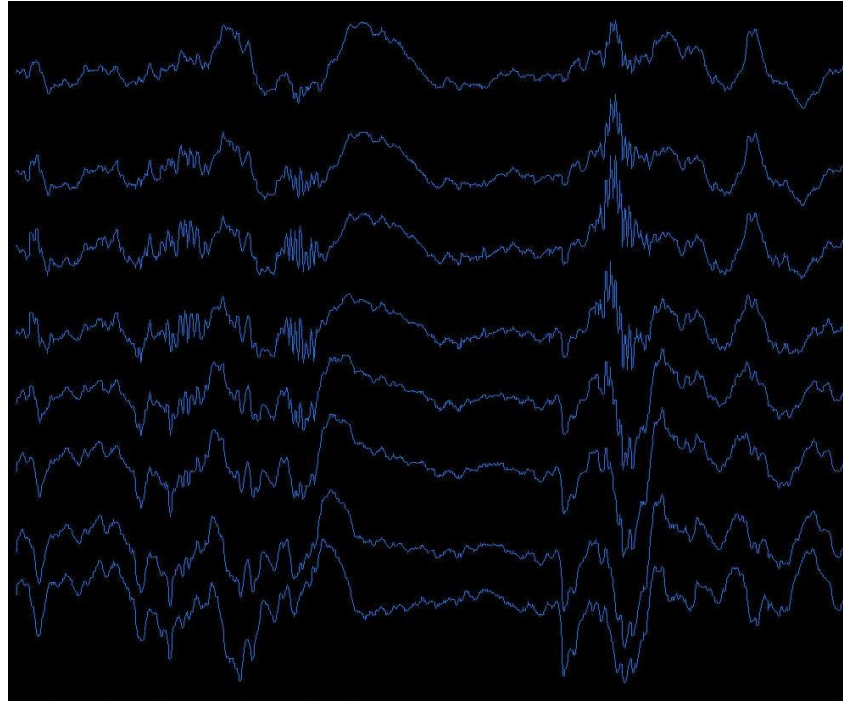
B: Theta-rhythm nested with gamma-oscillations from REM-sleep. One can see the gradual phase-shift of theta beneath the pyramidal cell layer and the phase-reversal of gamma-waves in the stratum radiatum.

A

B
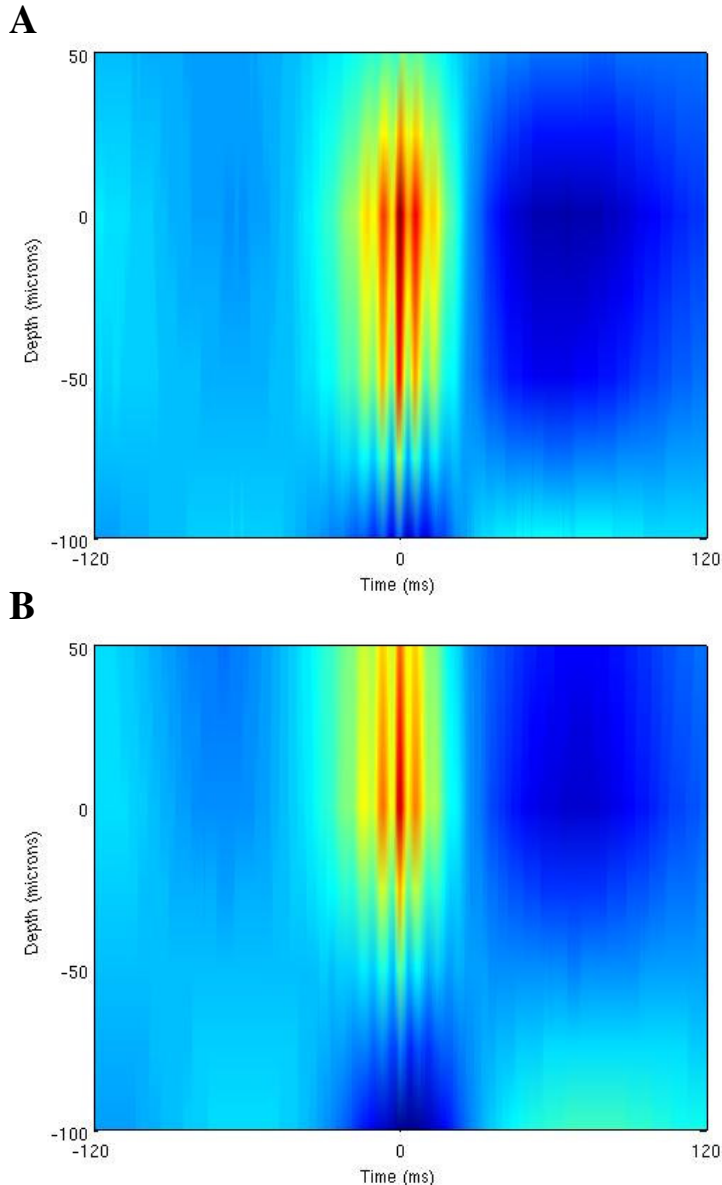
*Figure 20.: CSD-analysis of ripples from a WT (**A**) and a PV-GluR-A KO (**B**) mouse. Ripples were detected on a silicon probe-channel located in the pyramidal cell layer. Ripple-peaks were used as a trigger for the computation of average waveforms on distinct channels and the waveforms served for computing the CSD-maps. The plots show a time-segment of 120 ms around the ripple-peak, 0 depth indicates the pyramidal layer, positive values denote a direction towards stratum oriens, negative values mark a direction towards stratum radiatum. Around the ripple-peak one can see a sink in the stratum radiatum, resulting from the Schaffer-collateral input during sharp waves. It is combined with a current-source in the pyramidal layer which most probably results from perisomatic inhibition. We also find a current-source in the stratum radiatum and a sink in the pyramidal layer following sharp waves. The CSD-analysis indicates that there is no profound difference in the generation of sharp wave-ripples between WT and PV-GluR-A KO mice.*

The CSD-analysis provides evidence that the generation of ripples is confined to the pyramidal cell layer in the PV-GluR-A KO mice, and it is associated with dendritic depolarization in the stratum radiatum, indicating that the anatomical substrates of ripple-oscillations did not change in the mutant hippocampus.

Due to the precise arrangement of recording sites on silicon probes these recordings are suitable for coherence-analysis. Oscillations may look different in distinct recording sites of CA1 because projections may reach the targets with short time-delays that can cause measurable phase-offsets during gamma- and ripple-oscillations. This effect can be described by the phase-shift of oscillatory peaks. However, spectral parameters at a given recording site can also reflect inhomogeneities in the recorded cell-population. Thus, since fast excitatory transmission is reduced in PV-cells, we may speculate that individual interneurons would function rather independently

from each other and therefore the inhibition they inflict on pyramidal cells would be inhomogeneous. This could lead to a jitter in the timing of postsynaptic and action potentials of pyramidal cells, which would be visible on the spectral difference on distinct locations. To describe these phenomena we computed the cross-spectral coherence and interpeak-interval (difference in the interpeak-interval between oscillatory cycles of given site-pairs, IPI). It is of immense value that these measures are independent of signal-amplitudes and thus provide highly reliable results (see *Materials and Methods*).

Figure 21.: Cross-site coherence measures from WT (blue) and PV-GluR-A KO (red) mice implanted with silicon probes. On the electrode-shanks at the left and right side of the probe a given channel (located in the stratum pyramidale) was selected as a reference site. Coherence measures for distinct shanks with respect to the reference channel were calculated as an average of three pyramidal layer channels on the given shanks. The plotted results are averages of two animals (2 WT and 2 KO). One can see that neither the spectral parameters (A: cross-spectral coherence and B: IPI) nor the phase-coherence (C) differs significantly between the animal groups. Due to the huge standard deviations only the mean values are plotted.
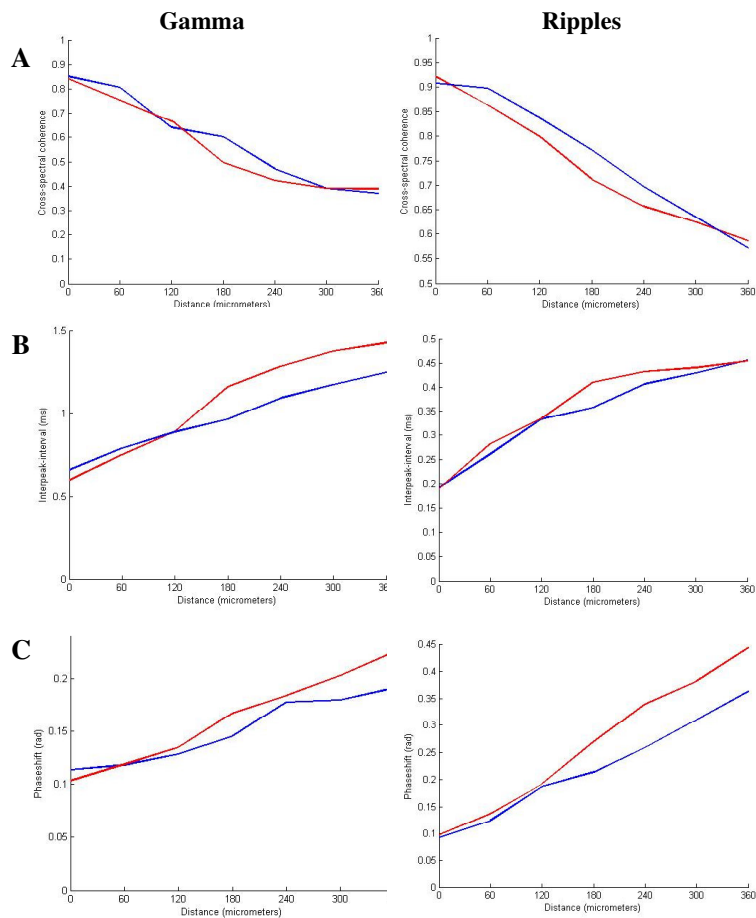
We recorded four mice with silicon probes, two KO and two WT animals, the KO and WT controls pairwise coming from the same litter. We found that in one animal pair the examined parameters did not differ significantly, however, in the other pair we found a slight decrease in cross-spectral and phase-coherence both with respect to gamma- and ripple-oscillations. Overall, when pooling the results we do not find these alterations significant, implying that synchrony in the

gamma- and ripple-frequency bands is not significantly perturbed in the spatial dimension upon reducing excitatory input in PV-cells (*figure 21.*).

Unitary analysis in the PV-GluR-A KO animals

To understand, how unitary activity underlies oscillatory phenomena, we isolated pyramidal cells and interneurons from tetrode- and silicon probe-recordings. Tetrodes are the most powerful tools in recording multiple single units from freely moving and behaving animals* whereas silicon probes, depending on the spacing of the recording sites can also be useful but not to that extent (at least with intersite-spacings more than 50 μm they are less powerful).

*To understand the tetrode-principle, one should imagine an experimentator walking in a dark forest on a sunny afternoon. Several birds, belonging to distinct species are singing in the trees but due to the leaves and low light-penetration the scientist would not see them. However, he hears their songs coming from different directions. The bird-songs reach the two ears of the investigator with some time-delay, and also with a power-difference due to the different distances the sound waves travel to reach the ears and due to the shadowing effect of the head on the ear which is located more distant to the bird. Therefore he can estimate the direction and the distance of a given bird based on these principles. If he is an ornithologist, he will also be able to distinguish between birds based on the peculiarities of their song (like pitch-frequency, intonation etc.), even if they come from similar directions. If there are two people walking there, the spatial arrangement of their four ears will increase the spatial resolution and species-recognition to an even higher degree. Due to the different action potential waveforms that pyramidal cells and interneurons emit and due to the amplitude-distributions on the four tetrode-channels they can also be sorted quite efficiently.

Pyramidal cells and interneurons can be easily distinguished in our recordings by distinct features, such as spike width, firing rate and autocorrelations (*see Materials and Methods*). The main advantage of our recordings compared to those from anaesthetized preparations relies in the more physiological circumstances a given cell is examined in since animals are not affected by the narcotics. Besides, one can record the same cell for several days, and also microcircuits can be examined given the relatively big number of cells isolated from a stereotrode. However, since we cannot fill the cells, the histological verification is more problematic. We cannot clearly distinguish between many of the interneuron-subtypes. Nevertheless, in many cases the location of the cell and/or firing patterns are predictive (*figure 22.,* Csicsvári et al., 1999b). We can also correlate our data with those obtained from anaesthetized animals since in those experiments many interneurons show distinct features regarding oscillations.

At a microcircuit level we can also relate the activity of cells relative to each other. The cross-correlation of cells can be indicative of whether there is excitatory or inhibitory transmission between the examined cells. In *figure 10. (Materials and Methods*) one can see two pyramidal units and an interneuron recorded from CA3. The cross-correlations indicate that there is a relatively high
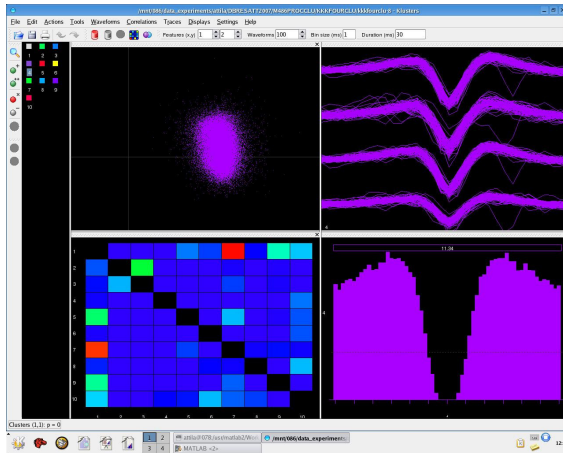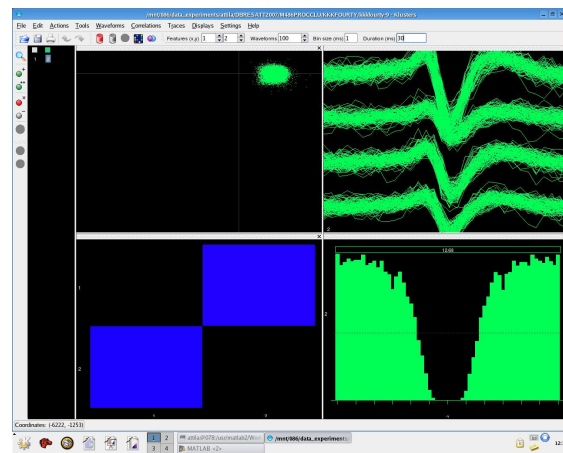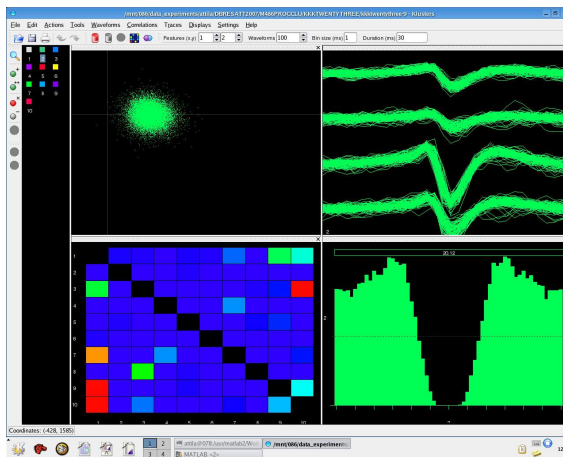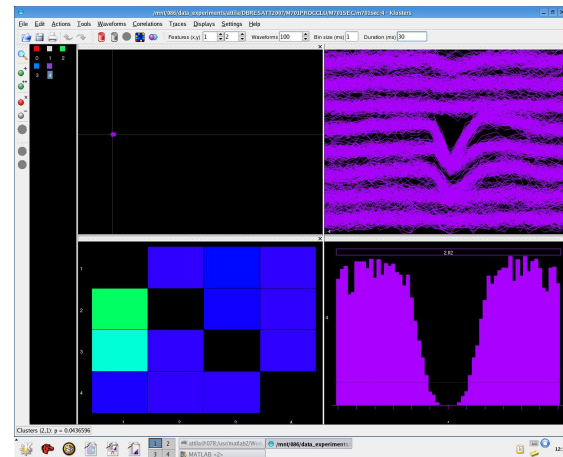
*Figure 22.: Interneurons from specific locations of our recordings. **A**: a putative CA1-basket cell, with characteristic autocorrelation. **B**: a putative O-LM interneuron (however, it can also be a basket cell) suggested by its location (CA1 stratum oriens). **C**: a putative basket cell from the DG. **D**: an "intermediate cell", the autocorrelation resembles that of interneurons but the firing rate is only ~3 Hz. A, B and C were recorded from a KO animal with tetrodes, D is from a WT mouse implanted with a silicon probe. For visual inspection the first 30 ms range of the autocorrelations is selected.*

probability that both pyramidal cells innervate the interneuron (shown by the positive peaks close to the zero ms bin) whereas the interneuron probably inhibits one of the pyramidal units (shown by the negative deflection next to the positive peak). *In vitro* experiments on neocortical slices showed that special interneurons can also excite pyramidal cells (Szabadics et al., 2006), therefore it would be interesting to show this phenomenon in hippocampal *in vivo* recordings as well, based on the analysis of cross-correlation functions. A monosynaptic excitatory coupling from an interneuron to a principal neuron would be an *in vivo* proof for that. Cross-correlations of cell-combinations of

different tetrodes can also reveal synaptic connections between distant cells, an advantage, which due to the thin slice-preparations, cannot be achieved *in vitro*.

From the huge number of cells recorded from the PV-GluR-A KO mice and their WT littermates, we selected 42 pyramidal cells and 24 interneurons from the CA1 of WT mice, and 134 pyramidal units and 99 interneurons from the CA1 of PV-GluR-A KO mice. The selected cells had an isolation distance of at least 30 (*see Materials and Methods*). Besides, we had recordings from 24 CA3-pyramidal cells and 11 CA3-interneurons from a KO animal, and we also recorded 1 DG-interneuron that satisfied the named criteria in both a WT and in a KO animal. These recordings were mainly from two mice implanted with several tetrodes but silicon probes also contributed substantially. From this pool we selected 34 pyramidal cells from the WT and 114 from the KO group, and 17 WT and 62 KO interneurons based on more stringent criteria. These cells were chosen based on a redundancy-screen that excluded those neurons that could be recorded more than once and had a higher probability of being the same. All the selected units were recorded in CA1.

Isolation distances for the selected units
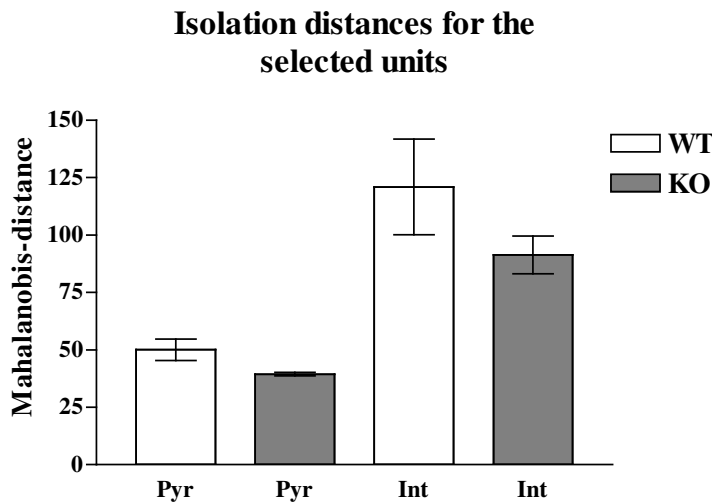
Figure 23.: The isolation distances of the selected pyramidal cells (Pyr, single units) and interneurons (Int, mainly multiunits). The isolation distances were not significantly different between pyramidal cells of WT (50.139±4.697, means and standard errors from 34 cells) and KO mice (39.461±0.815, 114 cells) and between interneurons of WT (120.990±20.784, 17 cells) and KO animals (91.423±8.215, 62 cells; p=0.156, Wilcoxon rank sum test). However, interneurons generally have a higher isolation distance than pyramidal cells.

We used only single units from pyramidal cells but also multiunits from interneurons. The contamination percentage of a given interneuron was approximated using its autocorrelation function. The area in the first 2 ms of this function (refractory period) was compared to the asymptotic rate of the neuron. In this way we got a rough estimation of the percentage of spikes in a given cluster that originated from a different, "contaminating" unit (*figure 24.*). The isolation distance did not differ significantly between WT and KO interneurons (*figure 23.*), nor did it for pyramidal cells. We did not find a significant difference between the contamination percentage of WT and KO interneurons either (*figure 24.*).

Contamination degree of interneurons

Figure 24.: The contamination degree of WT and KO interneurons, expressed as a percentage of the refractory and asymptotic firing rate. There is no significant difference between the groups, (19.053±3.303 for WT and 21.105±1.789 for KO; p=0.59, t-test). Mean values with standard errors are plotted.
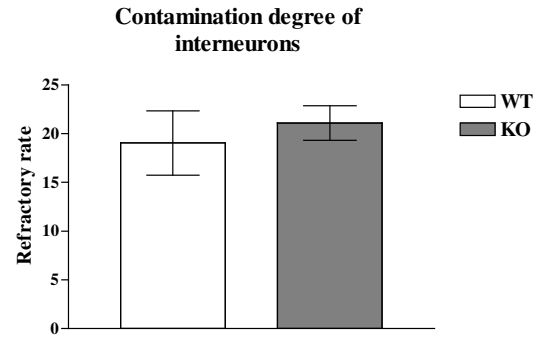
I mentioned that in extracellular recordings units are usually indicated by negative deflections. However, sometimes we find small positive potentials at the beginning of spikes. These could represent hyperpolarization just before spikes are generated and the recorded spikes may be "rebound spikes". By measuring the time between the positive and negative peaks of the spike-signals we can have a rough estimate of the duration of action potentials. In our practice, however, we measured the spike-width between the points with 25 % amplitude of the maximal negative peak. As mentioned above, interneurons express specific sets of ion-channels, which contribute to the short spike-width whereas pyramidal cells have a slower action potential and usually have longer-lasting after-hyperpolarizations. Neither pyramidal cells nor interneurons showed significant difference in their spike-width when we compared WT with PV-GluR-A KO mice (*figure 25.*, p=0.11 and 0.68 for pyramidal cells and interneurons, Wilcoxon rank sum tests). However, it is also not surprising since AMPA-currents usually do not contribute much to the currents of action potentials but rather to excitatory postsynaptic currents, and are activated at more negative membrane potentials whereas sodium channels open only at more positive values.
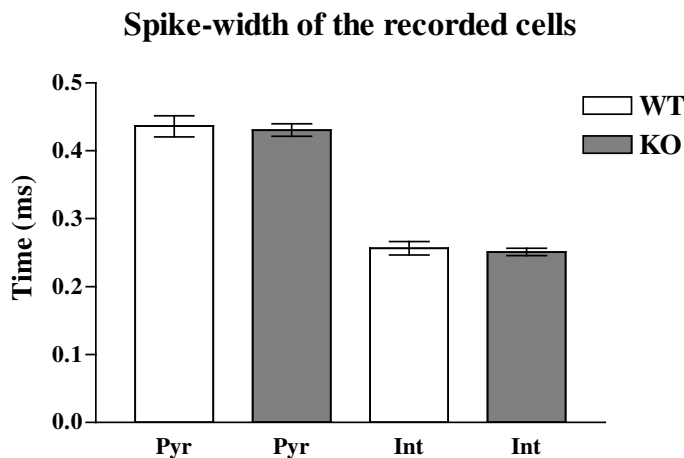
Spike-width of the recorded cells

Figure 25.: The spike-width of cells. Pyramidal cells (Pyr) have a longer action potential and consequently a bigger spike-width (0.436±0.015 ms for pyramidal cells of WT and 0.430±0.009 ms for those of KO) than interneurons (Int, WT: 0.256±0.009 ms and KO: 0.251±0.005 ms) where the expression of certain K^+-channels ensures a faster action potential (see Introduction). However, the spike-width of the same cell-type did not differ between genotypes (p=0.11 for pyramidal cells, and 0.68 for interneurons, Wilcoxon rank sum test).

Unitary firing rates in distinct behavioural states

First we determined the average firing rates of CA1 pyramidal cells and interneurons in WT and PV-GluR-A KO mice respectively. Interestingly, there was no significant difference either for pyramidal neurons (0.370±0.044 Hz for 34 WT units and 0.491±0.045 Hz for 114 KO units, p=0.72, Wilcoxon rank sum test) or local circuit neurons (15.904±1.367 Hz for 17 WT and 15.570±0.908 Hz for 62 KO interneurons, p=0.40, Wilcoxon rank sum test). There was only a very slight tendency towards an increased firing rate in pyramidal cells but it did not reach statistical significance (*figure 26.*). An explanation for this phenomenon could rely in the diversity of interneurons we recorded. Since we cannot really discriminate between PV-cells and other interneuron-subtypes that in fact comprise the majority of the hippocampal interneuron-family, our results do not exclude the presence of silent or slowly-firing PV-cells in the CA1 area of the hippocampus.
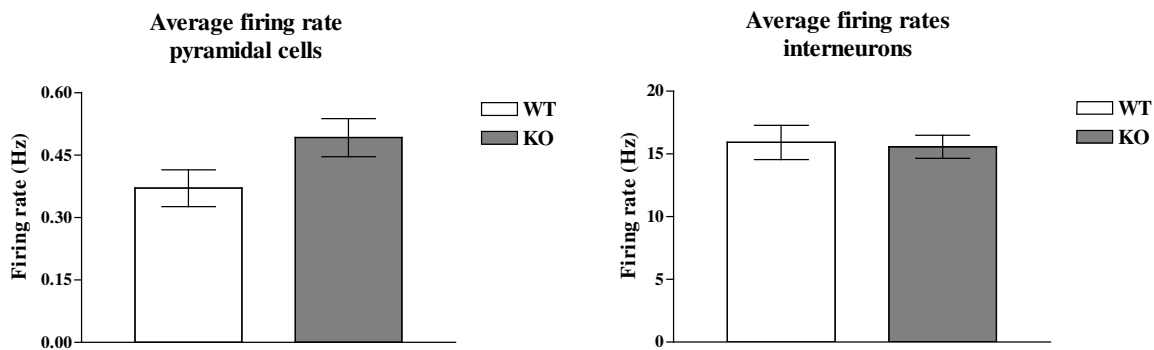
Figure 26.: Average firing rates of pyramidal cells and interneurons in WT and PV-GluR-A KO animals. Mean values and standard errors of the distributions are plotted.

The characteristic firing mode differs between the two cell types. Pyramidal cells tend to fire in bursts, meaning that within bursts very short time-periods elapse between successive action potentials but after emitting a burst the cell can stay silent for a longer time-interval, even seconds. This effect overall leads to a lower average firing rate of principal cell-activity. Interneurons discharge with a much higher frequency, however, usually less likely in bursts, so their activity is less clustered in time. To gain insight into these kinetical parameters we also looked at the bursting firing frequencies of the well-isolated units (*see Materials and Methods and figure 27.*).

Pyramidal cells in KO mice displayed an overall higher bursting frequency (157.630±7.401 Hz and 198.280±3.693 Hz for 34 cells from WT and 114 pyramidal cells from KO animals, respectively, p<0.0001, Wilcoxon rank sum test). Interneurons, however, did not differ in this respect (104.400±7.041 Hz for 17 WT and 94.416±3.793 Hz for 62 KO interneurons, p=0.21,

Wilcoxon rank sum test). This observation implies that even though PV-cells have a diminished excitatory drive, interneurons overall can be efficiently recruited during faster discharges. Thus, additional mechanisms may be involved in their "acceleration".
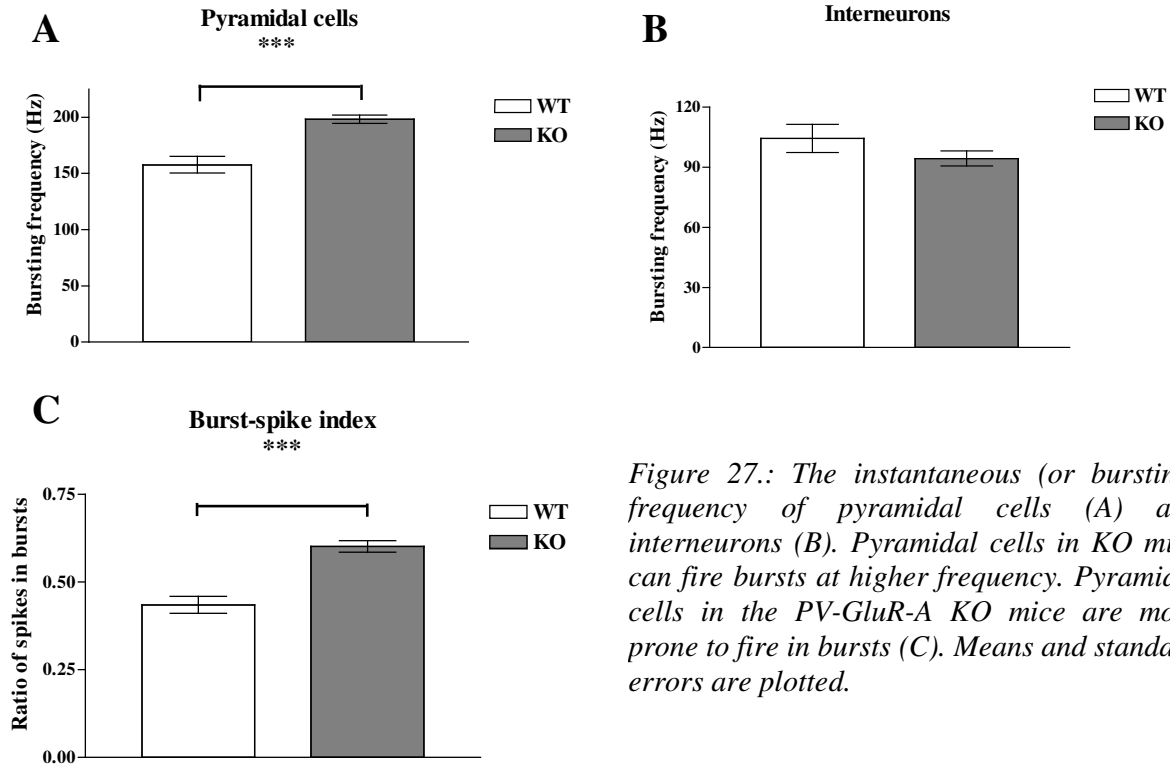

Figure 27.: The instantaneous (or bursting) frequency of pyramidal cells (A) and interneurons (B). Pyramidal cells in KO mice can fire bursts at higher frequency. Pyramidal cells in the PV-GluR-A KO mice are more prone to fire in bursts (C). Means and standard errors are plotted.

We were also interested in the propensity of pyramidal cells to fire in bursts. Therefore we determined the "burst-spike index" for pyramidal cells (*figure 27.C*), by counting the spikes that were emitted during bursts and relating it to the overall number of action potentials that a given cell emitted. Whereas in WT mice this ratio is 0.434 ± 0.024, in PV-GluR-A KO mice it is 0.601 ± 0.016, indicating that on average 43 % of the spikes of WT pyramidal cells is clustered in bursts whereas in PV-GluR-A KO mice roughly 60 % of the spikes belongs to burst firing. This difference is also highly significant ($p < 0.0001$, Wilcoxon rank sum test).

The mechanisms underlying cellular behaviour are most likely dissimilar during different behavioural and network states, therefore we analyzed unitary activity during different oscillations: theta-, gamma- and ripple-activity respectively. The most interesting finding was that during theta-oscillations pyramidal cells fired with a significantly lower average rate in PV-GluR-A KO mice than in WT mice (2.631 ± 0.449 Hz for 32 WT and 1.981 ± 0.189 Hz for 113 KO pyramidal cells, $p = 0.012$, Wilcoxon rank sum test, *figure 28.*). However, even though there is a slight tendency towards a decreased firing rate of interneurons in KO animals during theta-rhythm (29.801 ± 2.379 Hz for WT and 24.845 ± 1.636 Hz for KO, 17 and 62 cells respectively, $p = 0.09$, Wilcoxon rank sum

test), this effect is not statistically significant. We do not see any difference in pyramidal cell or local circuit neuron firing during ripples (*fig. 29.*).
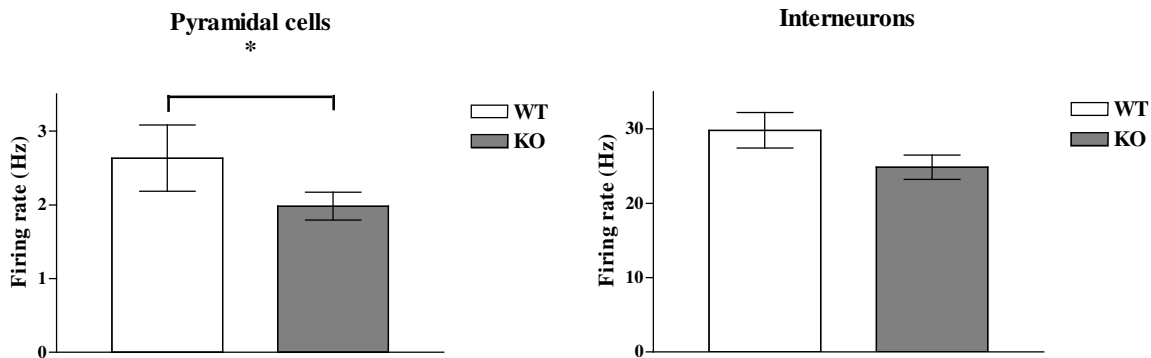

Figure 28.: Unitary firing rates during theta-oscillations. Pyramidal cells of the KO group fire significantly less in these states.
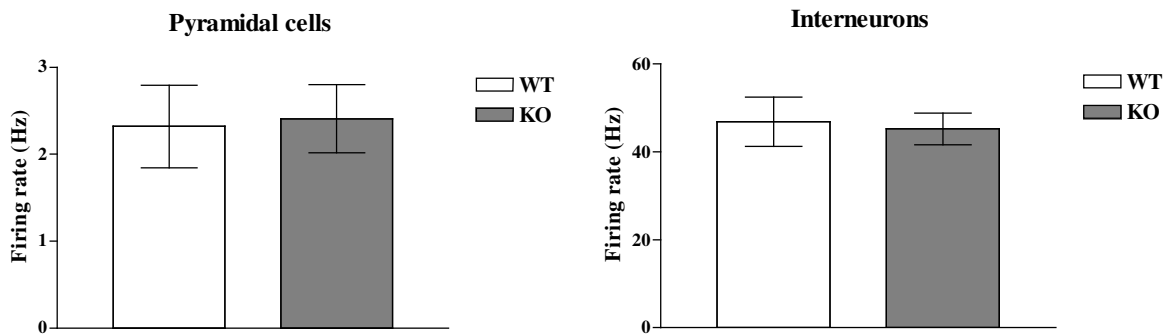

Figure 29.: Firing rates during ripple-oscillations. Neither pyramidal cells (2.321±0.473 Hz and 2.409±0.391 Hz for 31 WT and 111 KO pyramidal cells, p=0.140, Wilcoxon rank sum test), nor interneurons (46.853±5.596 Hz and 45.228±3.607 Hz for 17 WT and 59 KO interneurons respectively, p=0.825, t-test) show any change during ripple-oscillations.

The increased "burstiness" of pyramidal cells and their decreased average firing rate during theta-oscillations in KO mice tempted us to analyze bursting characteristics in distinct oscillatory forms. Interestingly, when we looked at instantaneous (or bursting) frequency of pyramidal cells in theta-related states, we found a significant increase (87.831±8.614 Hz for 30 WT and 139.020 ±5.407 Hz for 106 KO pyramidal neurons, p<0.0001, t-test, *figure 30.A*). Thus, even though pyramidal cells in the PV-GluR-A KO mice fire on average less during theta-oscillations, when bursts occur, they can accelerate to a higher rate than pyramidal cells in WT mice. It is of note that even though the gene-deletion is PV-cell specific, we find the main effect on pyramidal cells. This observation suggests that network mechanisms are brought about by an interplay between pyramidal cells and interneurons in the mouse hippocampus.
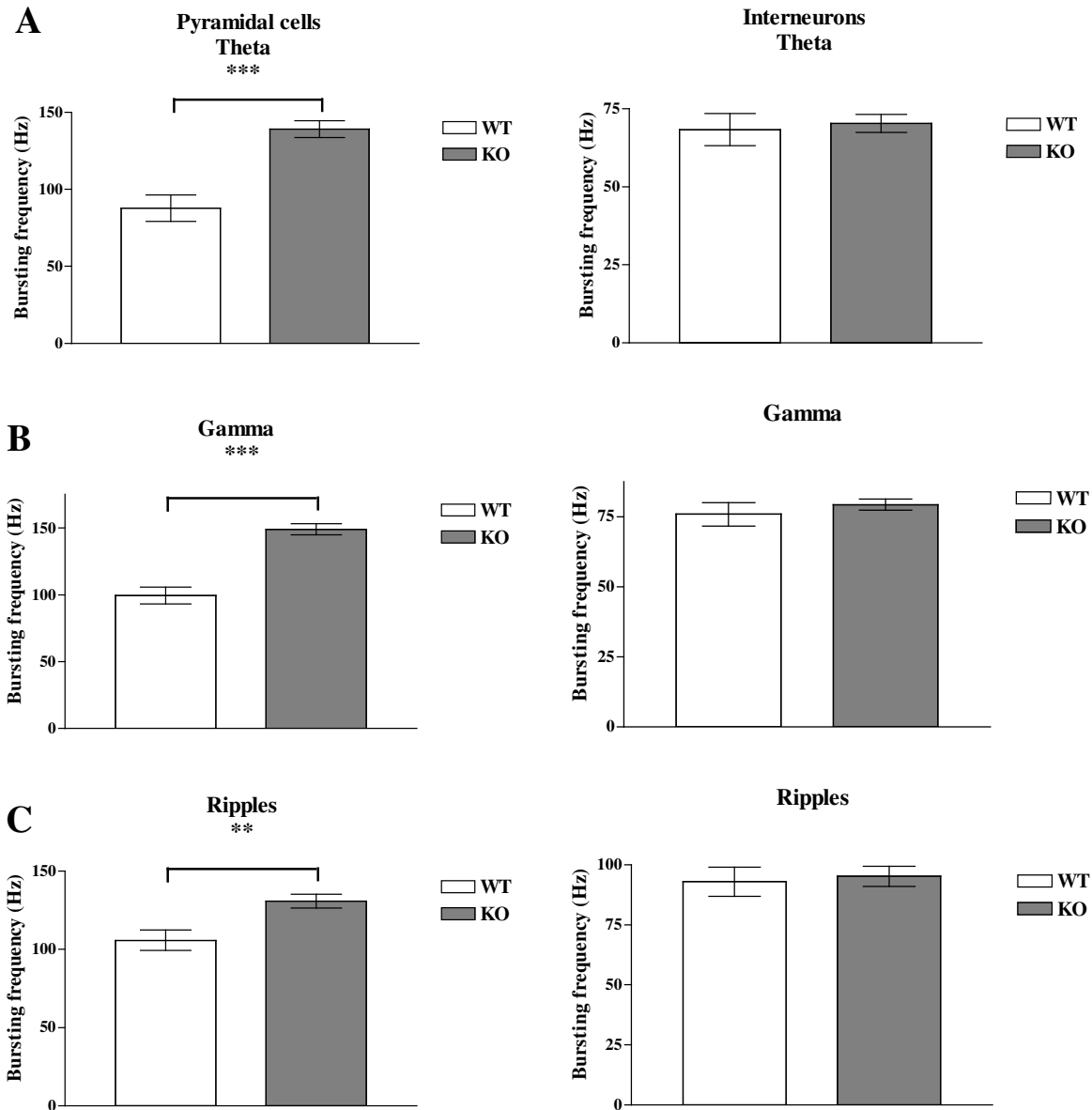
Bursting frequencies in different oscillations

*Figure 30.: Instantaneous, reflecting bursting frequencies of pyramidal cells and interneurons in theta-related behavioural states (**A**), during gamma- (**B**) and ripple- (**C**) oscillations. The pyramidal cells of the KO group display a marked increase in this parameter.*

The bursting frequency of pyramidal cells was also higher for gamma- and ripple-events (Gamma: 99.547±6.291 Hz for 34 WT and 148.940±4.169 Hz for 114 KO cells, p<0.0001; ripples: 105.840±6.541 Hz for 30 WT and 130.930±4.334 Hz for 108 KO pyramids, p<0.01, Wilcoxon rank sum tests) even though this effect was not so pronounced as in case of the theta-rhythm. Interneurons did not show any alteration in KO compared to WT mice (Theta: 68.348±5.109 Hz for 17 WT and 70.320±2.888 Hz for 62 KO interneurons, p=0.98, Wilcoxon rank sum test; gamma:

75.862±4.185 Hz for 17 WT and 79.292±1.956 Hz for 62 KO interneurons, p=0.43, t-test; ripples: 92.960±6.118 Hz for 17 WT and 95.220±4.162 Hz for 59 KO interneurons, p=0.78, t-test; *figure 30. A, B and C*.).

Ripples are highly synchronous events when 10-15 % of pyramidal cells discharge together in a 100 ms time-window. However, a given pyramidal cell does not discharge in every ripple: depending on the cell, the percentage of ripples a principal cell contributes to can be from 0 to up to 50 % or even more (Ylinen et al., 1995). This suggests that there are pyramidal cells that have a more stable contribution whereas others fire rarely. We also approached this problem by computing the firing rate of cells in all ripples and selectively in the ripples in which they were active. In this computation we became the former measure by accounting for the overall length of all the ripples (even if the cell was not active in most of them) present in the recording and the latter value was received by accounting for the overall length of only those ripples where the given cell was active. Very interestingly for pyramidal units the latter values are roughly 8-10 times as big as the first (17.858±0.577 Hz versus 2.321±0.473 Hz for WT pyramidal cells and 20.170±0.821 Hz versus 2.409±0.391 Hz for KO pyramids, means and standard errors), indicating that on average a pyramidal cell is involved in the generation of 10 % of the ripples (*figure 31*.).
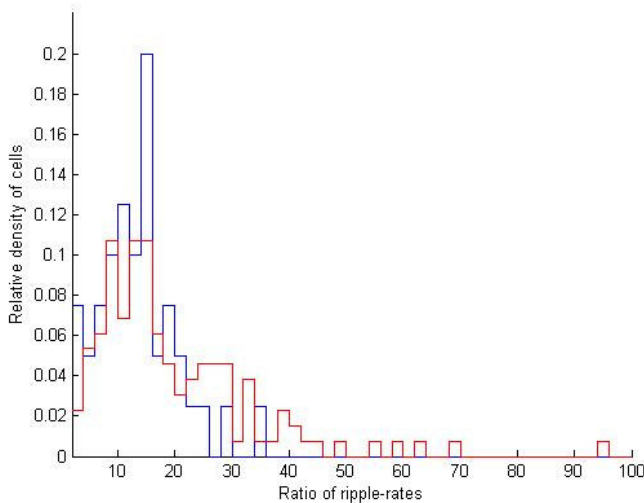

Figure 31.: Distribution of pyramidal cells regarding their involvement in ripple-generation or ripple-participation. The firing rate of each pyramidal cell was computed all over the detected ripples and only in those ripples in which they were active. The ratio of these two values served as an approximation to evaluate, how extensively a given cell contributes to ripple-oscillations with spike-emission. WT is blue, KO is red.

However, the situation is different for interneurons: in their case these numbers are not really different (52.005±4.832 Hz versus 46.853±5.596 Hz for WT and 50.072±3.205 Hz versus 45.228±3.607 Hz for KO interneurons), indicating that interneurons have a more general contribution to ripples whereas pyramidal cells may contribute in a more specific way to their generation. Overall, as suggested by previous data (Csicsvári et al., 2000) and also revealed by our study, distinct ripples may be brought about by different cell-assemblies which might also have an internal coordination, and interneurons can participate more generally by controlling the whole cell-

population. By analyzing the actual firing rate of interneurons during ripples, we find that in most cases both in wild types and in mutants they increase their firing rate. However, this observation holds true only in a general sense.

The literature suggests that interneurons can be grouped into several classes according to their behaviour during ripple- and theta-oscillations. Most interneurons located in the stratum pyramidale increase their firing rate all over the ripple-event. Some cells, however, have a double peak on the cross-correlations between the ripple-peaks and their spikes. Thus, they are active in the very beginning and at the end of the ripple-episode, with background activity levels in the middle of the oscillatory event, most probably for they also receive a strong inhibition there. "Anti-sharp wave cells", located mainly in the stratum oriens decrease their firing during ripples (Csicsvári et al., 1999b). *Figure 32.* shows an example of a "sharp wave-ON cell". PV-positive basket cells indeed have been shown to increase their firing during ripples (Klausberger et al., 2003) whereas CCK-cells usually do not increase it (Klausberger et al., 2005), and axo-axonic cells are only active in the beginning of these ultrafast oscillatory epochs and remain silent afterwards (Klausberger et al., 2003). O-LM cells are silent during ripples in anaesthetized rats (Klausberger et al., 2003), therefore they may correspond to the real "anti-sharp wave cells". Interestingly, even though in anaesthetized rats O-LM cells tend to fire in the trough of theta-waves, in freely moving animals most interneurons in the stratum oriens were also bound to the descending slope of theta-waves, just as most interneurons from the pyramidal cell layer (Csicsvári et al., 1999b). Axo-axonic (chandelier) cells fire preferentially on the peak of theta-waves in anaesthetized rats (Klausberger et al., 2003).
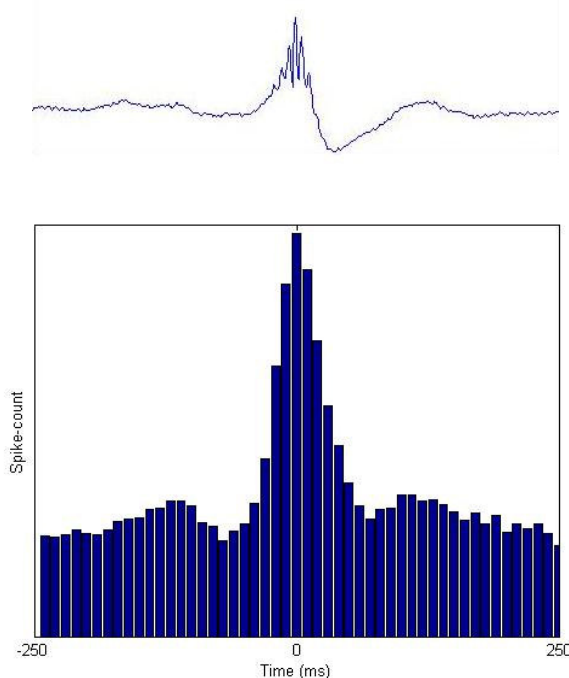
Figure 32.: A "sharp wave-ON cell" from a KO animal. The firing probability of the interneuron was computed as a function of time-difference from the ripple-peak (cross-correlation). I plotted a 250 ms region around the ripple-peaks with a 10 ms bin-size. On the upper trace an average ripple-waveform is shown, indicating that the recording position was at the border between stratum oriens and pyramidale. This location also suggests that most probably the interneuron was a basket cell.
On the lower trace one can see that notwithstanding the decreased excitatory drive on PV-cells this cell was recruited to ripple-events very efficiently.

Thus, we have some hints, which interneurons belong to the "sharp wave-ON" and "anti-sharp wave" categories, even though it is difficult to verify this *in vivo*. Altogether these results also indicate that notwithstanding the decreased excitatory drive on PV-cells most of them can still be efficiently recruited by ripple-oscillations.

Rhythmic modulation of unitary activity during distinct oscillations

LFP-oscillations represent the spatiotemporal summations of EPSPs and IPSPs at a population-level. Since action potential firing is related to the course of EPSP, there is a relation between the phase of oscillations and unitary activity. We call this phenomenon phase-locking. Based on previous studies (Csicsvári et al., 1999b, Buzsáki et al., 2003) it was suggested that during theta-rhythm interneurons fire preferentially on the descending slope of theta-waves while pyramidal cells have a double peak, just shortly after the theta-trough and around the theta-peak. During ripples pyramidal units are the most active near the ripple-troughs while interneurons prefer the ascending slopes which is not surprising considering the monosynaptic excitatory coupling between pyramidal cells and inhibitory neurons in CA1. As shown in pharmacologically induced gamma-oscillation models *in vitro* (Mann et al., 2005) and also *in vivo* (Penttonen et al., 1998; Csicsvári et al., 2003b), pyramidal cells are generally phase-locked to the trough of gamma-oscillations (recorded in the pyramidal cell layer) and interneurons follow them with a small phase-lag and are positioned on the ascending slope of gamma-waves indicating again a monosynaptic connection between the participating elements.

We also examined phase-locking of pyramidal cells and interneurons in WT and PV-GluR-A KO mice. The mean phase of averaged spike-phase histograms of pyramidal cells did not differ much between WT and KO mice either during gamma- or ripple-oscillations. In agreement with the literature, the maximum firing probability of pyramidal cells was roughly in the trough of gamma-oscillations (315.98±8.92 and 330.08±3.90 degrees for 26 WT and 90 KO pyramidal neurons; circular means and standard errors of the circular means; 0 and 360 degrees being the trough of the oscillatory wave and 180 degrees denoting the peak of it; p=0.33, to compare circular means Watson-Wheeler circular test is used throughout this chapter) and very close to the trough of ripple-oscillations (289.98±5.08 versus 280.48±3.11 degrees from 26 and 98 pyramidal cells from WT and KO animals respectively, p=0.28). However, in our study, contrary to the literature the maximal firing probability of pyramidal cells is during the descending slope of theta-waves (266.83±5.99 and 288.78±4.40 degrees for 29 WT and 103 KO pyramids, p=0.02). When analyzing interneurons, we

Pyramidal cells **Interneurons**
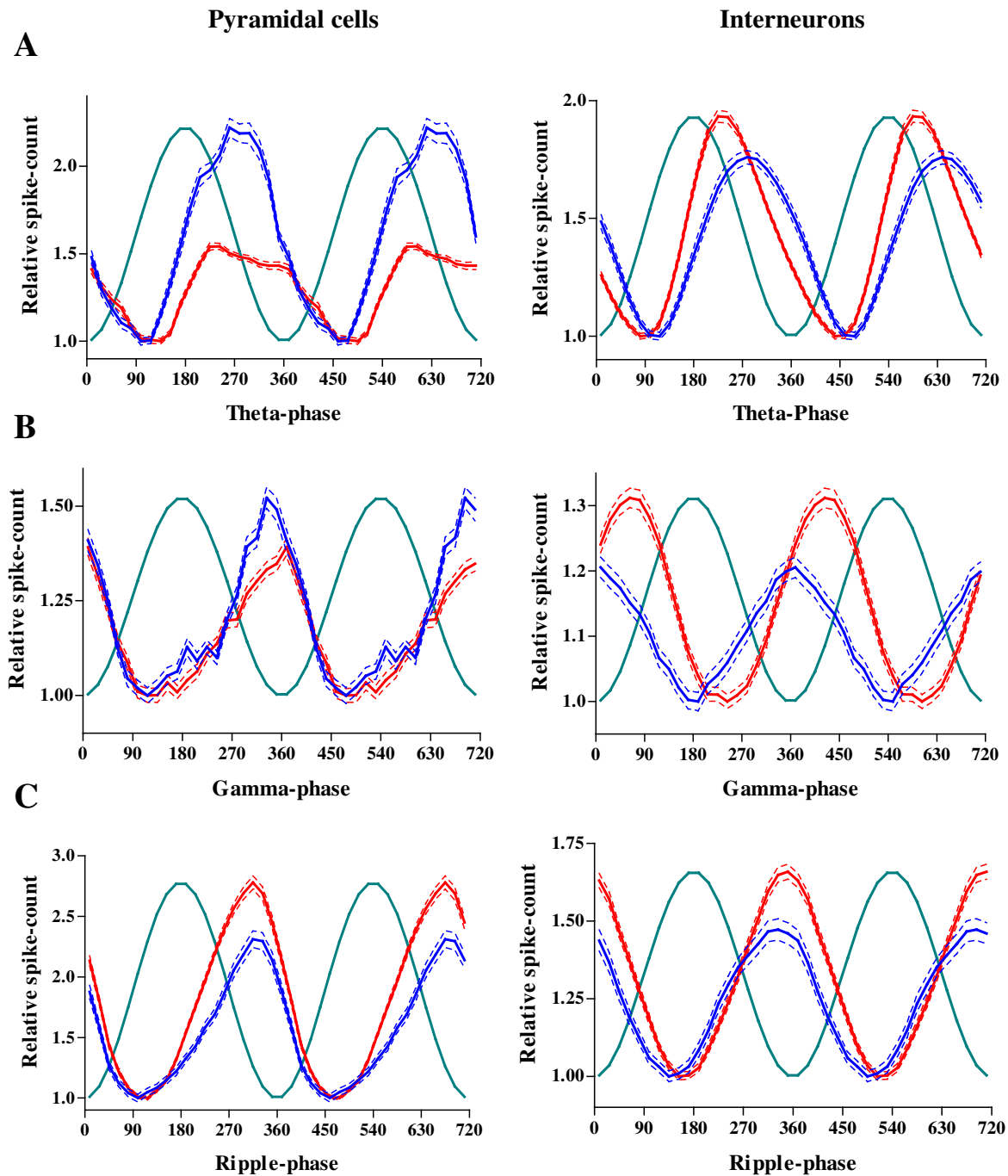
A

B

C

*Figure 33.: Phase-modulation of pyramidal cells (left panels) and interneurons (right panels) during distinct oscillations. Cells from WT animals are indicated with blue, those of KO with red. During theta-oscillations (**A**) pyramidal cells were less well modulated in the mutants whereas interneurons were tuned a bit more sharply. In theta-related gamma-rhythm (**B**), interneurons displayed an increased modulation depth in KO mice whereas pyramidal cells showed a decreased modulation. In ripples (**C**) both principal cells and interneurons were more sharply modulated. One can also see that during gamma, interneurons in KO mice are relatively delayed compared to those in WT mice. The same holds true for ripples. Note that on these plots the spike-counts in each phase-bin are normalized to the trough of the modulation curves, therefore troughs are always represented by the value 1. The phase-values are given in degrees, the green curve represents an oscillatory reference-wave.*

found a phase-shift in the spike-phase histograms both for theta-, gamma- and ripple-oscillations. Surprisingly interneurons tended to discharge a bit "earlier" on the descending slope of theta-waves in the KO group (*figure 33.A*, 289.68±9.73 degrees for 17 WT and 267.40±4.71 degrees for 62 KO interneurons). However, this effect was not significant (p=0.84). During gamma-oscillations (gamma nested within theta-rhythm) interneurons fired slightly later in the KO than in the WT group (*figure 33.B,* 2.83±9.65 degrees for 16 WT and 56.175±4.05 degrees for 60 KO interneurons, p=0.15), not in the troughs as the WT interneurons did but rather on the ascending slopes of gamma-waves. Even though this tendency was not significant, we also found it during ripples of the KO mice when comparing it with cells from the WT mice (*figure 33.C,* 288.35±11.14 versus 341.44±4.57 degrees for 16 WT and 59 KO interneurons, p=0.18). To sum up these results, it seems that during gamma-oscillations of WT mice interneurons followed the pyramidal cells with a slight phase lag (around 45 degrees) which became much longer (almost 90 degrees) in PV-GluR-A KO mice. During ripples of WT mice the pyramidal cells and local circuit neurons fired almost at the same time but in the PV-GluR-A mutants there was a delay of almost 60 degrees.

Interestingly, during theta-oscillations pyramidal cells in KO animals displayed a reduced modulation depth (relative difference between the peak and trough of the spike-phase histograms, p=0.0002, paired t-test for 20 phase-bins covering a complete oscillatory cycle) while the difference between the phase-modulation of interneurons turned out not to be significant (p=0.84). During gamma-oscillations (gamma related to theta-oscillations, this means during exploration or REM-sleep) pyramidal cells from PV-GluR-A KO animals were less modulated by the local field than their WT counterparts (p=0.0062). Interneurons, however, were more sharply tuned in the mutants (p=0.0011). During ripples the depth of modulation was higher for both KO pyramidal units and interneurons compared to WT units (p=0.0016 for pyramidal cells and p=0.002 for interneurons, paired t-tests). Altogether the increased modulation depth of both cell types in the KO mice during ripples is in line with the increased ripple-power we usually find in PV-GluR-A KO mice.

We also estimated whether the recorded units have a certain phase-preference regarding the oscillations (*figure 34.*). The Rayleigh test performed on every unit indicated that all interneurons had a certain theta-phase-preference in WT as well as in KO animals whereas a majority but not all pyramidal cells were significantly modulated by the theta-rhythm (24 from 29 pyramids in the WT and 94 from 103 pyramids in the KO group).

As also suggested by previous studies (Csicsvári et al., 1999b), many pyramidal cells may be place cells that show phase-precession during theta-oscillations. Therefore they may not have such a strong phase-preference. Interestingly, practically all interneurons were significantly modulated by the gamma-rhythm, (16 cells from 16 WT and 58 from 60 interneurons in the KO)

whereas roughly half of the pyramidal cells showed such phase-locking to gamma (15 from 26 in the WT and 50 from 90 in the KO group). The majority of both pyramidal cells (25 from 26 WT and 91 from 98 KO) and interneurons (14 from 16 WT an 58 from 59 KO) were significantly modulated by ripple-waves.

Pyramidal cells   **Interneurons**

A

B

C
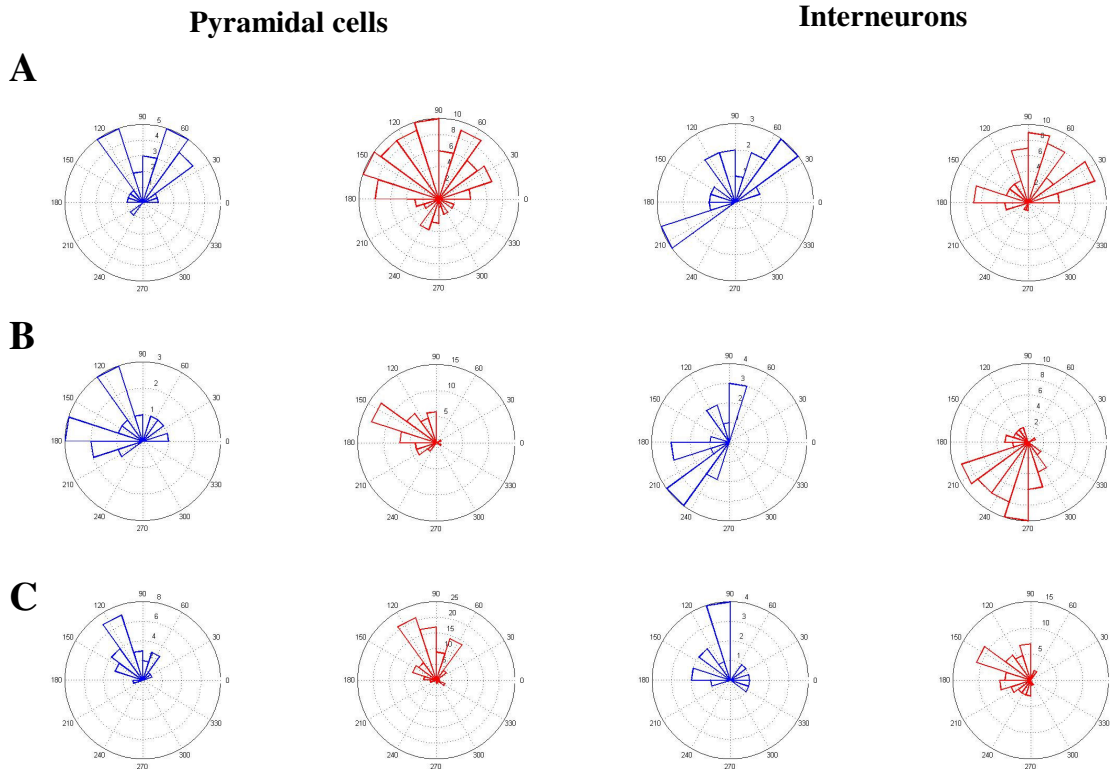
Figure 34.: Preferred phases of significantly modulated units during theta-oscillations (A), gamma- (B) and ripple-rhythms (C). Cells from WT animals are marked with blue, those from KO mice with red colour. The preferred phases are plotted on circular histograms in a way that the zero phase (and consequently the 360 degrees, on the right side of the circle) indicate the peak of a given oscillatory wave and 180 degrees denote the trough (left side of the plots). Therefore the descending slopes of oscillatory waves are represented by the upper half of the circles and the ascending slopes by the lower halves. The wave proceeds on the plots in a counterclockwise fashion. One can see that while there is not much difference regarding pyramidal cells, interneurons in KO mice have altered preferred phases with respect to gamma- and ripple-oscillations, corresponding well with unitary phase-modulation histograms.

DISCUSSION

Analyzing *in vivo* recordings from PV-GluR-A KO mice we made several interesting observations. Even though PV-cells in the hippocampus of these mice are supposed to have a significantly reduced excitatory input and therefore are thought to be partially uncoupled from the excitatory network, we did not find a strong deficit in the generation of gamma- and ripple-oscillations. Surprisingly, ripples tended to be of even higher amplitude in KO than in WT mice and we did not find pronounced changes in the gamma-power either. However, we saw a modest gamma-frequency decrease during REM-sleep of these animals. Interestingly, *in vitro* these mice exhibited a strongly reduced gamma-power (Fuchs et al., 2007, *figure 35.*). Now we have to clarify what circumstances could have led to these disparate results. The *in vitro* study was performed in horizontal CA3-slices using a kainate-application protocol. One might speculate that an intact hippocampus (as in our experiments) might not be as vulnerable to the genetic defect as a slice-preparation since many of the anatomical connections are destroyed in the slice. We cannot rule out either that other brain structures might adjust their input to the changed hippocampal circuitry, thereby providing a different sort of compensation, and it is actually known that parahippocampal structures, like the entorhinal cortex, have an impact on hippocampal gamma-generators (Bragin et al., 1995). Oscillations evoked *in vitro* peak around 30 Hz, thus, they are considerably slower than gamma-oscillations *in vivo*, which have a more or less homogeneous spectral distribution between 30 and 80 Hz. In this manner the gamma-oscillations we examine may be of a different nature and origin than gamma-oscillations *in vitro*. Another possibility is that different hippocampal subregions might show different sensitivity to the genetic defect.

Figure 35.: Gamma-oscillations induced by kainate-application in WT and PV-GluR-A KO animals. The upper panel shows the kainate-concentration dependence of gamma-oscillations in vitro. In the lower panel, example traces of gamma-oscillations in WT and KO mice are shown. The power of gamma-oscillations (measured between 20 and 80 Hz, plotted in the lower right corner) is significantly reduced in the mutants.
Figure is from Fuchs et al., 2007.
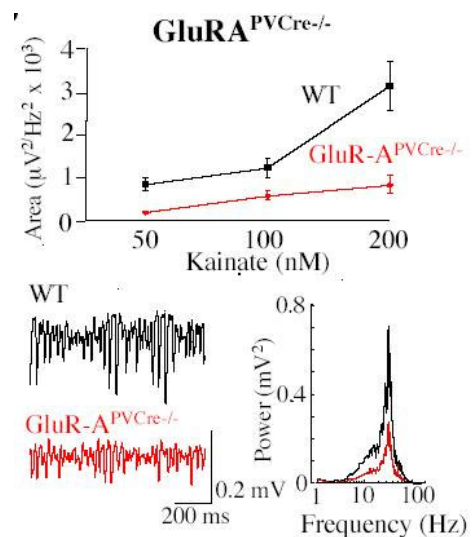
The increased ripple-power we see in PV-GluR-A KO mice could be related to the overall higher excitability of the pyramidal cell-network, due to the underperformance of local circuit

neurons, even though this excitability *in vivo* does not reach the threshold for epileptic phenomena. Indeed, perisomatic inhibition is thought to be very strong during ripples, requiring a very strong dendritic excitation on a given pyramidal cell to make it fire during the event. Thus, a weaker inhibition would result in increased pyramidal cell firing, making the ripples more pronounced. However, a higher ripple-power does not necessarily mean more cells that fire but can also mean that individual IPSPs and EPSPs get bigger or that compound postsynaptic potentials get bigger. The amplitude of compound postsynaptic potentials can be related to the number of cells participating in the potential-fluctuations or to the precise short-time synchrony between them. The same number of cells, if more synchronized, can bring about bigger local field potential fluctuations. Interestingly, pyramidal cells in PV-GluR-A KO mice did not fire more during ripples than pyramidal neurons from the WT group, even though their bursting frequency was higher during ripple events. Interestingly, it is rather the increased modulation depth of cell-firing which seems to be responsible for the higher ripple-power in the KO mice. Secondary mechanisms like gap junctions can also take over the synchronizing function of perturbed inhibition in the oscillogenesis. As a consequence, an increased number of spikelets could also result in a higher ripple-power. Eventually decreased inhibition might be favourable for antidromic spike-propagation and can shift ripple-frequency towards higher values in computer network models (Traub et al., 2000). However, this scenario would also mean more cells firing during ripples which we actually do not find. We cannot rule out that different interneuron-subpopulations might "reinnervate" the network in a different pattern which would lead to an altered balance between excitation and inhibition. In other words, in conventional knockouts we cannot rule out developmental effects. However, since PV-expression starts only around two weeks of age in mice, early developmental alterations can be excluded.

To understand how millisecond-scale synchrony is brought about in ranges of several millimeters during gamma- and ripple-oscillations belongs to the daunting questions of electrophysiology given that interneuron axons generally do not span more than several hundred micrometers. Ripples, however, are synchronized relatively well along the longitudinal axis of the hippocampal formation and its output pathways, regions spanning several millimeters (Chrobak & Buzsáki, 1996), even though as our results also suggest, there is a substantial drop in the phase-coherence already in a few hundred micrometers. To exert their synchronizing effect, interneurons need either a very precise and coordinated coupling to the excitatory network or very reliable gap junction-coupling between themselves (Traub et al., 1998). Recent research also suggests that long-range interneuron projections exist between the hippocampus, subiculum, presubiculum and other retrohippocampal structures and many of these interneurons increase their firing during ripples

(Jinno et al., 2007). Interestingly, most of these cells are PV-negative. Our results suggest that by compromising the excitatory neurotransmission on PV-cells, the network can still synchronise very efficiently. Thus, additional mechanisms, possibly also different cell-types seem to be involved as well in this form of network synchrony. An alternative explanation could be that the "excitatory deinnervation" of PV-cells "forces" them to switch back to their developmentally premature state when GABA can have an excitatory effect. This mechanism could be brought about by the altered expression of KCC2- and NKCC1-molecules, as proposed for pyramidal cells in temporal lobe epilepsy after traumatic lesions (Cohen et al., 2002; Stein & Nicoll, 2003). In this scenario, phasic GABAergic currents in PV-cells could substitute for the missing glutamatergic input.

Among hippocampal oscillations the theta-rhythm deserves big attention since its relation to cognitive functions has been suggested many times. In human subjects for example the performance of navigation tasks promotes synchrony in the theta-range and there is a correlation between the difficulty of the task and the actual theta-power (Kahana, 2006). The theta-rhythm in the hippocampus also seems to be preserved in the PV-GluR-A KO mice. However, given the many neurotransmitter systems involved in theta-generation (Yoder & Pang, 2005) we cannot exclude that compensatory effects stand behind this phenomenon. Hippocampal interneurons also receive GABAergic innervation from septal interneurons and they provide the septum with a reciprocal GABAergic projection. As a consequence, theta-generation could be perturbed in the septohippocampal loop. On the other hand, the septal nuclei also provide hippocampal interneurons with cholinergic input. In this manner, septal pacemakers can maintain a normal theta-rhythm even in the PV-GluR-A mutants. This theta can still modulate gamma-oscillations in a normal way. In any case, it would be interesting to record from the hippocampus and the medial septum simultaneously, to reveal in more detail the features of theta-generation.

Our unitary findings indicate that by compromising the excitation of PV-cells, the firing rates of interneurons do not change substantially even if we find a slight tendency towards decreased interneuronal firing rate during theta-oscillations. However, since we cannot discriminate between different interneuron-subpopulations in our interneuron-pool, this result can indicate a substantially underperforming PV-cell-population together with an unaltered or slightly compensating subpopulation of other GABAergic cells, be that CCK-positive neurons or interneurons expressing other markers. In a different scenario, PV-cells may possess "pacemaker"-properties, in which case they could generate action potentials without substantial excitatory input. As a result, their overall firing rates might not change much but the firing precision of basket cells could decrease, a possible outcome corroborated by the results on *in vitro* gamma-oscillations from GluR-D KO mice. However, as we saw, the PV-GluR-A KO mice are also different from the GluR-

D KO animals in this respect, because interneurons in PV-GluR-A KO animals displayed an increased phase-modulation during gamma- as well as ripple-oscillations. Interneurons in the PV-GluR-A KO mice increase their firing rate during ripples as WT interneurons do, however, additional mechanisms, such as gap junctions can also take part in this process or might become prevailing.

Interestingly, the main effect of modifying interneurons can be measured on pyramidal cells in a more sensitive way. Even though the average firing rate of principal cells was unaltered in the PV-GluR-A mutants, these pyramidal cells could accelerate to higher values during bursts, which is the favoured mode of pyramidal cell discharge. In addition to that, pyramidal cells in the PV-GluR-A KO mice were more likely to participate in bursts than those in WT mice. The higher bursting frequency is even more prominent during theta-oscillations. Pyramidal cells in KO mice exhibited a lower firing rate during theta-periods than their WT counterparts but surprisingly their bursting frequency was higher than those in WT mice. Thus, we see a complex phenotype. It seems that during theta-oscillations pyramidal cells from PV-GluR-A KO mice reach their firing threshold more rarely than principal cells from WT mice but when they reach it, they can fire faster. Experiments carried out in the Buzsáki-lab (Harris et al., 2001) have shown that the longer a pyramidal cell is silent, the more likely it responds with burst firing. It is assumed that this property is in connection with the depolarization block of their fast Na^+-channels. In this manner, it takes longer for a perturbed inhibitory network to relieve this block on pyramidal neurons, but when this is achieved, the pyramidal cells can fire faster most probably because of the suboptimal function of inhibitory cells. Pyramidal cells in PV-GluR-A KO mice also exhibit normal average firing rates during ripples, however, their bursting frequency is also higher during ripples compared to WT animals.

As discussed in the *Results* section, we do not find drastic changes in the phase-preference of either pyramidal cells or interneurons in PV-GluR-A KO mice, even though putative basket cells preferentially discharged at a slightly earlier theta-phase in the mutant compared to WT mice and also during gamma- and ripple-oscillations interneurons were delayed in the KO animals. However, the modulation depth of KO interneurons exceeded that of the WT control especially in gamma- and ripple-oscillations. These phenomena can result from the insufficient excitation the interneurons receive, because PV-cells would reach their firing threshold only in more circumscribed oscillatory phases. The delay of interneurons related to the gamma-phase (and also ripple-phase) indicates a problem with the activation of interneurons in feed-forward or feed-back excitation and this delay can also explain the gamma-frequency decrease we find in REM-sleep (*figure 18.*, magnified and replotted on *figure 36.*). Interestingly, PV-cells in GluR-D KO mice showed a weaker modulation in

in vitro gamma-oscillations (*figure 37.*) and this would also mean a decreased phase-modulation with respect to gamma-oscillations *in vivo*.
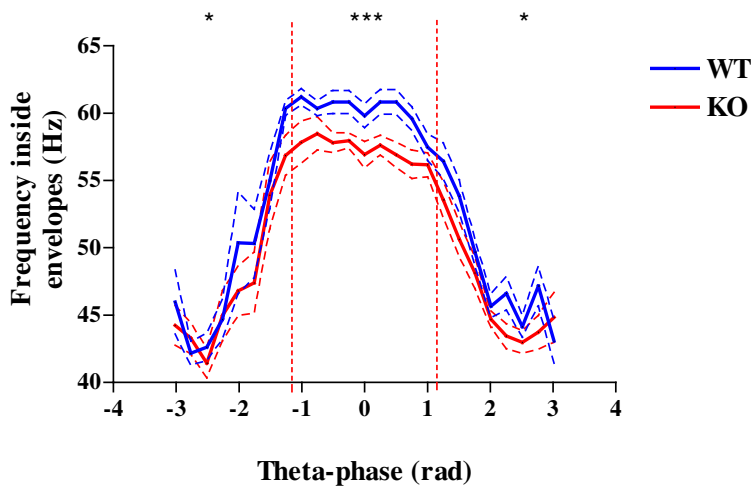

Figure 36.: PV-GluR-A KO mice display a reduction in the REM-gamma-frequency, which is most pronounced on peak of the theta-waves.
See the part on oscillatory analysis and fig. 18 for more details.

Figure 37.: Decreased phase-locking of PV-cells in pharmacologically induced gamma-oscillations in GluR-D KO mice. On the left ten oscillatory waves and the same number of action potentials are seen as an overlay. On the right the precise distribution of action potentials with respect to the peak of the gamma-waves is seen.
Figure is from Fuchs et al., 2007, Neuron.
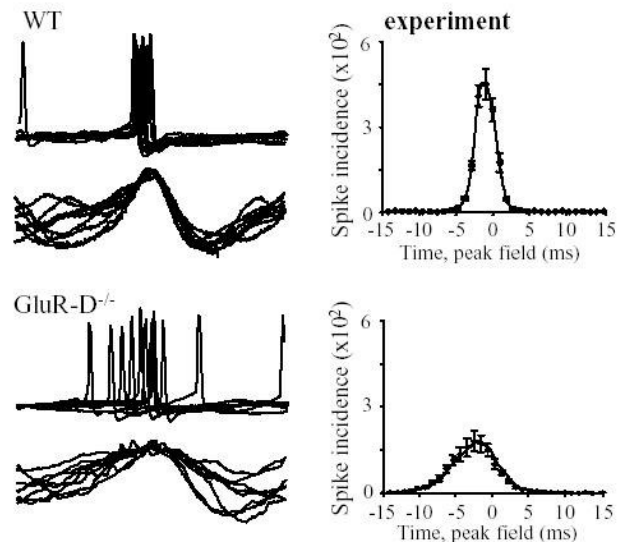
However, we cannot directly relate *in vitro* findings from GluR-D KO mice with *in vivo* results from PV-GluR-A KO mice because the GluR-D subunit also determines the fast kinetics of glutamate receptors. Thus, slowing down the AMPA-currents on PV-cells by deleting GluR-D may have a more profound effect on the spiking precision which could lead to a decreased gamma-phase-modulation *in vitro*, an outcome which we see in GluR-D KO mice but do not find in PV-GluR-A mutants. The decreased phase-modulation in the GluR-D-mutants can also account for the more pronounced gamma-power decrease and the slight gamma-frequency decrease in those animals (Fuchs et al., 2007), a result, which is different from that obtained in PV-GluR-A KO mice *in vivo*, even if we see a slight gamma-frequency decrease during REM-sleep in the latter.

We also find a higher modulation depth for pyramidal neurons and interneurons in PV-GluR-A KO mice during ripple-oscillations. To understand this finding let us imagine that due to

the perturbed excitatory drive of interneurons, more pyramidal cells are recruited to a given sharp-wave in the CA3-region of PV-GluR-A KO than in WT mice. As a consequence, CA1-interneurons receive a proportionally stronger drive, which could approach or even exceed the levels in WT mice. The stronger drive together with the altered sensitivity of interneurons could bring interneurons into motion in a more synchronised way. Thus, by auxiliary mechanisms the interneurons can be even sharper modulated and the sharper modulation of the interneurons can also be responsible for the sharper modulation depth of pyramidal cells later on. The mutant ripples would be the "fruit" of an altered, more synchronised inhibition and a more sharply tuned excitation, but still not reaching the threshold for epileptic discharges.

Even though it is tempting to correlate decreased gamma-power with cognitive deficits, we could not reproduce the *in vitro* results on gamma-oscillations *in vivo*. However, pyramidal cells in the PV-GluR-A KO mice behaved in a different way than those in WT mice, especially during theta-oscillations. The unitary analysis suggests that pyramidal cells fire overall less frequently during awake exploration and REM-sleep in KO animals. This may affect the navigation skills and memory-acquisition of these mice since hippocampal principal cells may be less accessible for excitatory inputs in the named behavioural states. However, in certain cases, pyramidal cells could fire with higher-frequency bursts. Altogether these features can make their activity less predictable and less controllable. A decreased firing precision can be harmful to the stability of cell-assemblies and in a similar way to the consolidation and stability of place fields. This can explain why PV-GluR-A KO animals underperform in short-term memory tests, such as T-maze and novel object recognition. The increased bursting frequency of CA1 pyramidal neurons during ripples might also mean that less well potentiated pyramidal cells also respond with burst firing in the actual oscillatory episode. This may lead to memory-consolidation in a less contrasted way and therefore may also lead to memory problems in the long run, even though the reference memory of the PV-GluR-A mutant mice seemed to be intact. Another possibility could be that as a consequence of compromised inhibition gap junctional coupling might be enhanced and this would interfere with the function of pyramidal neurons more profoundly, making their output less controllable. This model, however, is unlikely and would suggest that gap junctions are atavistic remains in the central nervous system and instead of being useful devices, they increase its noise-level.

Outlook

The altered network synchrony observed in the CA1 hippocampal subregion in PV-GluR-A KO mice raises many interesting questions. Analysis of place cells and place fields in these mice

will be carried out next and will be useful to establish links between single-cell activity and behaviour. The impaired performance of the mutants in the novel object recognition tests suggests that pattern completion and pattern separation may also be perturbed in these animals. These functions have been associated with the CA3 region (Nakazawa et al., 2002) and DG (McHugh et al., 2007). Therefore *in vivo* recordings from CA1, CA3 and DG during cognitive tasks and in remapping experiments could further enhance our understanding of cognitive alterations in the PV-GluR-A KO mice.

To reduce the probability of developmental alterations in knockout mice, we will resort to viral-injection exteriments in distinct hippocampal subfields using adult "floxed" GluR-A mice. The Cre-gene in these viruses, however, should be under the control of PV-promoter, which has not yet been achieved.

ACKNOWLEDGEMENTS

LITERATURE

Amaral DG & Witter MP (1995): Hippocampal formation. The rat nervous system, Second edition, Academic Press Inc, 443-493

Ashby MC, Maier SR, Nishimune A & Henley JM (2006): Lateral diffusion drives constitutive exchange of AMPA receptors at dendritic spines and is regulated by spine morphology. The Journal of Neuroscience, 26:7046-7055

Baranauskas G, Tkatch T, Nagata K, Yeh JZ & Surmeier DJ (2003): Kv3.4 subunits enhance the repolarizing efficiency of Kv3.1 channels in fast-spiking neurons. Nature Neuroscience, 6:258-266

Bartos M, Vida I & Jonas P (2007): Synaptic mechanisms of synchronized gamma oscillations in inhibitory interneuron networks. Nature Reviews Neuroscience, 8:45-56

Ben-Ari Y, Gaiarsa J-L, Tyzio R & Khazipov R (2007): GABA: a pioneer transmitter that excites immature neurons and generates primitive oscillations. Physiol. Reviews, 87:1215-1284

Behrens CJ, van den Boom LP, de Hoz L, Friedman A & Heinemann U (2005): Induction of sharp wave-ripple complexes *in vitro* and reorganization of hippocampal networks. Nature Neuroscience, 8:1560-1567

Blatow M, Rozov A, Katona I, Hormuzdi SG, Meyer AH, Whittington MA, Caputi A & Monyer H (2003): A novel network of multipolar bursting interneurons generates theta frequency oscillations in neocortex. Neuron, 38:805-817

Bliss TVP & Collingridge GL (1993): A synaptic model of memory: long-term potentiation in the hippocampus. Nature, 361:31-39

Bliss TVP & Lømo T (1973): Long-lasting potentiation of synaptic transmission in the dentate area of the anaesthetized rabbit following stimulation of the perforant path. Journal of Physiology, 232:331-356

Bragin A, Jandó G, Nádasdy Z, Hetke J, Wise K & Buzsáki G (1995): Gamma (40-100 Hz) oscillation in the hippocampus of the behaving rat. The Journal of Neuroscience, 15: 47-60

Bruzzone R, Hormuzdi SG, Barbe MT, Herb A & Monyer H (2003): Pannexins, a family of gap junction proteins expressed in brain. PNAS, 100:13644-13649

Buhl DL, Harris KD, Hormuzdi SG, Monyer H & Buzsáki G (2003): Selective impairment of hippocampal gamma oscillations in connexin-36 knock-out mice *in vivo*. The Journal of Neuroscience, 23:1013-1018

Burnashev N (2005): Dynamic modulation of AMPA receptor-mediated synaptic transmission by polyamines in principal neurons. Focus on "Polyamines modulate AMPA receptor-dependent synaptic response in immature layer V pyramidal neurons". Journal of Neurophysiology, 93:2371

Buzsáki G (2004): Large-scale recording of neuronal ensembles. Nature Neuroscience, 7:446-451

Buzsáki G (2006): Rhythms of the brain. Oxford University Press

Buzsáki G (1989): Two-stage model of memory trace formation: A role for "noisy" brain states. Neuroscience, 31:551-570

Buzsáki G, Bragin A, Chrobak JJ, Nádasdy Z, Sík A, Hsu M & Ylinen A (1994): Oscillatory and intermittent synchrony in the hippocampus: Relevance to memory trace formation. Temporal coding in the brain. Springer-Verlag Berlin Heidelberg, 145-172

Buzsáki G, Buhl DL, Harris KD, Csicsvári J, Czéh B & Morozov A (2003): Hippocampal network patterns of activity in the mouse. Neuroscience 116:201-211

Buzsáki G & Draguhn A (2004): Neuronal oscillations in cortical networks. Science, 304:1926-1929

Cacucci F, Lever C, Wills TJ, Burgess N & O'Keefe J (2004): Theta-modulated place-by-direction cells in the hippocampal formation in the rat. The Journal of Neuroscience, 24:8265-8277

Chen L, Chetkovich DM, Petralia RS, Sweeney NT, Kawasaki Y, Wenthold RJ, Bredt DS & Nicoll RA (2000): Stargazin regulates synaptic targeting of AMPA receptors by two distinct mechanisms. Nature, 408:936-943

Chrobak JJ & Buzsáki G (1996): High-frequency oscillations in the output networks of the hippocampal-entorhinal axis of the freely behaving rat. The Journal of Neuroscience, 16:3056-3066

Cohen I, Navarro V, Clemenceau S, Baulac M & Miles R (2002): On the origin of interictal activity in human temporal lobe epilepsy *in vitro*. Science, 298:1418-1421

Csicsvári J, Henze DA, Jamieson B, Harris KD, Sirota A, Barthó P, Wise KD & Buzsáki G (2003a): Massively parallel recording of unit and local field potentials with silicon-based electrodes. J Neurophysiol, 90:1314-1323

Csicsvári J, Hirase H, Czurkó A, Mamiya A & Buzsáki G (1999a): Fast network oscillations in the hippocampal CA1 region of the behaving rat. The Journal of Neuroscience, 19:RC20:1-4

Csicsvári J, Hirase H, Czurkó A, Mamiya A & Buzsáki G (1999b): Oscillatory coupling of hippocampal pyramidal cells and interneurons in the behaving rat. The Journal of Neuroscience, 19:274-287

Csicsvári J, Hirase H, Mamiya A & Buzsáki G (2000): Ensemble patterns of hippocampal CA3-CA1 neurons during sharp wave-associated population events. Neuron, 28:585-594

Csicsvári J, Jamieson B, Wise KD & Buzsáki G (2003b): Mechanisms of gamma oscillations in the hippocampus of the behaving rat. Neuron, 37:311-322

Cunningham MO, Davies CH, Buhl EH, Kopell N & Whittington MA (2003): Gamma oscillations induced by kainate receptor activation in the entorhinal cortex *in vitro*. The Journal of Neuroscience, 23:9761-9769

Cunningham MO, Whittington MA, Bibbig A, Roopun A, LeBeau FEN, Vogt A, Monyer H, Buhl EH & Traub RD (2004): A role for fast rhythmic bursting neurons in cortical gamma oscillations *in vitro*. PNAS, 101:7152-7157

Delpire E (2000): Cation-chloride cotransporters in neuronal communication. News Physiol Sci., 15:309-312

Denk W & Svoboda K (1997): Photon upmanship: Why multiphoton imaging is more than a gimmick? Neuron, 18:351-357

Dragoi G & Buzsáki G (2006): Temporal encoding of place sequences by hippocampal cell assemblies. Neuron, 50:145-157

Dragoi G, Harris KD & Buzsáki G (2003): Place representation within hippocampal networks is modified by long-term potentiation. Neuron, 39:843-853

Draguhn A, Traub RD, Schmitz D & Jefferys JGR (1998): Electrical coupling underlies high-frequency oscillations in the hippocampus *in vitro*. Nature, 394:189-192

Ego-Stengel V & Wilson MA (2007): Spatial selectivity and theta phase precession in CA1 interneurons. Hippocampus, 17:1-17

Feldmeyer D, Kask K, Brusa R, Kornau HC, Kolhekar R, Rozov A, Burnashev N, Jensen V, Hvalby Ø, Sprengel R & Seeburg PH (1999): Neurological dysfunctions in mice expressing different leveles of the Q/R site-unedited AMPAR subunit GluR-B. Nature Neuroscience, 2:57-64

Fisahn A, Pike FG, Buhl EH & Paulsen O (1998): Cholinergic induction of network oscillations at 40 Hz in the hippocampus in vitro. Nature, 394:186-189

Fonyó A (1997): Az orvosi élettan tankönyve. Medicina Könyvkiadó Rt.

Foster DJ & Wilson MA (2006): Reverse replay of behavioural sequences in hippocampal place cells during the awake state. Nature, 440:680-683

Freund TF (2003): Interneuron Diversity series: Rhythm and mood in perisomatic inhibition. TRENDS in Neurosciences, 26:489-495

Freund TF & Katona I (2007): Perisomatic inhibition. Neuron, 56:33-42

Fries P, Schröder JH, Roelfsema PR, Singer W & Engel AK (2002): Oscillatory neuronal synchronization in primary visual cortex as a correlate of stimulus selection. The Journal of Neuroscience, 22:3739-3754

Fuchs EC, Zivkovic AR, Cunningham MO, Middleton S, LeBeau FEN, Bannermann DM, Rozov A, Whittington MA, Traub RD, Rawlins JNP & Monyer H (2007): Recruitment of parvalbumin-positive interneurons determines hippocampal function and associated behaviour. Neuron, 53:591-604

Fuentealba P, Begum R, Capogna M, Jinno S, Márton LF, Csicsvári J, Thomson A, Somogyi P & Klausberger T (2008): Ivy cells: A population of nitric-oxide-producing, slow-spiking GABAergic neurons and their involvement in hippocampal network activity. Neuron, 57:917-929

Fürst Zs (1998): Gyógyszertan. Medicina Könyvkiadó Rt.

Furukawa H, Singh SK, Mancusso R & Gouaux E (2005): Subunit arrangement and function in NMDA receptors. Nature, 438:185-192

Geiger JRP, Melcher T, Koh DS, Sakmann B, Seeburg PH, Jonas P & Monyer H (1995): Relative abundance of subunit mRNAs determines gating and Ca^{2+} permeability of AMPA receptors in principal neurons and interneurons in rat CNS. Neuron, 15:193-204

Gewaltig MO, Diesmann M & Aertsen A (2001): Propagation of cortical synfire activity: survival probability in single trials and stability in the mean. Neural Netw., 14:657-673

Giocomo LM, Zilli EA, Fransén E & Hasselmo ME (2007): Temporal frequency of subthreshold oscillations scales with entorhinal grid cell spacing. Science, 315:1719-1722

Gray CM & Singer W (1989): Stimulus-specific neuronal oscillations in orientation columns of cat visual cortex. PNAS, 86:1698-1702

Gulyás AI, Megías M, Emri ZS & Freund TF (1999): Total number and ratio of excitatory and inhibitory synapses converging onto single interneurons of different types in the CA1 area of the rat hippocampus. The Journal of Neuroscience, 19:10082-10097

Hafting T, Fyhn M, Molden S, Moser MB & Moser EI (2005): Microstructure of a spatial map in the entorhinal cortex. Nature, 436:801-806

Hanley JG, Khatri L, Hanson PI & Ziff EB (2002): NSF ATPase and α-/β-SNAPs disassemble the AMPA receptor-PICK1 complex. Neuron, 34:53-67

Harris KD, Henze DA, Csicsvári J, Hirase H & Buzsáki G (2000): Accuracy of tetrode spike separation as determined by simultaneous intracellular and extracellular measurements. Journal of Physiology, 401-414

Harris KD, Henze DA, Hirase H, Leinekugel X, Dragoi G, Czurkó A & Buzsáki G (2002): Spike train dynamics predicts theta-related phase precession in hippocampal pyramidal cells. Nature, 417: 738-741

Harris KD, Hirase H, Leinekugel X, Henze DA & Buzsáki G (2001): Temporal interaction between single spikes and complex spike bursts in hippocampal pyramidal cells. Neuron, 32:141-149

Hashimoto K, Fukaya M, Qiao X, Sakimura K, Watanabe M & Kano M (1999): Impairment of AMPA receptor function in cerebellar granule cells of ataxic mutant mouse stargazer. The Journal of Neuroscience, 19:6027-6036

Hazan L, Zugaro M & Buzsáki G (2006): Klusters, NeursoScope, NDManager: a free software suite for neurophysiological data processing and visualization. J. Neurosci. Methods, 155:207-216

Higuchi M, Single FN, Köhler M, Sommer B, Sprengel R & Seeburg PH (1993): RNA editing of AMPA receptor subunit GluR-B: a base-paired intron-exon structure determines position and efficiency. Cell, 75:1361-1370

Hormuzdi SG, Pais I, LeBeau FEN, Towers SK, Rozov A, Buhl EH, Whittington MA & Monyer H (2001): Impaired electrical signaling disrupts gamma frequency oscillations in connexin 36-deficient mice. Neuron, 31:487-495

Isomura Y, Sirota A, Özen S, Montgomery S, Mizuseki K, Henze DA & Buzsáki G (2006): Integration and segregation of activity in entorhinal-hippocampal subregions by neocortical slow oscillations. Neuron, 52:871-882

Jinno S, Klausberger T, Marton LF, Dalezios Y, Roberts JDB, Fuentealba P, Bushong EA, Henze D, Buzsáki G & Somogyi P (2007): Neuronal diversity in GABAergic long-range projections from the hippocampus. The Journal of Neuroscience, 27:8790-8804

Kahana MJ (2006): The cognitive correlates of human brain oscillations. The Journal of Neuroscience, 26:1669-1672

Kamondi A, Acsády L & Buzsáki G (1998): Dendritic spikes are enhanced by cooperative network activity in the intact hippocampus. The Journal of Neuroscience, 18:3919-3928

Kandel ER, Schwartz JH & Jessell TM (2000): Principles of neural science, 4th Edition, McGraw-Hill, New York

Kentros CG, Agnihotri NT, Streater S, Hawkins RD & Kandel ER (2004): Increased attention to spatial context increases both place field stability and spatial memory. Neuron, 42:283-295

Khazipov R, Sirota A, Leinekugel X, Holmes GL, Ben-Ari Y & Buzsáki G (2004): Early motor activity drives spindle bursts in the developing somatosensory cortex. Nature, 432:758-761

Kim E & Sheng M (1996): PDZ domain proteins of synapses. Nature Reviews Neuroscience, 5:771-781

Klausberger T, Magill PJ, Marton LF, Roberts JDB, Cobden PM, Buzsáki G & Somogyi P (2003): Brain-state- and cell-type-specific firing of hippocampal interneurons *in vivo*. Nature, 421:844-848

Klausberger T, Marton LF, Baude A, Roberts JDB, Magill PJ & Somogyi P (2004): Spike timing of dendrite-targeting bistratified cells during hippocampal network oscillations *in vivo*. Nature Neuroscience, 7:41-47

Klausberger T, Marton LF, O'Neill J, Huck JHJ, Dalezios Y, Fuentealba P, Suen WY, Papp E, Kaneko T, Watanabe M, Csicsvári J & Somogyi P (2005): Complementary roles of cholecystokinin- and parvalbumin-expressing GABAergic neurons in hippocampal network oscillations. The Journal of Neuroscience, 25:9782-9793

Kocsis B, Bragin A & Buzsáki G (1999): Interdependence of multiple theta generators in the hippocampus: a partial coherence analysis. The Journal of Neuroscience, 19:6200-6212

Lamsa KP, Heeroma JH, Somogyi P, Rusakov DA & Kullmann DM (2007): Anti-Hebbian long-term potentiation in the hippocampal feedback inhibitory circuit. Science, 315:1262-1266

Larson J, Wong D & Lynch G (1986): Patterned stimulation at the theta frequency is optimal for the induction of hippocampal long-term potentiation. Brain Research, 368:347-350

Leutgeb JK, Leutgeb S, Treves A, Meyer R, Barnes CA, McNaughton BL, Moser MB & Moser EI (2005): Progressive transformation of hippocampal neuronal representations in "morphed" environments. Neuron, 48:345-358

Lytton WW & Lipton P (1999): Can the hippocampus tell time? The temporo-septal engram shift model. Computational Neuroscience. Neuroreport 10:2301-2306

Maguire EA, Gadian DG, Johnsrude IS, Good CD, Ashburner J, Frackowiak RSJ & Frith CD (2000): Navigation-related structural change in the hippocampi of taxi drivers. PNAS, 97:4398-4403

Maier N, Güldenagel M, Söhl G, Siegmund H, Willecke K & Draguhn A (2002): Reduction of high-frequency network oscillations (ripples) and pathological network discharges in hippocampal slices from connexin 36-deficient mice. Journal of Physiology, 541:521-528

Maier N, Nimmrich V & Draguhn A (2003): Cellular and network mechanisms underlying spontaneous sharp wave-ripple complexes in mouse hippocampal slices. Journal of Physiology, 550: 873-887

Mann EO, Suckling JM, Hajós N, Greenfield SA & Paulsen O (2005): Perisomatic feedback inhibition underlies cholinergically induced fast network oscillations in the rat hippocampus *in vitro*. Neuron, 45:105-117

Marin O & Rubenstein JLR (2003): Cell migration in the forebrain. Annual Review of Neuroscience, 26:441-483

Markram H, Lübke J, Frotscher M & Sakmann B (1997): Regulation of synaptic efficacy by coincidence of postsynaptic APs and EPSPs. Science, 275:213-215

Maurer AP, Cowen SL, Burke SN, Barnes CA & McNaughton BL (2006): Phase precession in hippocampal interneurons showing strong functional coupling to individual pyramidal cells. The Journal of Neuroscience, 26:13485-13492

Mayer LM (2005): Glutamate receptor ion channels. Current Opinion in Neurobiology, 15:282-288

McHugh TJ, Blum KI, Tsien JZ, Tonegawa S & Wilson MA (1996): Impaired hippocampal representation of space in CA1-specific NMDAR1 knockout mice. Cell, 87:1339-1349

McHugh TJ, Jones MW, Quinn JJ, Balthasar N, Coppari R, Elmquist JK, Lowell BB, Fanselow MS, Wilson MA & Tonegawa S (2007): Dentate gyrus NMDA receptors mediate rapid pattern separation in the hippocampal network. Science, 317:94-99

McNaughton BL, Battaglia FP, Jensen O, Moser EI & Moser MB (2006): Path integration and the neural basis of the 'cognitive map'. Nature Reviews Neuroscience, 7:663-678

McNaughton BL, O'Keefe J & Barnes CA (1983): The stereotrode: a new technique for simultaneous isolation of several single units in the central nervous system from multiple unit records. Journal of Neuroscience Methods, 8:391-397

Messinger A, Squire LR, Zola SM & Albright TD (2005): Neural correlates of knowledge: Stable representation of stimulus associations across variations in behavioral performance. Neuron, 48: 359-371

Mitzdorf U (1985): Current source-density method and application in cat cerebral cortex: Investigation of evoked potentials and EEG phenomena. Physiological Reviews, 65:37-100

Mizumori SJ, Barnes CA & McNaughton BL (1990): Behavioural correlates of theta-on and theta-off cells recorded from hippocampal formation of mature young and aged rats. Experimental Brain Research, 80:365-373

Mody I & Pearce RA (2004): Interneuron Diversity Series: Diversity of inhibitory neurotransmission through GABA$_A$ receptors. TRENDS in Neurosciences, 27:569-575

Nakazawa K, McHugh TJ, Wilson MA & Tonegawa S (2004): NMDA receptors, place cells and hippocampal spatial memory. Nature Reviews Neuroscience, 5:361-372

Nakazawa K, Quirk MC, Chitwood RA, Watanabe M, Yeckel MF, Sun LD, Kato AK, Carr CA, Johnston D, Wilson MA & Tonegawa S (2002): Requirement for hippocampal CA3 NMDA receptors in associative memory recall. Science, 297:211-218

Nakazawa K, Sun LD, Quirk MC, Rondi-Reig L, Wilson MA & Tonegawa S (2003): Hippocampal CA3 NMDA receptors are crucial for memory acquisition of one-time experience. Neuron, 38:305-315

O'Keefe J & Dostrovsky J (1971): The hippocampus as a spatial map. Preliminary evidence from unit activity in the freely-moving rat. Brain Research, 34:171-175

O'Neill J, Senior T & Csicsvári J (2006): Place-selective firing of CA1 pyramidal cells during sharp wave/ripple network patterns in exploratory behavior. Neuron, 49:143-155

Penttonen M, Kamondi A, Acsády L & Buzsáki G (1998): Gamma frequency oscillation in the hippocampus of the rat: intracellular analysis *in vivo*. European Journal of Neuroscience, 10:718-728

Ponomarenko AA, Knoche A, Korotkova TM & Haas HL (2003a): Aminergic control of high-frequency (~200 Hz) network oscillations in the hippocampus of the behaving rat. Neuroscience Letters, 348:101-104

Ponomarenko AA, Korotkova TM & Haas HL (2003b): High frequency (200 Hz) oscillations and firing patterns in the basolateral amygdala and dorsal endopiriform nucleus of the behaving rat. Behavioural Brain Research, 141:123-129

Ponomarenko AA, Korotkova TM, Sergeeva OA & Haas HL (2004): Multiple GABA$_A$ receptor subtypes regulate hippocampal ripple oscillations. European Journal of Neuroscience, 20:2141-2148

Price CJ, Cauli B, Kovács ER, Kulik A, Lambolez B, Shigemoto R & Capogna M (2005): Neurogliaform neurons form a novel inhibitory network in the hippocampal CA1 area. The Journal of Neuroscience, 25:6775-6786

Ranck JB Jr. (1984): Head-direction cells in the deep cell layers of dorsal presubiculum in freely moving rats. Soc. Neurosci. Abstr., 10:599

Raymond CR & Redman SJ (2006): Spatial segregation of neuronal calcium signals encodes different forms of LTP in rat hippocampus. Journal of Physiology, 570:97-111

Redish D (1999): Beyond the cognitive map. From place cells to episodic memory. MIT Press

Reymann KG & Frey JU (2007): The late maintenance of hippocampal LTP: Requirements, phases, `synaptic tagging´, `late-associativity´ and implications. Neuropharmacology, 52:24-40

Robbe D, Montgomery SM, Thome A, Rueda-Orozco PE, McNaughton BL & Buzsáki G (2006): Cannabinoids reveal importance of spike timing coordination in hippocampal function. Nature Neuroscience, 9:1526-1533

Rozov A, ZilberterY, Wollmuth LP & Burnashev N (1998): Facilitation of currents through rat Ca^{2+}-permeable AMPA receptor channels by activity-dependent relief from polyamine block. Journal of Physiology, 511:361-377

Sargolini F, Fyhn M, Hafting T, MacNaughton BL, Witter MP, Moser MB & Moser EI (2006): Conjunctive representation of position, direction, and velocity in entorhinal cortex. Science, 312:758-762

Schmitz D, Schuchmann S, Fisahn A, Draguhn A, Buhl EH, Petrasch-Parwez, Dermietzel R, Heinemann U & Traub RD (2001): Axo-axonal coupling: A novel mechanism for ultrafast neuronal communication. Neuron, 31:831-840

Scoville WB & Milner B (1957): Loss of recent memory after bilateral hippocampal lesions. Journal of Neurology, Neurosurgery and Psychiatry, 20:11-21

Segovia G, Yagüe AG, García-Verdugo JM & Mora F (2006): Environmental enrichment promotes neurogenesis and changes the extracellular concentrations of glutamate and GABA in the hippocampus of aged rats. Brain Research Bulletin, 70:8-14

Siapas AG, Lubenov EV & Wilson MA (2005): Prefrontal phase locking to hippocampal theta oscillations. Neuron, 46:141-151

Somogyi P, Tamás G, Lujan R & Buhl EH (1998): Salient features of synaptic organisation in the cerebral cortex. Brain Research Reviews 26:113-135

Stein V & Nicoll RA (2003): GABA generates excitement, Neuron, 37:375-378

Steriade M (1999): Coherent oscillations and short-term plasticity in corticothalamic networks. TRENDS in Neurosciences, 22:337-345

Stevens A & Price J (1996): Evolutionary Psychiatry. A new beginning. Routledge

Szabadics J, Varga Cs, Molnár G, Oláh Sz, Barzó P & Tamás G (2006): Excitatory effect of GABAergic axo-axonic cells in cortical microcircuits. Science, 311:233-235

Szirmai I (2005): Neurológia. Medicina

Szirmai I, Kamondi A & Kovács T (2000): A neurológiai betegvizsgálat alapjai. Semmelweis Egyetem Orvostudományi Kar, Neurológiai Klinika

Traub RD & Bibbig A (2000): A model of high-frequency ripples in the hippocampus based on synaptic coupling plus axon-axon gap junctions between pyramidal neurons. The Journal of Neuroscience, 20:2086-2093

Traub RD, Bibbig A, LeBeau FEN, Cunningham MO & Whittington MA (2005): Persistent gamma oscillations in superficial layers of rat auditory neocortex: experiment and model. Journal of Physiology, 562:3-8

Traub RD, Spruston N, Soltesz I, Konnerth A, Whittington MA & Jefferys JGR (1998): Gamma-frequency oscillations: A neuronal population phenomenon, regulated by synaptic and intrinsic cellular processes, and inducing synaptic plasticity. Progress in Neurobiology, 55:563-575

Uchizono K (1965): Characteristics of excitatory and inhibitory synapses in the central nervous system of the cat. Nature, 207:642-643

Ulanovsky N & Moss CF (2007): Hippocampal cellular and network activity in freely moving echolocating bats. Nature Neuroscience, 10:224-233

Vida I, Bartos M & Jonas P (2006): Shunting inhibition improves robustness of gamma oscillations in hippocampal interneuron networks by homogenizing firing rates. Neuron, 49:107-117

Vogt A, Hormuzdi SG & Monyer H (2005): Pannexin1 and pannexin2 expression in the developing and mature rat brain. Molecular Brain Research, 141:113-120

Whitlock JR, Heynen AJ, Shuler MG & Bear MF (2006): Learning induces long-term potentiation in the hippocampus. Science, 313:1093-1097

Whittington MA & Traub RD (2003): Interneuron Diversity series: Inhibitory interneurons and network oscillations *in vitro*. TRENDS in Neurosciences, 26:676-682

Wonders CP & Anderson SA (2006): The origin and specification of cortical interneurons. Nature Reviews Neuroscience, 7:687-696

Wolansky T, Clement EA, Peters SR, Palczak MA & Dickson CT (2006): Hippocampal slow oscillation: A novel EEG state and its coordination with ongoing neocortical activity. The Journal of Neuroscience, 26:6213-6229

Wood ER, Dudchenko PA, Robitsek RJ & Eichenbaum H (2000): Hippocampal neurons encode information about different types of memory episodes occurring in the same location. Neuron, 27: 623-633

Xia J, Zhang X, Staudinger J & Huganir RL (1999): Clustering of AMPA receptors by the synaptic PDZ domain-containing protein PICK1. Neuron, 22:179-187

Ylinen A, Bragin A, Nádasdy Z, Jandó G, Szabó I, Sík A & Buzsáki G (1995): Sharp wave-associated high-frequency oscillation (200 Hz) in the intact hippocampus: network and intracellular mechanisms. The Journal of Neuroscience, 15:30-46

Yoder RM & Pang KC (2005): Involvement of GABAergic and cholinergic medial septal neurons in hippocampal theta rhythm. Hippocampus, 15:381-392

Zamanillo D, Sprengel R, Hvalby Ø, Jensen V, Burnashev N, Rozov A, Kaiser KMM, Köster HJ, Borchardt T, Worley P, Lübke J, Frotscher M, Kelly PH, Sommer B, Andersen P, Seeburg PH, Sakmann B (1999): Importance of AMPA receptors for hippocampal synaptic plasticity but not for spatial learning. Science, 284:1805-1811

Zhang ZJ & Reynolds GP (2002): A selective decrease in the relative density of parvalbumin-immunoreactive neurons in the hippocampus in schizophrenia. Schizophrenia Research, 55:1-10

Zsiros V & Maccaferri G (2005): Electrical coupling between interneurons with different excitable properties in the stratum lacunosum-moleculare of the juvenile CA1 rat hippocampus. The Journal of Neuroscience, 25:8686-8695